

YMEP 2018 FINAL TECHNICAL REPORT
Report on the Stratigraphy and Structure of the CL and HJ Properties

NTS: 106C01, 106C02, 106C07, 106C08 Mayo Mining District, Yukon Territories, Canada

CL: 64°15'17" N 132° 44'12" W
HJ: 64°12'34" N 132° 25'45" W

CLAIMS:

CL 1-493 (YF42001-YF42493)
CL 494-501 (YD156278-YD156285)
HJ 1-405 (YF41401-YF41805)
HJ 406-412 (YD156286-YD156292)

WORK PERFORMED:
July 22 – 30, 2018

Effective Date: January 24, 2019

Prepared for:
Carlincore Resources Ltd.

Prepared by:

Carl Schulze, BSc, PGeo



YMEP FINAL TECHNICAL REPORT
Report on the Stratigraphy and Structure of the CL and HJ Properties

Effective Date: January 24, 2019

Prepared for:
Carlincore Resources Ltd.
200-204 Lambert Street
Whitehorse YT
Y1A 3T2

Prepared by:
Aurora Geosciences Ltd.
Main Office: 3506 McDonald Drive, Yellowknife, NT, X1A 2H1
Phone: (867) 902.2729 Fax: (867) 920-2739
www.aurorageosciences.com

Author:
Carl Schulze, BSc., P.Geo.

TABLE OF CONTENTS

1	EXECUTIVE SUMMARY.....	1
2	INTRODUCTION	2
3	LOCATION & ACCESS	3
4	PROPERTY DESCRIPTION	3
5	CLIMATE & PHYSIOGRAPHY.....	7
6	EXPLORATION HISTORY.....	7
6.1	PRE-2016 EXPLORATION	7
6.2	2016 EXPLORATION	10
6.2.1	<i>Pre-season Desktop Analysis.....</i>	10
6.3	2016 FIELDWORK	12
7	REGIONAL & PROPERTY GEOLOGY	18
7.1	REGIONAL GEOLOGY.....	18
7.2	PROPERTY GEOLOGY.....	23
8	2018 WORK PROGRAM	26
8.1	NORTHWEST (NW) PART OF AREA 2 (HJ BLOCK)	28
8.2	SOUTHEAST (SE) PART OF AREA 1 (CL BLOCK)	30
8.2.1	<i>Southeast (SE) part of Area 1 (CL block)</i>	30
8.2.2	<i>Southeast 2 (SE2) part of Area 1 (CL Block)</i>	32
8.2.3	<i>Northwest (NW) part of Area 1 (CL Block)</i>	33
9	SAMPLING METHODOLOGY, ANALYSIS AND SECURITY.....	35
9.1	ROCK SAMPLES.....	35
9.2	CARBON ISOTOPE CHEMOSTRATIGRAPHY	35
10	DISCUSSION: STRUCTURAL EVOLUTION OF THE CL AND HJ CLAIMS.....	35
10.1	OVERVIEW.....	36
10.2	AREA 2 TRANSECT (HJ BLOCK)	36
10.3	AREA 1 SE TRANSECT (CL BLOCK).....	38
10.4	AREA 1 NW TRANSECT (CL CLAIMS).....	39
10.5	CARBON ISOTOPE CHEMOSTRATIGRAPHY	40
10.6	2018 ROCK SAMPLING.....	43
11	CONCLUSIONS	48
11.1.1	AREA 2 NW (HJ Block).....	48
11.1.2	AREA 1 SE (CL Block)	48
11.1.3	AREA 1 NW (CL Block).....	49
12	REFERENCES	50

LIST OF FIGURES

FIGURE 1: LOCATION MAP	4
FIGURE 2: CLAIM MAP, CL AND HJ CLAIMS	5
FIGURE 3: LOCATION OF CL AND HJ BLOCKS, ON A 15M RESOLUTION HILLSHADE DIGITAL ELEVATION MODEL BACKGROUND. MODIFIED FROM BENNETT (2016).....	6
FIGURE 4: REGIONAL GEOLOGICAL SETTING OF CL AND HJ PROPERTIES. GEOLOGY FROM GORDEY AND MAKEPEACE (1999). FIGURE MODIFIED FROM BENNETT (2016)	9
FIGURE 5: ANOMALOUS AU AND AS IN STREAM SEDIMENTS (2012-2015 DATA) (BENNETT, 2016)	13
FIGURE 6: ANOMALOUS Pb, Zn, Ag AND Au IN SOILS (2014-2015 DATA). FROM BENNETT (2016), LITHOLOGICAL UNITS FROM CHAKUNGAL (2014)....	14
FIGURE 7: ANOMALOUS Au AND Cu VALUES (BENNETT, 2016)	15
FIGURE 8: As-Sb AND Au-Sb SOIL ANOMALIES (BENNETT, 2016).....	16
FIGURE 9: ANOMALOUS Mo-Tl IN SOIL, CORRESPONDING TO AN INTERBEDDED BLACK SHALE AND SILSTONE UNIT (BENNETT, 2016).....	17
FIGURE 10: (a) ROCK SAMPLE WITH HIGHEST Au ASSAY (38 PPB Au). (b) SAMPLE WITH HIGHEST As ASSAY (2,159 PPM As). PHOTOS BY BENNETT (2016)	18
FIGURE 11: DEPOSITS WITHIN ATAC RESOURCES LTD's ANUBIS AND OSIRIS CLUSTERS, AND AS-IN-SOIL ANOMALIES. FROM: HTTP://WWW.ATACRESOURCES.COM/PROJECTS/RACKLA/NADALEEN-TREND.	20
FIGURE 12: BEDROCK GEOLOGY OF SOUTHERN CL PROPERTY (FROM MOYNIHAN, 2016).	21
FIGURE 13: BEDROCK GEOLOGY OF SOUTHERN HJ PROPERTY (FROM MOYNIHAN, 2016).	22
FIGURE 14: NEOPROTEROZOIC WINDERMERE SUPERGROUP STRATIGRAPHY (AFTER NARBONNE AND AITKEN, 1995), WITH PROPOSED CORRELATIONS TO UNITS ALONG THE RACKLA BELT (COLPRON, 2013). FIGURE FROM PYLE AND BENNETT, 2018	23
FIGURE 15: LOCAL AND REGIONAL STRATIGRAPHY AND DETAILED SECTIONS OF THE OSIRIS CLUSTER LOCAL STRATIGRAPHIC UNITS (COULTER ET AL, 2017; RISTORCELLI ET AL., 2018)	25
FIGURE 16: LOCATION OF TRANSECTS, CL AND HJ BLOCKS (PYLE AND BENNETT, 2018)	27
FIGURE 17: STRATIGRAPHIC LOG OF THE SECTION IN THE NORTHWEST PART OF AREA 2	29
FIGURE 18: STRATIGRAPHIC LOG OF THE SECTION IN THE SE PART OF AREA 1 (PYLE AND BENNETT, 2018).....	31
FIGURE 19: STRATIGRAPHIC LOG OF THE SECTION IN THE SE2 PART OF AREA 1	32
FIGURE 20: COMPOSITE STRATIGRAPHIC LOG OF THE SECTIONS IN THE NORTHWEST PART OF AREA 1	34
FIGURE 21: INTERPRETED STRUCTURAL DOMAINS FOR AREA 2 TRANSECT, SUPERIMPOSED ON HILLSHADE MODEL (PYLE AND BENNETT, 2018)	37
FIGURE 22: INTERPRETED STRUCTURAL DOMAINS FOR AREA 1SE TRANSECT (PYLE AND BENNETT, 2018)	39
FIGURE 23: NNW TRENDING LATE BRITTLE FAULT ZONE WITHIN AREA 1 NW (PYLE AND BENNETT, 2018).....	40
FIGURE 24: CARBON ISOTOPE CHEMOSTRATIGRAPHY OF THE EDICARAN WINDERMERE SUPERGROUP, THROUGH THE COMPOSITE SECTION IN THE NW PART OF AREA 1 (PYLE AND BENNETT, 2018).	42
FIGURE 25: SCATTER PLOT OF NIOBium VERSUS ZIRCONIUM.....	43
FIGURE 26: GROUPINGS OF GEOCHEMICAL DATA AND MEDIAN LINE PLOTS FOR AREAS 1 NW, 1 SE AND 2	44
FIGURE 27: ROCK SAMPLE LOCATIONS, AREA 1 NW	45
FIGURE 28: ROCK SAMPLE LOCATIONS, AREA 1 SE	46
FIGURE 29: ROCK SAMPLE LOCATIONS, FIGURE 2	47

LIST OF TABLES

TABLE 1. SUMMARY OF 2014-2016 SAMPLE COLLECTIONS.....	10
TABLE 2. PEARSON CORRELATION COEFFICIENTS (R VALUES) FOR SELECTED ELEMENTS FOR 2014 (TOP FIGURE) AND 2015 (BOTTOM FIGURE) SOIL SAMPLES	11

LIST OF APPENDICES

APPENDIX I.....	STATEMENT OF QUALIFICATIONS
APPENDIX II.....	CLAIM INFORMATION
APPENDIX III.....	PROJECT LOG
APPENDIX IV.	STATEMENT OF EXPENDITURES
APPENDIX V.	SAMPLE DESCRIPTIONS
APPENDIX VI.	GEOCHEMICAL ANALYSIS CERTIFICATES
APPENDIX VII.	FULL PYLE/ BENNETT REPORT

1 EXECUTIVE SUMMARY

Carlincore Resources Ltd. (“Carlincore”) in 2018 commissioned L. Pyle and V. Bennett, through Aurora Geosciences Ltd., to conduct a detailed evaluation of the stratigraphic and structural settings of two sub-areas of the CL and HJ claim blocks. These are: Area 1, comprising the southeastern portion of the CL property, and Area 2, covering the northwest corner of the HJ property. These were covered by a total of three transects: Area 1 SE and Area 1 NW respectively on Area 1 of the CL block, and Area 2 NW of the HJ block. This report describes the stratigraphic and structural evaluation of these three transects.

The CL and HJ properties comprise 501 and 412 Yukon quartz mining claims respectively, 100% owned by Carlincore and recorded in the Mayo Mining District. The CL property is centered at 64°15'17" N 132°44'12" W, and the HJ property is centered at 64°12'34" N 132° 25'45" W. The properties are located about 190 km northeast of the road-accessible Village of Mayo. The properties are accessible by helicopter, from Mayo, although fixed wing access to the Stewart Strip is also available, with permission by ATAC Resources Ltd.

Regional bedrock geology has been recently recompiled and re-interpreted by the Yukon Geological Survey. The properties are interpreted to be underlain by mainly Neoproterozoic clastic and lesser carbonate sedimentary rocks of the Windermere Supergroup comprising shelf and slope carbonate and clastic rocks of the Ogilvie Platform. The CL and HJ properties are located several kilometres north of the east-west trending regional-scale Dawson Thrust, separating Windermere rocks from Neoproterozoic to Lower Cambrian Selwyn Basin, Hyland Group coarse- and fine-grained clastic rocks. The CL and HJ properties are located directly north of the east-west trending Kathleen Lakes fault, another east-west trending regional feature which remains poorly understood. The Carlin-style deposits and prospects of the Anubis and Osiris clusters within the Nadaleen trend, held by ATAC, are located within Windermere Supergroup rocks between the Kathleen Lakes fault and the Dawson Thrust.

In 2012 and 2013, Carlincore Resources Ltd. conducted detailed stream geochemical sampling and prospecting surveys on the HJ and CL properties. The program revealed a number of weak gold and path-finder element (As, Hg, Sn, Te, Tl) anomalies. This was followed up in 2014 by soil geochemical sampling, prospecting, rock sampling, and geological mapping. Additional soil and rock sampling were carried out in 2015. In 2016 a desktop study of existing geochemical and geological data was completed by Bennett, and further rock geochemical sampling was done. No significant mineralization was discovered; the highest gold (Au) value returned was 38 ppb Au and the highest arsenic (As) value was 2,159 ppm.

Stratigraphic and structural analysis, as well as rock sampling, were conducted in 2018. Area 1 SE comprises two stratigraphic units: the Rapitan Group and Ice Brook/ Keele Formation of the Windermere Supergroup. Strata comprises two 100% siliciclastic successions, which are also present within the Osiris cluster but are not mineralized hosts. The structural setting of Area 1 SE comprises an early generation of shallow SSW-plunging tight to open folds within the Rapitan Group that is overprinted by a later generation of fault-related folding. No mineralization associated with these faults was observed, and no

major shear zones or thrust faults, features that play an important role in mineral emplacement at the Osiris cluster, were mapped. Rock geochemical sampling at Area 1 SE returned elevated copper values, as well as the highest As value (20.4 ppm) returned in 2018.

Stratigraphy in Area 1 NW comprises about 20% carbonate and 80% heterolithic siliciclastics interpreted as units of the Windermere Supergroup. The basal unit is the Rapitan Group (siliciclastics), successively overlain by the Ice Brook/Keele Formation (siliciclastics), Ravenstthroat Formation (cap carbonates), Sheepbed Formation (mixed fine siliciclastics and carbonate), Gametrail Formation (dominated by carbonate debrites), Blueflower Formation (siliciclastics), and possibly the Risky Formation (carbonates). The Sheepbed and Gametrail formations have stratigraphic equivalents within the Osiris cluster stratigraphy of the Rackla Gold Belt trend.

Area 1 NW hosts the most intact section of prospective carbonate host rocks, including the widest section of carbonate stratigraphy within the three transects. These include dolostone within the Ravenstthroat Formation and limestones within the Sheepbed, Gametrail, Blueflower and Risky (?) formations. Mineralization within the Osiris cluster occurs within the Nadaleen and Gametrail formations, the stratigraphic equivalents of the Sheepbed and Gametrail formations on the CL and HJ blocks. However, no mineralization was observed in 2018. The dominant structural grain is NNE-trending and west-dipping. No major brittle- ductile shear zones or thrust faults where observed. The area is characterized by a suite of N, NE-ENE and NW late brittle structures that may be coeval and may represent part of a Riedel shear system.

Stratigraphy in Area 2 consists of mudrock, sandstone, and conglomeratic sandstone with rare dolostone beds. Stratigraphy remains unconstrained in a regional context, and further work is warranted to determine age and stratigraphic position of the transect examined. However, the predominance of siliciclastics over carbonate lithologies lowers potential for sediment-hosted gold prospects.

Area 2 consists of three structural domains , the largest of which is characterized by late NE and ENE trending brittle faults with only minor amounts of displacement, and associated shallow to moderate ENE-plunging folds. No major thrust faults or shears zones occur in Area 2, and no mineralization was observed.

2 INTRODUCTION

In 2018 Aurora Geosciences Ltd. (“Aurora”) was commissioned by Carlincore Resources Ltd. (“Carlincore”) to conduct a detailed evaluation of the stratigraphic and structural settings of two sub-areas of the CL and HJ properties, respectively. The CL and HJ properties, located in east-central Yukon directly north of the Nadaleen Trend of Carlin-style deposits, are 100% owned by Carlincore. The survey was conducted from July 22 to July 30, 2018 by Leanna Pyle (P.Geo., Ph.D.) of VI Geoscience Services Ltd., and Venessa Bennett (P.Geo., Ph.D. A.Dip (GIS/RS) of Geomantia Consulting. Three transects were selected and surveyed; these cover Area 1 NW and Area 1 SE in the southeastern part of the CL block, and Area 2 NW in the HJ block.

This report reviews the results of stratigraphic and structural evaluation of these transects. Total expenditures for 2018 on both properties stand at CDN\$83,300.

All geographic locations in this report are relative to North American Datum 1983 (NAD 83). Non-geodetic coordinates are expressed in Universal Transverse Mercator (UTM) Zone 8N metric coordinates. All measurements are expressed in metric units unless they are quoted from historic reports expressed in other units of measure. Angles of azimuth are expressed relative to true north unless otherwise stated.

3 LOCATION & ACCESS

The CL property is centered at 64°15'17" N 132° 44'12" W, on NTS map sheets 106C\02 and 106C\07. The HJ property is centered at 64°12'34" N 132° 25'45" W, on NTS map sheets 106C\01 and \106C02. Both are located within the Mayo Mining District, Yukon (Figure 1). The properties are located about 190 km northeast of the road-accessible Village of Mayo (pop. 200, 2016 census) which provides basic grocery, fuel and hardware supplies, as well as accommodations. Mayo also has a serviced airstrip with regularly commercial air service, and is the location of the mining recorder's office for the Mayo mining district.

The properties are accessible by helicopter, with the closest road access located at the community of Keno City about 55 road-km northeast of Mayo. In 2018, ATAC Resources Ltd. allowed Aurora the use of its privately-owned Stewart River airstrip for fixed wing access from Mayo. From there, the properties were accessed by helicopter on a daily set-out basis.

4 PROPERTY DESCRIPTION

The CL property comprises 501 contiguous Yukon quartz mining claims covering about 10,460 hectares (25,840 acres). The HJ property comprises 412 quartz claims covering 8,603 hectares (21,250 acres). Both properties are located directly adjacent to the south side of the Peel Watershed Land Use planning region, currently excluded from new staking activity (Figures 2 and 3). Claim information is summarized in Appendix II.

The claims comprising each property may be retained in good standing by performing applicable assessment work in the amount of \$100 per claim per year, or by paying the same amount as "cash in lieu" of assessment work. A \$5.00 administration fee per each \$100 worth of filing is also applicable.

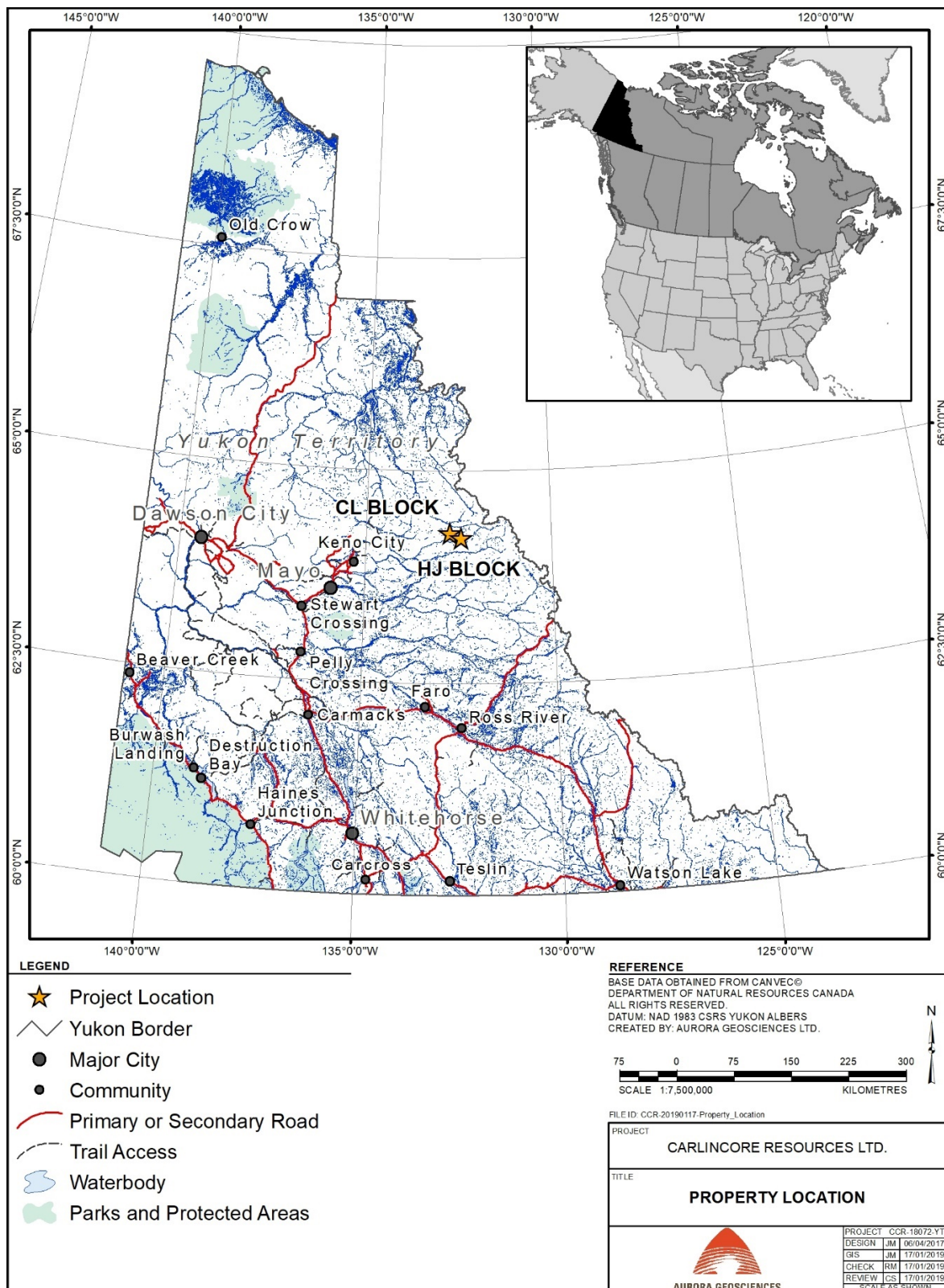
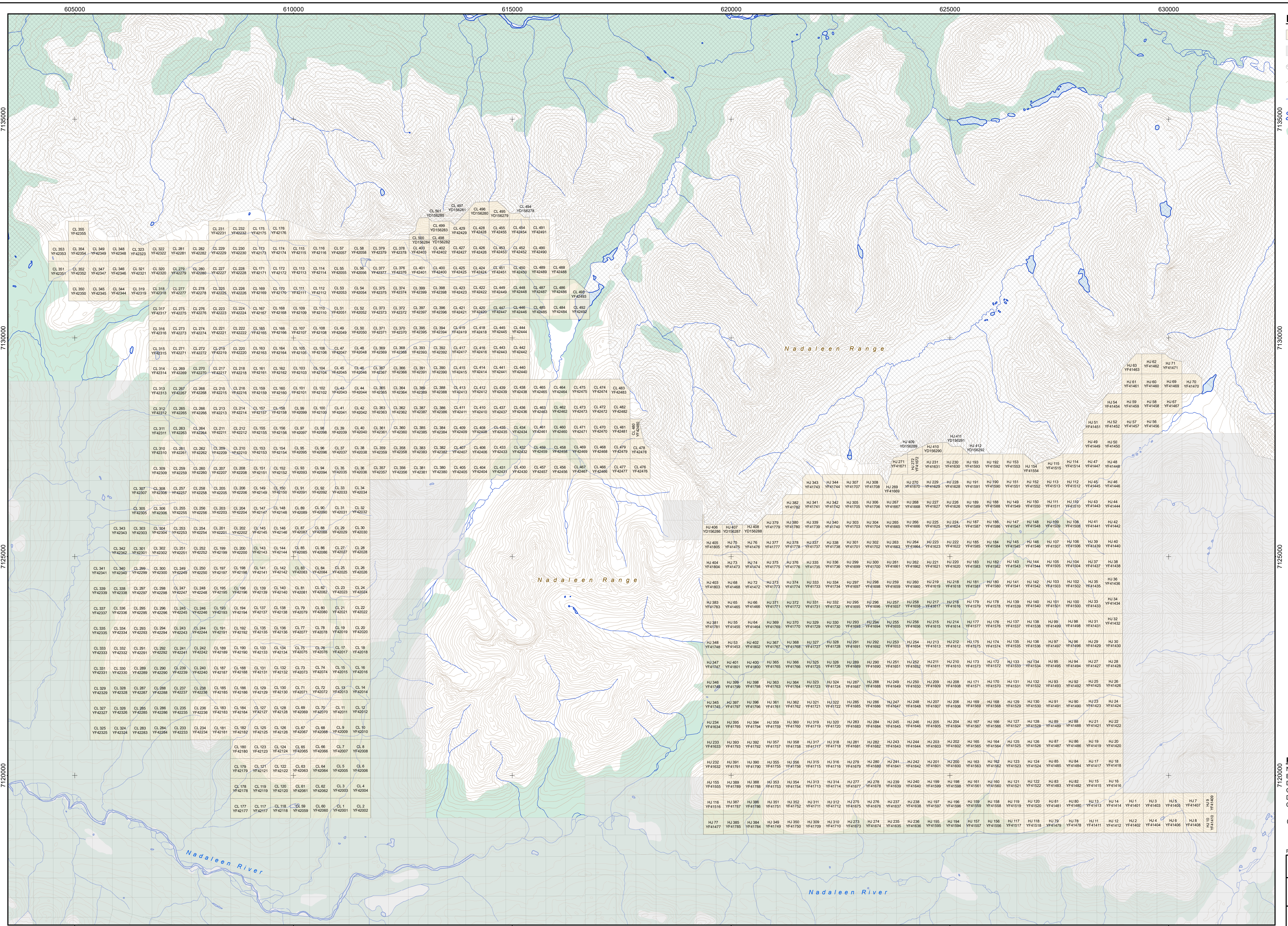


Figure 1: Location Map



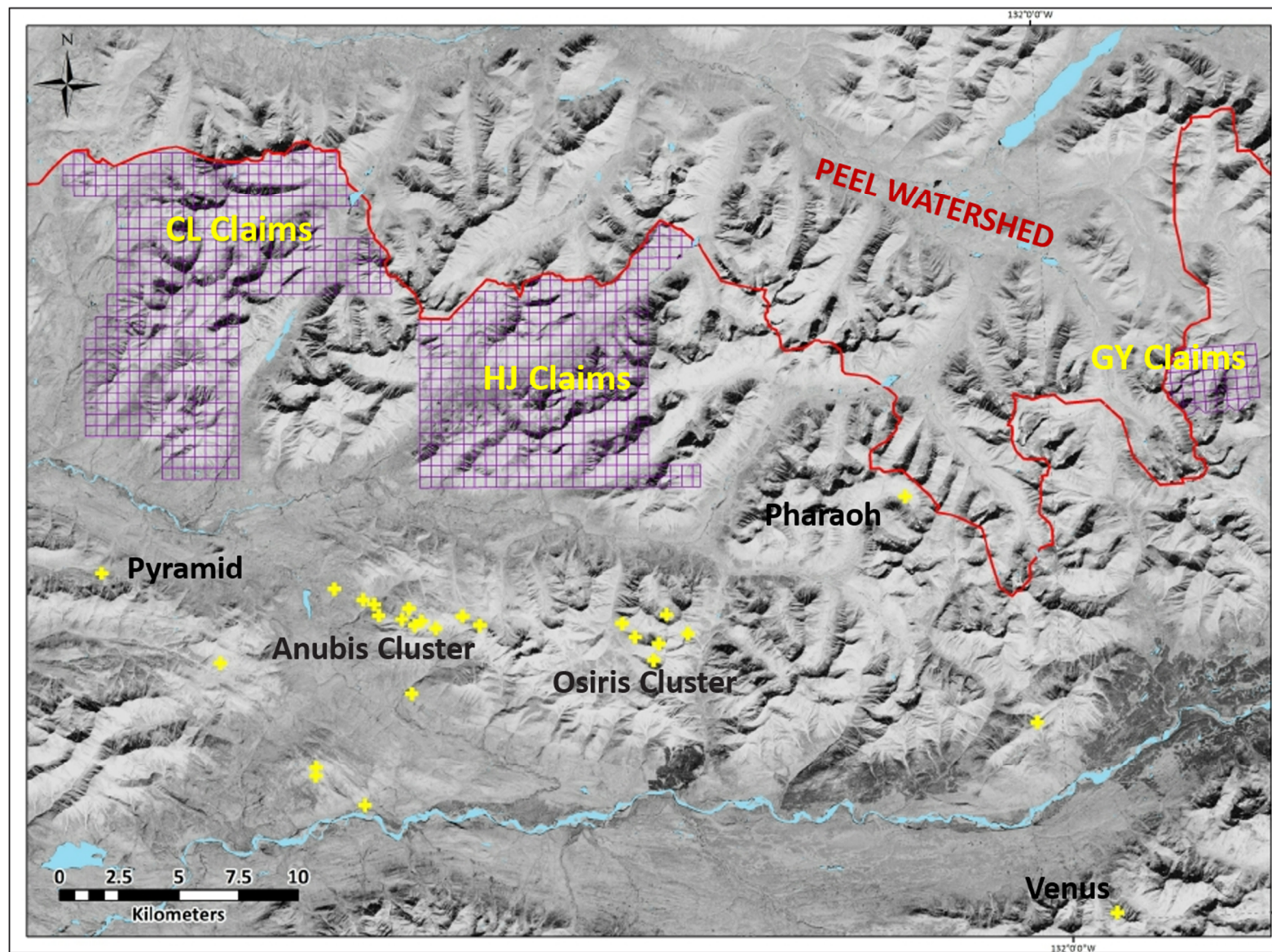


Figure 3: Location of CL and HJ blocks, on a 15m resolution hillshade digital elevation model background. Modified from Bennett (2016).

5 CLIMATE & PHYSIOGRAPHY

This section was taken verbatim, with minor modifications, from the 2016 assessment report titled “Assessment Report: Geochemical and Remote Sensing Analysis, Geochemical Sampling and Prospecting of the HJ, CL and GY Properties” by Leonard Gal, MSc, PGeo.

The climate and physiography section has been modified after the Ecological Stratification Working Group (1995) and Mitchell (2015). The CL and HJ properties are located within the Taiga Cordillera Eco-zone and the Selwyn Mountain Eco-region. The northern continental climate experienced by the region is marked by mild summers and long cold winters. The mean annual temperature is -4.5°C, comprising a mean summer temperature of 11°C and mean winter temperature of -19.5°C. On average the region receives 600 – 750 mm precipitation annually. The area is generally snow free between late May and mid-September.

The properties lie in the Selwyn Mountains (Figures 1, 2 and 4) at elevations ranging between 900 and 2,000 m above sea level (asl). Northwest and northeast trends dominate the generally dendritic drainage pattern. Streams drain southward into the Nadaleen River, a tributary of the Stewart River. The region has been glaciated, although there is abundant outcrop exposure along ridges and stream cutbanks, as well as significant colluvial cover (mainly talus slopes). Glacial till occurs mainly in valley bottoms.

The tree line in the area occurs at about 1,500 m asl. At higher elevations the eco-region is characterized by alpine tundra vegetation, comprising mainly crustose lichens, dwarf willows, mountainous avens, dwarf willow and shrubs. At the lower elevations subalpine open woodland vegetation comprises stunted subalpine fir, occasional black and white spruce, willow, dwarf birch and Labrador tea.

6 EXPLORATION HISTORY

6.1 PRE-2016 EXPLORATION

This section, to pre-2016 work, is taken with minor modifications from the 2016 assessment report titled: “Assessment Report: Geochemical and Remote Sensing Analysis, Geochemical Sampling and Prospecting of the HJ, CL and GY Properties” by Leonard Gal, MSc, PGeo.

There is no record of historical work prior to 2012 conducted on the current claims. However, several companies have explored for base and precious metals in the general area. In 1975, McIntyre Mines Ltd. conducted prospecting and a soil geochemistry survey roughly eight kilometres west of the CL property, followed by a drill program to test for lead-zinc mineralization (Birkland, 1976). In 1977 McIntyre Mines Ltd. also explored for and discovered lead-zinc mineralization roughly four kilometres south of the CL claims (Floyd and Arnold, 1977).

In 1976-1977, a Geological Survey of Canada (GSC) regional stream sediment survey was conducted in the area at an average sample density of one per 13 km² (Hornbrook et al., 1990). The results of this survey

indicated weakly anomalous gold and associated trace elements within or proximal to the Carlincore properties. A second GSC stream sediment survey in 2001 in the area yielded weakly anomalous gold (9 ppb) and arsenic (21 ppm; Heon 2003). These regional stream sediment anomalies were a factor in the initial acquisition of the ground.

The Yukon Geological Survey and the GSC partnered in an aeromagnetic survey over the area in 2006-2007 (Kiss et al., 2008). This survey identified a large magnetic high anomaly centered roughly on the CL property, possibly representing an underlying intrusive body (Kalkowski, 2014).

Recent exploration increased significantly with the discovery of sediment-hosted gold mineralization within the Rackla Belt in east-central Yukon. Work by ATAC Resources Ltd. ("ATAC") during 2006-2009 led to the discovery of the Tiger deposit (Figure 4), with measured and indicated oxide and sulphide resources of 5.68 Mt at 2.66 g/t Au; containing 485,700 ounces of gold (<http://www.atacresources.com/projects/rackla/rau-trend/tiger-deposit>). The Tiger deposit is hosted within Paleozoic carbonates, and located west of Carlincore's properties.

In 2010, ATAC made its initial discoveries along the Nadaleen Trend directly to the south, in the eastern part of the Rackla Belt. Initial regional geochemical sampling was followed up by prospecting, mapping, grid sampling, and drilling which outlined sediment-hosted gold mineralization akin to the Carlin trend gold deposits of Nevada, USA. To date, geochemical anomalies, in particular occurrences of realgar, an arsenic sulphide, consistent with Carlin-style mineralization have been found over a regional strike length of 70 km, indicating a regionally significant system (Bennett, 2016). ATAC exploration has outlined gold occurrences in the Osiris and Anubis clusters (Figures 3 and 4), each less than 10 km from the southern boundary of Carlincore's properties. Drilling in 2013 at the Conrad zone in the Osiris cluster yielded gold values to 4.23 g/t Au over 68.58 m and 5.40 g/t Au over 33.86 m. At the Orion target in the Anubis cluster, 2015 rotary air blast drilling yielded results to 3.97 g/t Au over 47.24m (<http://www.atacresources.com/projects/rackla/nadaleen-trend>).

In 2012, Anthill Resources Ltd. discovered a sediment-hosted gold occurrence (the "Venus" prospect) southeast of the main Nadaleen Trend. This indicates potential for additional exploration targets in favourable rocks outside the Nadaleen trend.

Carlincore acquired their properties in 2012, and, in 2012-2013, conducted stream geochemical sampling and prospecting on the HJ and CL properties. All significant drainages were sampled and prospected, and a number of gold and path-finder element (As, Hg, Sn, Te, Tl) anomalies were outlined (Kalkowski, 2014).

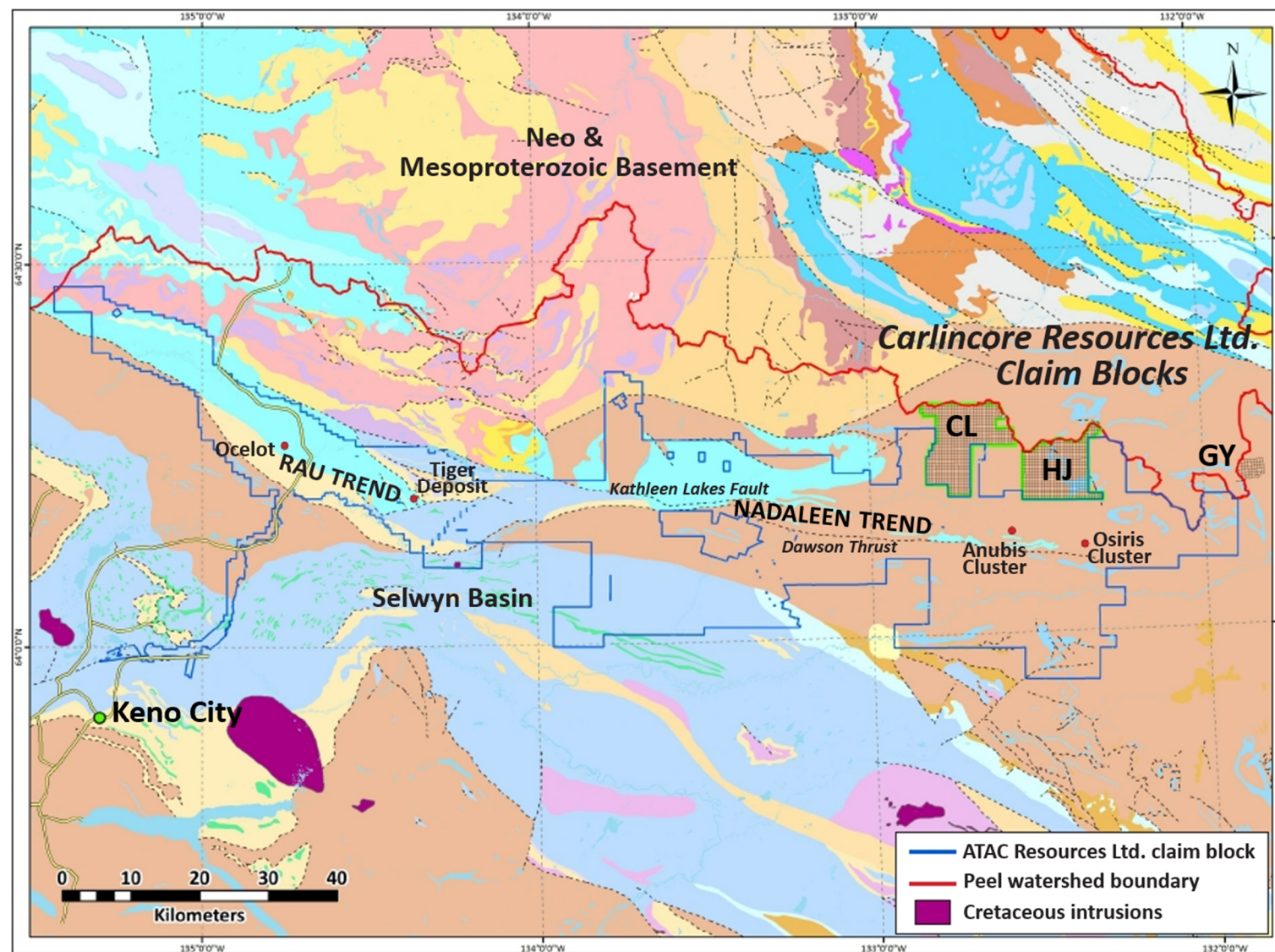


Figure 4: Regional geological setting of CL and HJ properties. Geology from Gordey and Makepeace (1999). Figure modified from Bennett (2016)

The reconnaissance work was followed up in 2014 with soil geochemical surveys, geological mapping and prospecting on the CL and HJ properties (Kalkowski, 2014). Soil sampling identified a number of areas anomalous in gold and trace elements associated with Carlin-type mineralization. Soil geochemical values up to 22.2 ppb Au, 117 ppm As, 1.23 ppm Tl, 5.3 ppm Hg and 6.6 ppm Sb were obtained. Geological mapping identified calcareous lithologies and structural features favourable for hosting Carlin-type gold mineralization. However, no mineralization or alteration was observed at surface. Rock samples yielded up to 20 ppb Au and 129 ppm As. A sample of black shale yielded 0.12% molybdenum and 0.28% zinc (Kalkowski, 2014).

In 2015, Carlincore carried out further sampling on the CL and HJ properties. A total of 157 rock samples were collected from areas outlined by previous anomalous stream sediment and soil geochemistry, and from areas mapped in 2014 indicating favourable stratigraphy and structural settings. Additionally, 1,905 soil samples, including 864 from the CL and 1,198 from the HJ properties, were collected (Mitchell, 2015). No significant mineralization was observed, with rock samples yielding up to 60 ppb Au, 198.5 ppm As, and 801 ppm Cu (Mitchell, 2015).

In preparation for a 2016 field season, geochemical data from 2014-2015 was re-assessed and re-analyzed, and desktop lineament and spectral reflectance studies were done using remote-sensing data. The goal was to find target areas for follow-up exploration. This follow-up work was performed in the summer of 2016, and included prospecting and the collection and analysis of 141 rock and soil samples. Table 1 summarizes the number of geochemical samples collected from 2014-2016.

Table 1. Summary of 2014-2016 sample collections.

Year	Stream Sediment	Rock	Soil	Notes and Reference
2014	0	254	1920	Kalkowski (2014)
2015	0	157	1905	Mitchell (2015)
2016	7	141	*	*coarse textured "C" horizon material prepped and analyzed as rock. Bennett (2016)

6.2 2016 EXPLORATION

6.2.1 Pre-season Desktop Analysis

A review of 2014-2015 geochemical data was completed by Bennett (2016) to target priority areas for follow-up. This included multi-element Pearson correlation analysis, which was carried out on the soil and stream sediments datasets. Results of stream sediment correlation analysis indicate no significant Au-As correlation, with the highest statistically significant correlations occurring between Tl-Mo and Ag-Bi. Pearson correlation analysis of 2014-2015 soils also indicate a poor correlation between Au and As. Significantly, all currently known occurrences of sediment-hosted gold mineralization in Yukon are characterized by highly elevated As in soils (Bennett, 2016). Multi-element correlations in the 2014 soils data include: Tl-Mo and Au-Cu (Table 2). No significant correlations were seen between Au, As or other Carlin-type sediment-hosted pathfinder elements (e.g., Sb, Tl, Hg) (Gal, 2016).

Statistically significant correlations for the 2015 soil dataset included As-Sb and Mo-Tl. Gal (2016) concluded the lack of strong Au-As correlations and low absolute As in soil values suggest that sediment-hosted gold mineralization is either absent, or is at depth. The moderate As-Sb correlation, not indicated in the 2014 data set, is somewhat encouraging, and may be used as a secondary targeting vector for sediment-hosted gold exploration.

Table 2 shows Pearson correlation coefficients (*r* values) for selected elements for 2014 (top figure) and 2015 (bottom figure) soil samples, with some higher correlation pairs highlighted.

Table 2. Pearson correlation coefficients (*r* values) for selected elements for 2014 (top figure) and 2015 (bottom figure) soil samples

	Au	Ag	As	Tl	Hg	Sb	Mo	Bi	Cu	Pb	Zn	W
Au	1	0.13	-0.113	0.015	0.147	0.004	0.001	-0.076	0.419	-0.055	-0.006	0.065
	1	0.161	0.044	-0.007	-0.006	0.086	0.111	-0.123	0.099	0.015	-0.036	0.1
Ag		1	0.374	0.289	0.128	0.213	0.379	0.373	0.206	0.373	0.372	0.001
		1	0.258	0.154	0.084	0.233	0.204	0.323	0.109	0.266	0.303	-0.149
As			1	0.374	0.137	0.334	0.452	0.324	-0.002	0.47	0.214	-0.114
			1	0.092	0.118	0.614	0.221	0.461	0.116	0.357	0.238	-0.05
Tl				1	0.236	0.234	0.613	0.128	0.08	0.183	0.286	-0.052
				1	0.128	0.23	0.511	0.103	0.336	0.122	0.098	0.009
Hg					1	0.488	0.181	-0.042	0.154	0.016	0.12	0.085
					1	0.123	0.084	0.057	0.074	0.132	0.189	-0.061
Sb						1	0.322	0.051	0.073	0.134	0.198	0.27
						1	0.33	0.391	0.198	0.314	0.205	0.06
Mo							1	0.177	0.101	0.077	0.242	-0.045
							1	0.163	0.268	0.131	0.072	0.081
Bi								1	-0.012	0.384	0.117	-0.014
								1	0.377	0.567	0.371	-0.132
Cu									1	-0.014	0.07	0.327
									1	0.424	0.275	-0.085
Pb										1	0.261	-0.162
										1	0.534	-0.124
Zn											1	-0.139
											1	-0.114
W												1
												1

The desktop study showed that, of 281 rock samples collected in 2014-2015; nine returned Au values >20 ppb up to 60 ppb, and only three rocks returned As values >100 ppm, up to 198 ppm.

Pre-season work in 2016 included a detailed lineament analysis conducted by Bennett (2016) over the region encompassing the CL and HJ properties. This identified structural corridors, the most important which appeared to be WNW-oriented system, showing continuity from the CL and HJ claims to ATAC's

Pharaoh sediment-hosted gold occurrence. Several major NNE trending structures were also identified, as well as an abundance of east-trending lineaments (Gal, 2016).

A study of Landsat 8 surface reflectance data was also done by Bennett in 2016. The survey covered the CL, HJ and GY claims and the Osiris and Anubis clusters of ATAC Resources Ltd. The data were processed to produce a false colour Red-Green-Blue (RGB) composite image where specific band ratios corresponded to the different colour channels. This was tested over the well-exposed Osiris zone (ATAC Resources Ltd.), characterized by a prominent NW-trending clay + As alteration + gossan zone.

Areas of significant Fe concentration indicated by the Red channel of the RGB image correlate with a distinct stratigraphic unit in the central part of the CL property. Two locations where As in soil values were >100 ppm are associated with Landsat anomalies and may be related to gossan development along NE-trending faults. The HJ property exhibits considerably fewer zones of elevated Fe, which do not exhibit any strong spatial correlation to anomalous geochemical soil data.

Bennet (2016) integrated geochemical data, bedrock mapping, lineament analysis and the Landsat 8 surface reflectance data to identify 17 target areas, the highest having anomalous As in soil or known faults. These targets were followed up with ground truthing fieldwork in the summer of 2016 (Gal, 2016).

6.3 2016 FIELDWORK

Prospecting and rock, soil and stream sediment sampling were conducted on 11 of 17 target areas on the CL and HJ and GY claims. At the CL and HJ properties, a total of 132 rock grab, rock chip and soil samples (58 on the CL claims and 83 on the HJ claims) were collected in 2016. These include 14 soils re-sampled from pre-existing 2014–2015 pits, and 27 rock chips collected from the base of these pits, for a total of 41 samples. For these, Bennett (2006) compared and plotted original (2014–2015) and re-sampled (2016) results for selected pathfinder elements of interest (Au-As-Sb; Cu-Pb-Zn). This comparison showed poor reproducibility of results, with 2016 sampling returning lower Au values in almost all cases, as well as consistently lower As and Sb values. Bennett suggests that contamination may have occurred in the 2014–2015 datasets. Gal (2016) indicated that year-2016 samples were not analyzed by fire assay, and that different methods of sample preparation may have been employed.

The remaining 103 samples were collected during ground truthing of the target areas. Four samples returned Au values >10 ppb and 10 samples yielded As >100 ppm. The highest Au-in-rock geochemical value was 38 ppb (sample #1173495; Figure 10 (a)) from an ESE-trending brittle fault cutting a limestone debris flow unit in the NE part of the CL property. Soil sampling in this area returned anomalous Sb in soil values up to 18 ppm. Sample #1173471, from an E-trending brittle fault in the NE corner of the CL property, yielded the highest As value, of 2,159 ppm, recorded to date on the CL or HJ properties (Figure 10 (b)). No other significant mineralization was suggested by the 2016 analytical results.

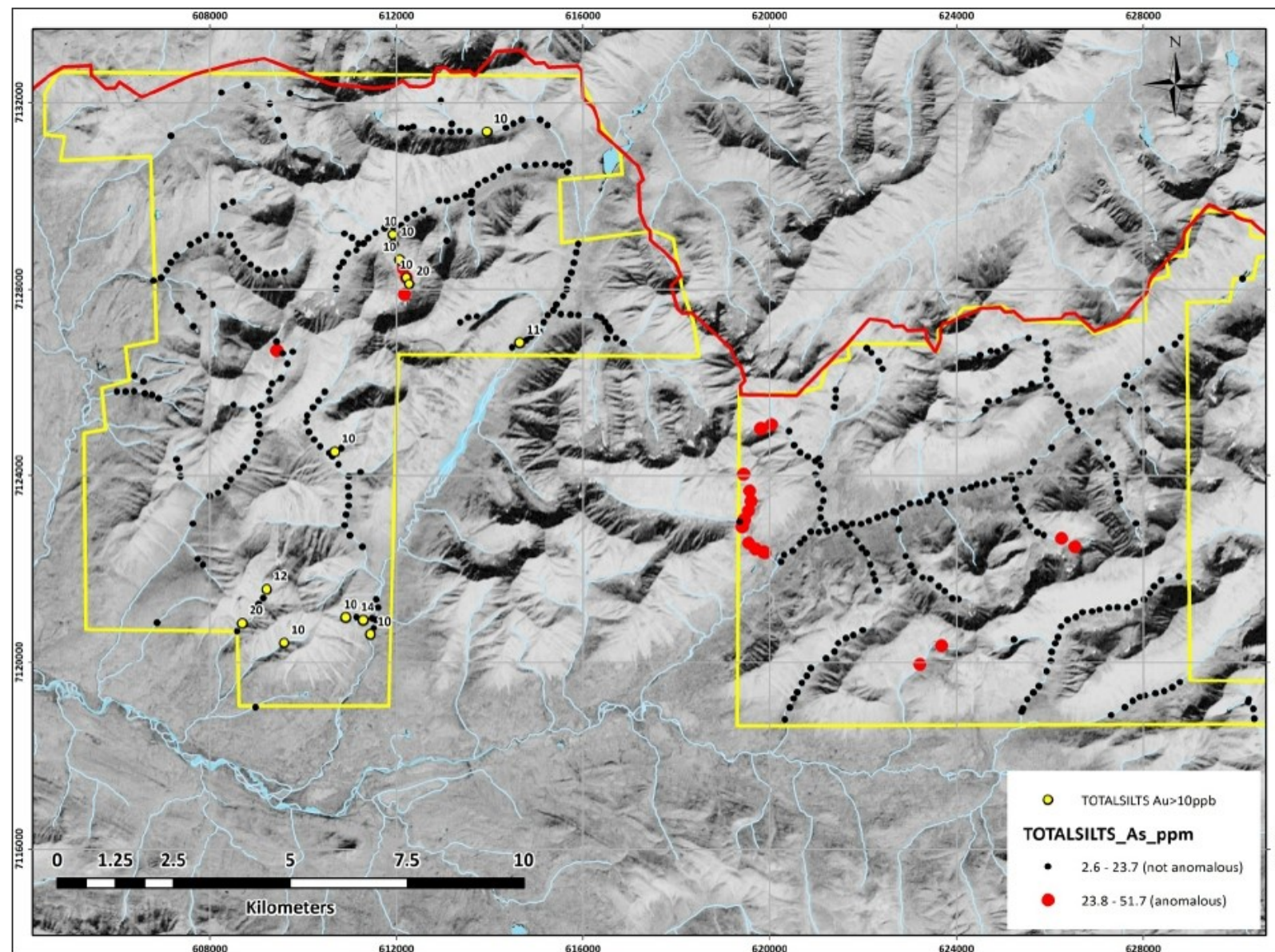


Figure 5: Anomalous Au and As in stream sediments (2012-2015 data) (Bennett, 2016).

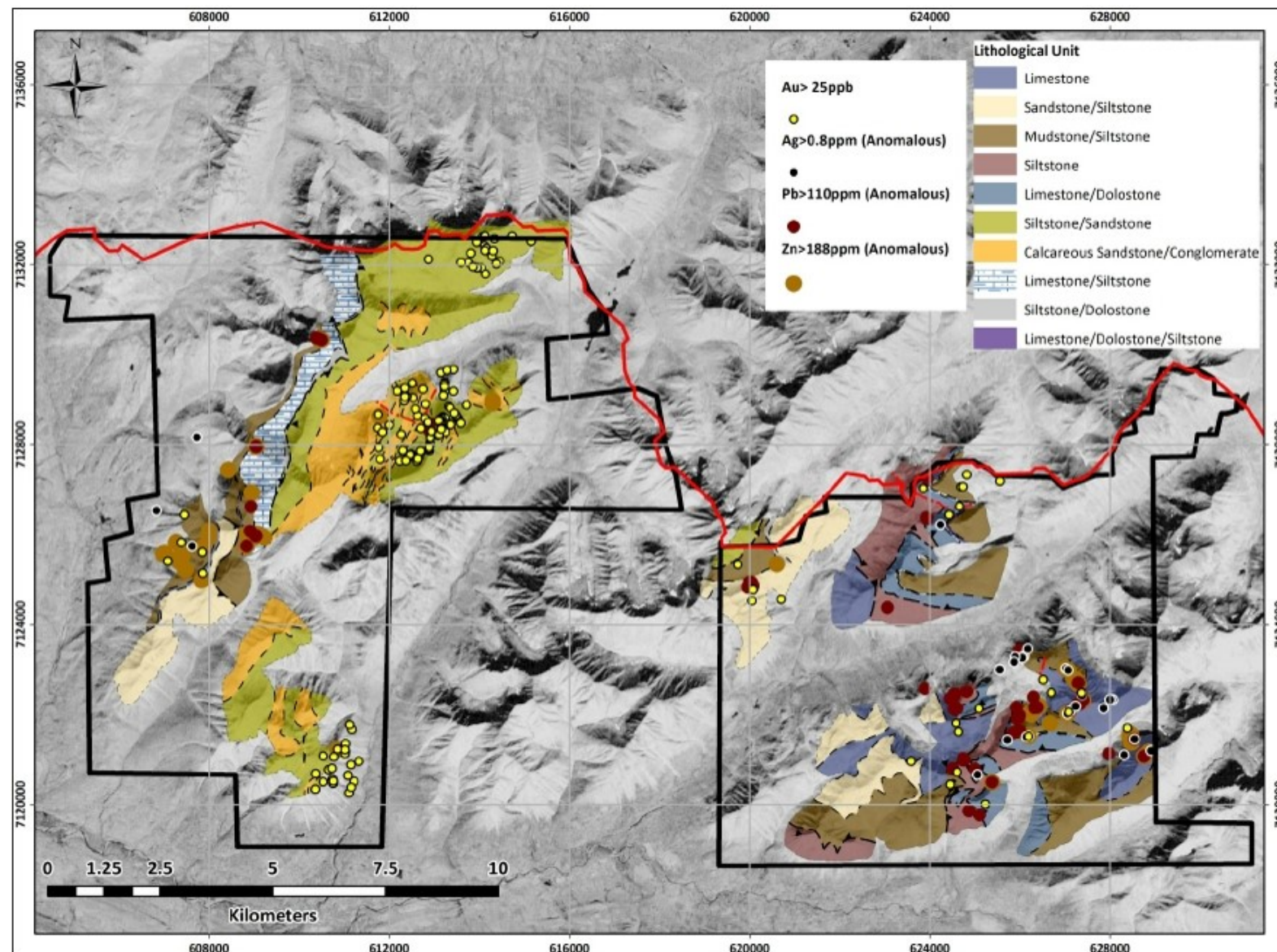


Figure 6: Anomalous Pb, Zn, Ag and Au in soils (2014-2015 data). From Bennett (2016), lithological units from Chakungal (2014).

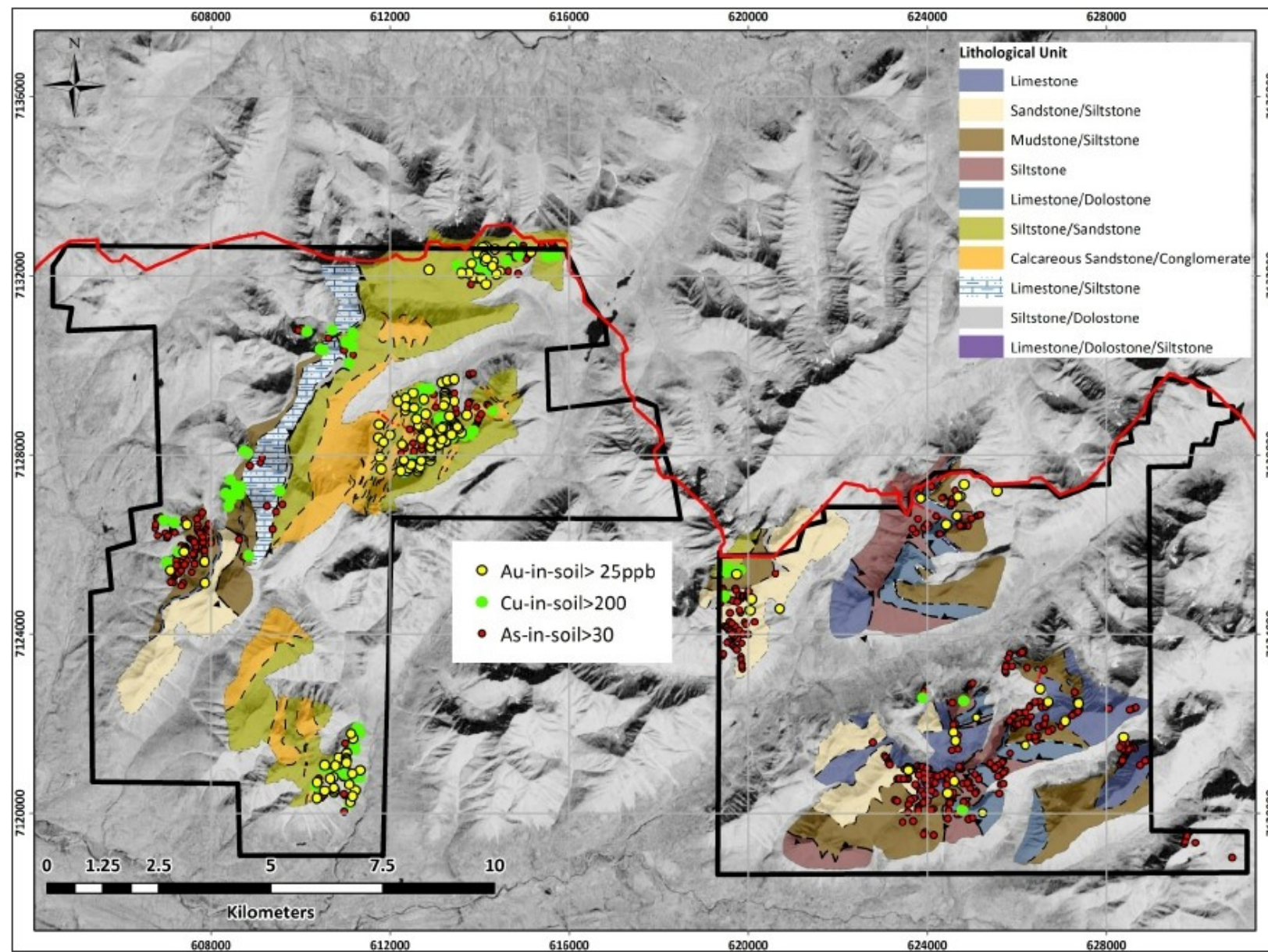


Figure 7: Anomalous Au and Cu values (Bennett, 2016)

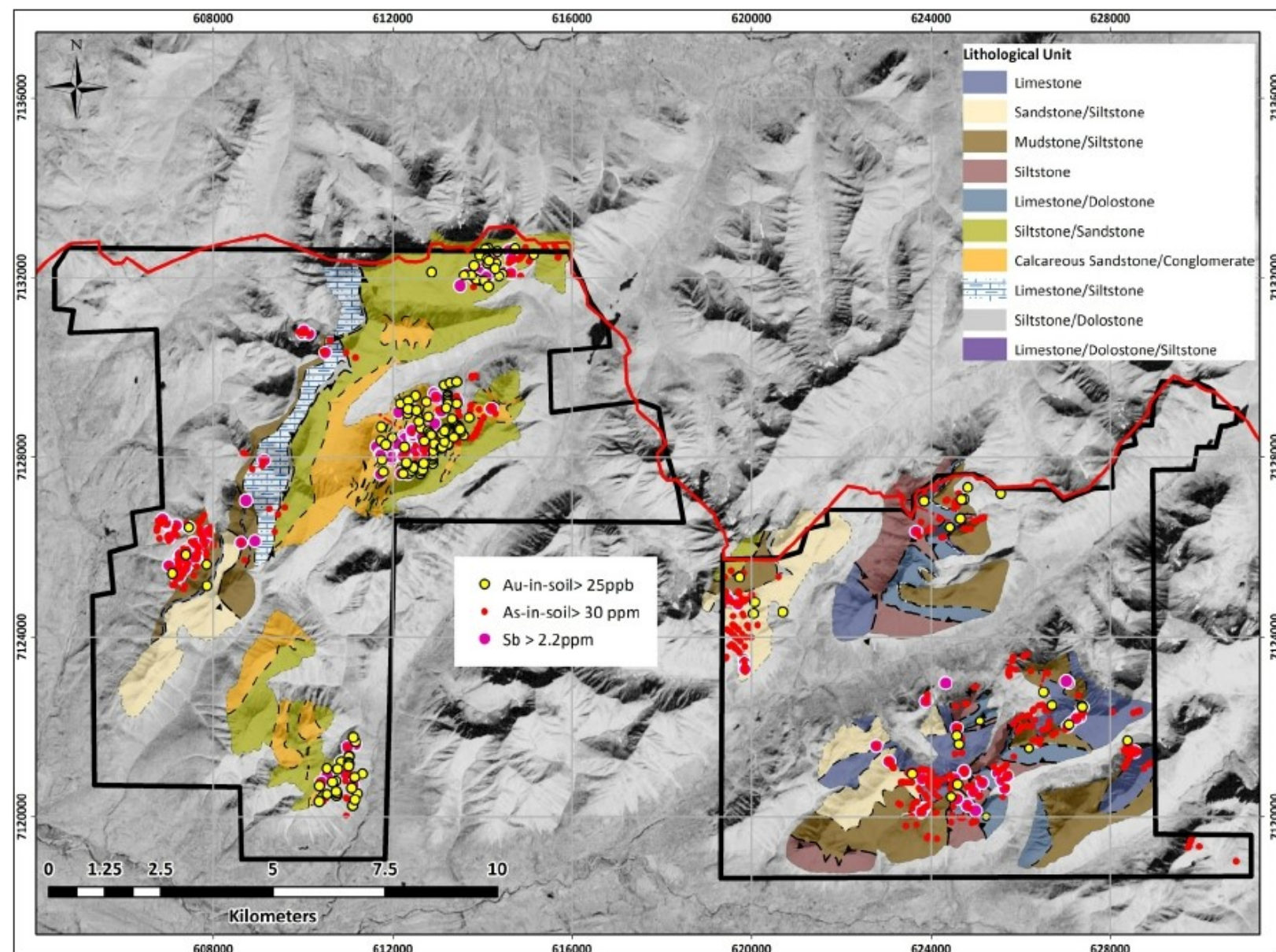


Figure 8: As-Sb and Au-Sb soil anomalies (Bennett, 2016)

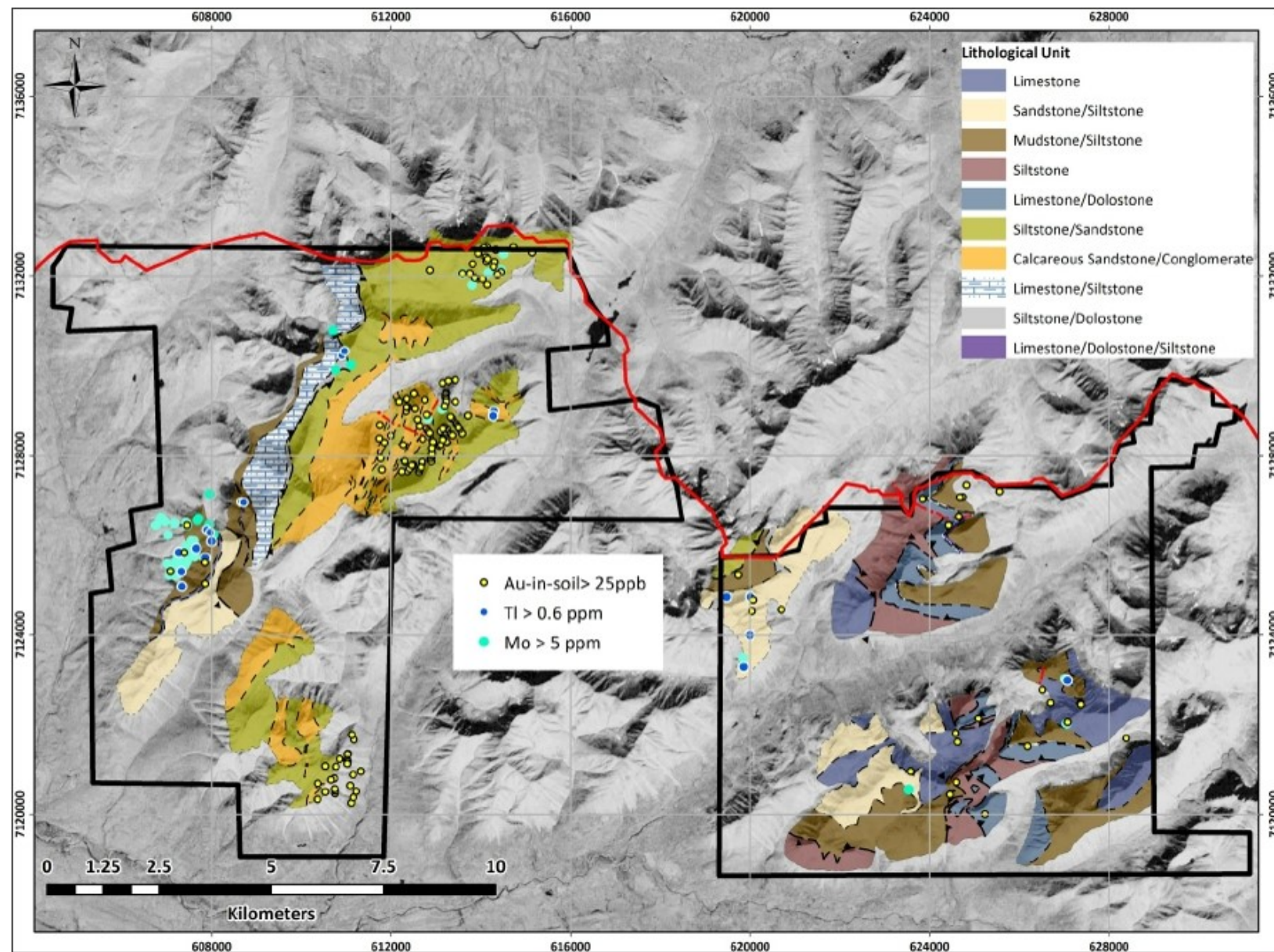


Figure 9: Anomalous Mo-Tl in soil, corresponding to an interbedded black shale and siltstone unit (Bennett, 2016)

The following figure shows the samples with the highest gold and arsenic values respectively from 2016 sampling.



Figure 10: (a) Rock sample with highest Au assay (38 ppb Au). (b) Sample with highest As assay (2,159 ppm As). Photos by Bennett (2016)

7 REGIONAL & PROPERTY GEOLOGY

7.1 REGIONAL GEOLOGY

This section is taken with modifications from the 2016 assessment report titled: "Assessment Report: Geochemical and Remote Sensing Analysis, Geochemical Sampling and Prospecting of the HJ, CL and GY Properties" by Leonard Gal, MSc, PGeo., in turn modified after Bennett (2016), Mitchell (2015) and Kalkowski (2014).

Published bedrock geological maps for the region include: 1:250 000 scale Nash Creek (NTS 106D; Green, 1972) and Nadaleen River (NTS 106C; Blusson, 1974), 1:50 000 scale Mount Westman (NTS 106D/1; Abbott 1990), Mt. Mervyn (NTS 106C/04; Chakungal and Bennett, 2010), and Mt. Ferrel (NTS 106C/3; Colpron 2012). Moynihan (2016) recently compiled the geology of NTS map-sheets: 105N/15, 105N/16, 105O/13, 106B/4, 106C/1, and 106C/2 at a 1:75 000 scale.

The CL and HJ properties are located towards the southern margin of the Meso and Neoproterozoic Windermere Supergroup comprising shelf and slope carbonate and clastic rocks of the Ogilvie Platform (Abbott, 1997, Moynihan, 2015, Moynihan, 2016), formed along the margins of the Ancient North American Continent. The CL and HJ properties are located several kilometres north of the east-west trending regional-scale Dawson Thrust, separating Windermere rocks from Neoproterozoic (approx. 580-560 My) to Lower Cambrian Selwyn Basin, Hyland Group coarse- and fine-grained clastic rocks. The Carlin-style deposits and prospects of the Anubis and Osiris clusters within the Nadaleen trend, held by ATAC, are located within Windermere Supergroup rocks between the CL and HJ properties and the Dawson Thrust (Figure 4).

The Hyland Group rocks, forming the basal sequence of the Selwyn Basin, are interpreted as roughly coinciding with the onset of rifting in the southern Canadian Cordillera (Moynihan et al., 2015). Moynihan demonstrated continuity between the Neoproterozoic to Cambrian Hyland Group succession with that of the Windermere Supergroup of the Yukon Block across the eastern end of the Dawson thrust zone. The Dawson thrust has been interpreted as a Neoproterozoic normal or growth fault, re-activated by Mesozoic compressive forces which played a significant role in focusing mineralizing fluids that formed Nadaleen trend deposits and prospects (Mair et al., 2006; Colpron et al., 2013). Mineralization in the Nadaleen trend is bounded to the south by the Dawson thrust, and to the north by the Kathleen Lakes fault structure (Figure 11). The Kathleen Lakes structure is poorly understood but may be another re-activated Neoproterozoic normal fault. Host rocks to Carlin-style occurrences in the Nadaleen Trend are middle Proterozoic to middle Paleozoic limestones, including rocks thought to be equivalent to Gametrail and Risky formations (Figures 12 and 13).

Figures 12 and 13, showing mapping by Moynihan, 2016, on the CL and HJ properties respectively, are included in this report, partly to include the revised stratigraphic succession as of 2016.

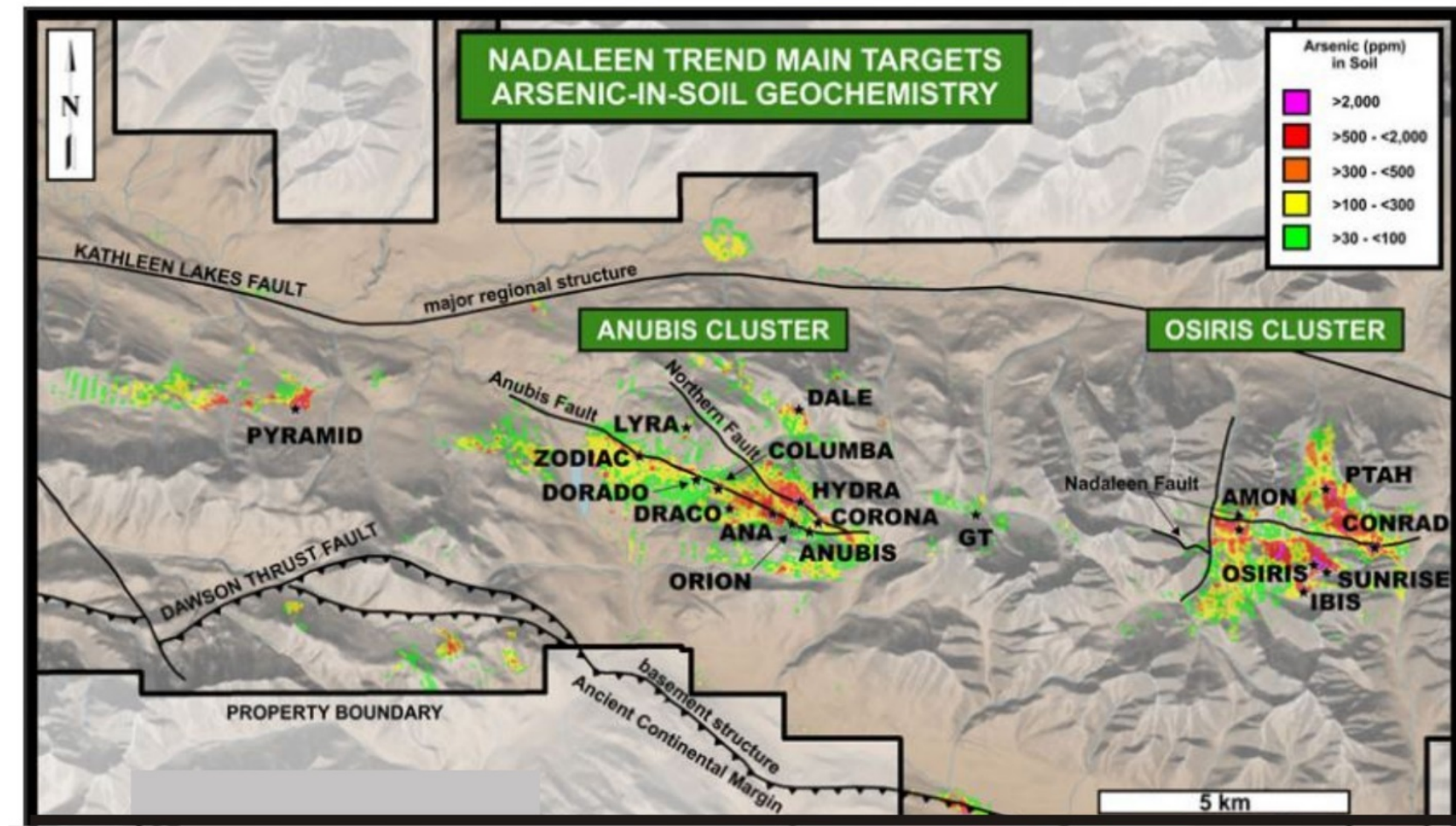
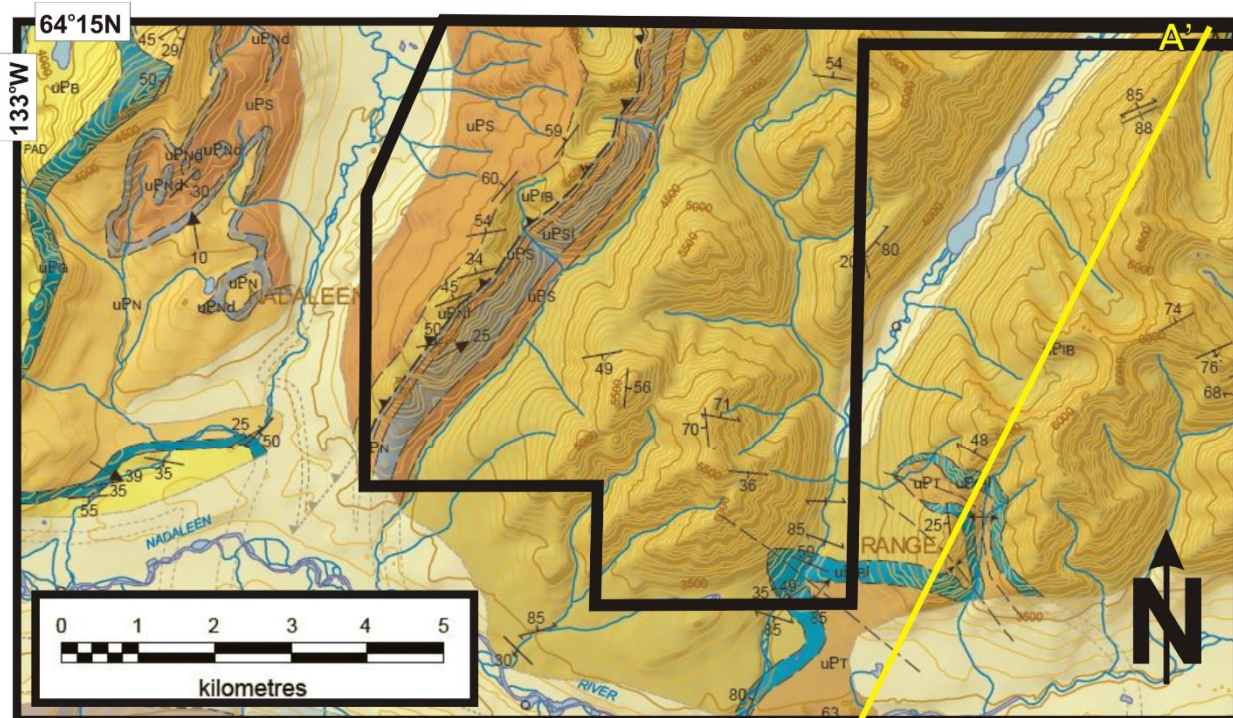
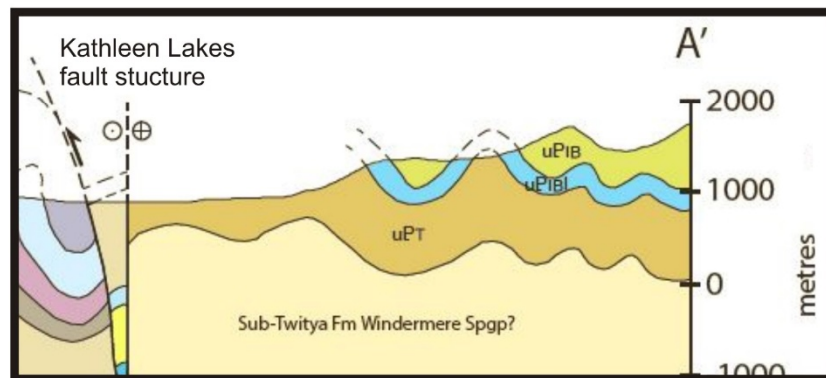


Figure 11: Deposits within ATAC Resources Ltd's Anubis and Osiris clusters, and As-in-soil anomalies. From: <http://www.atacresources.com/projects/rackla/nadaleen-trend>.

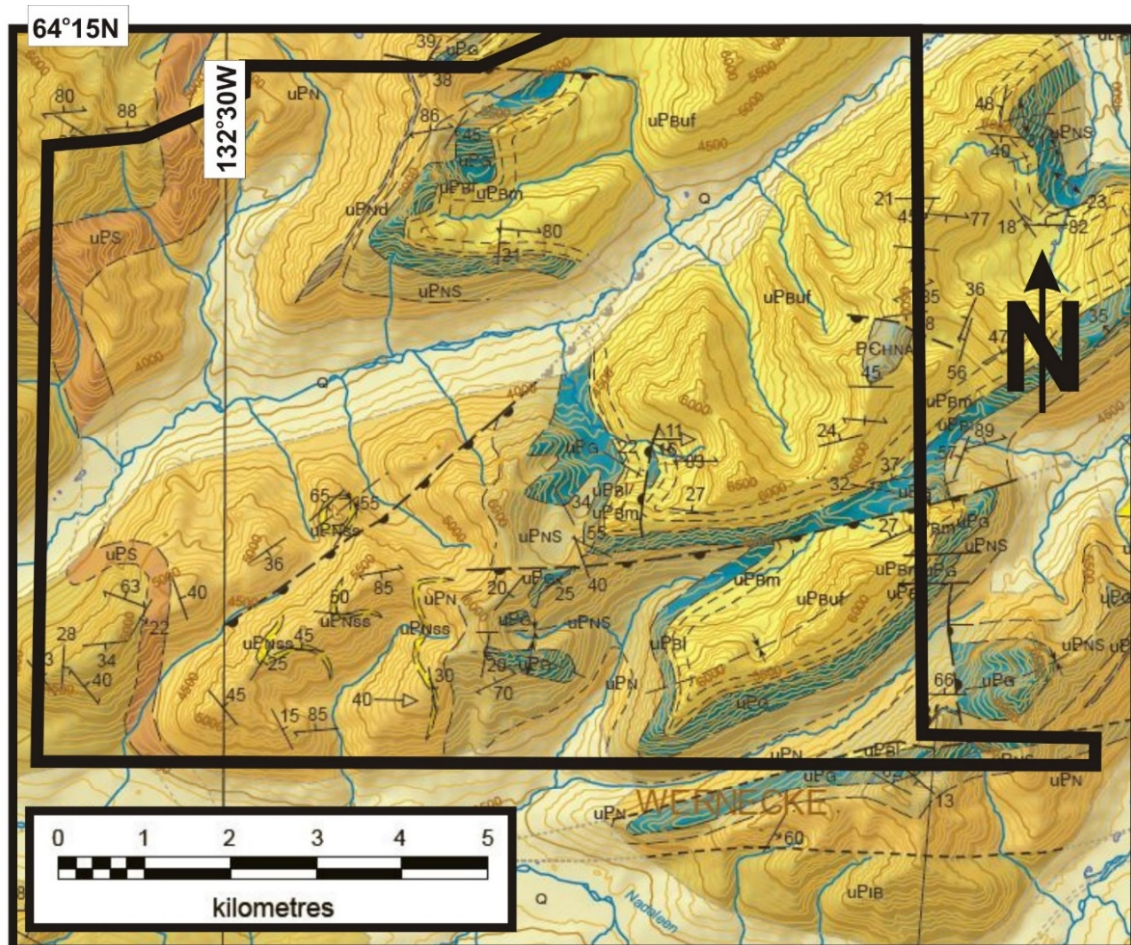
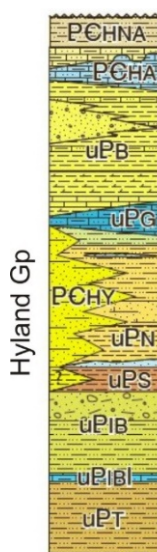
**LEGEND**

PCHNA	Ingta Fm
PCHA	Risky Fm
uPB	Blueflower Fm
uPG	Gametrail Fm
PCHY	Nadaleen fm
uPN	Sheepbed Fm
uPIB	Ice Brook Fm
uPIBI	Twitya Fm
uPT	



Geology, legend, cross section from Moynihan (2016)

Figure 12: Bedrock geology of southern CL property (from Moynihan, 2016).

**LEGEND**

Ingta Fm

Risky Fm

Blueflower Fm

Gametrail Fm

Nadaleen fm

Sheepbed Fm

Ice Brook Fm

Twitya Fm

Geology, and legend from Moynihan (2016)

Figure 13: Bedrock geology of southern HJ property (from Moynihan, 2016).

7.2 PROPERTY GEOLOGY

Although the property geology was mapped in 2016, property geology in this section is based on the 2018 stratigraphic and structural evaluation study by Pyle and Bennett, titled “**Yukon Gold Project East Central Yukon, Canada. Report On the Stratigraphy and Structure of the CL and HJ Claims**”. Details of the 2018 survey results are shown in Section 8. The full Pyle/ Bennett report is attached as Appendix VII.

The CL and HJ claims are underlain by a broad sequence of Windermere Supergroup limestone to dolostone, fine clastic and lesser coarse clastic sediments. The stratigraphic succession, indicating the Ediacaran Windermere Supergroup succession and proposed correlations to the Rackla Belt and the Basal Selwyn Basin successions, is shown in Figure 14 below. The focus of the 2018 program was stratigraphic and structural evaluation of the Neoproterozoic Windermere Supergroup units.

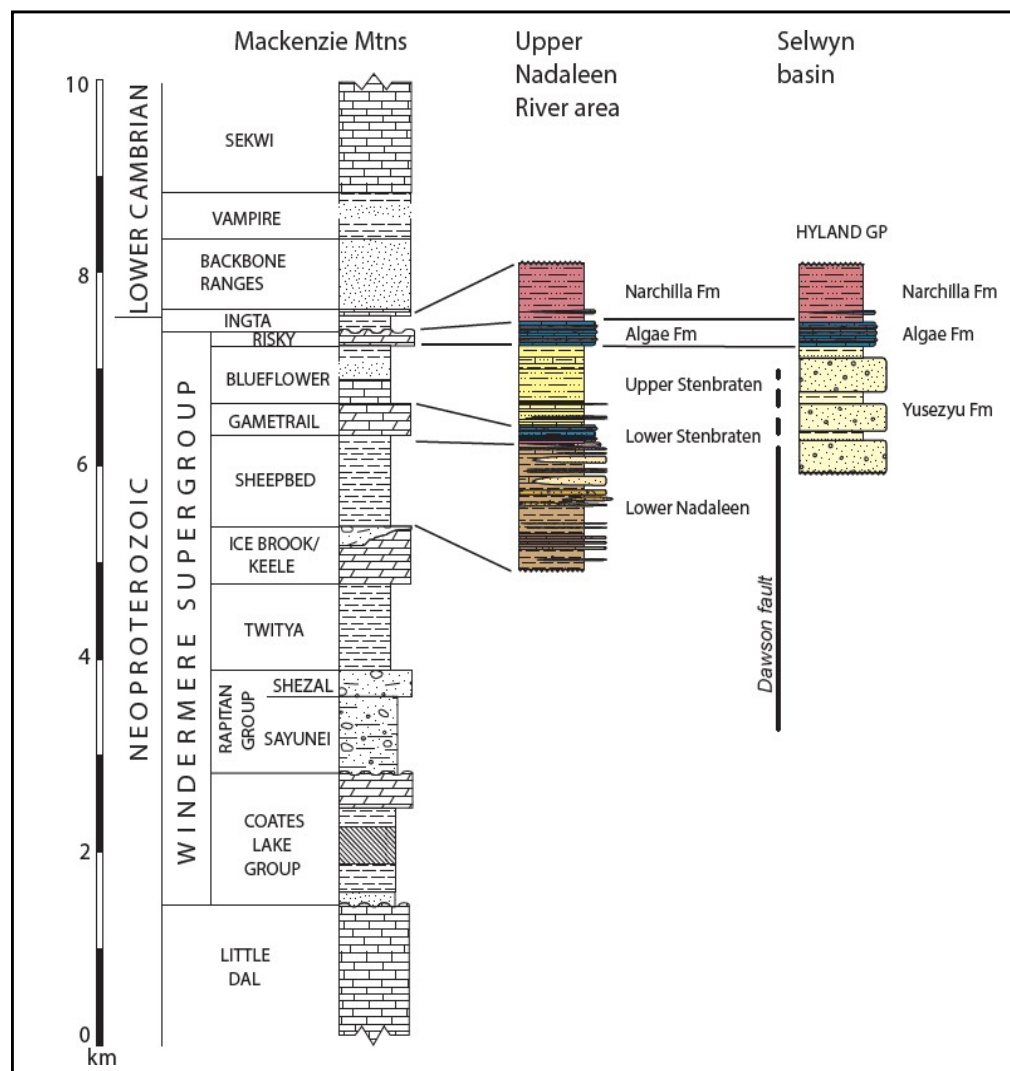


Figure 14: Neoproterozoic Windermere Supergroup stratigraphy (after Narbonne and Aitken, 1995), with proposed correlations to units along the Rackla belt (Colpron, 2013). Figure from Pyle and Bennett, 2018

The CL and HJ claims are located north of the Kathleen Lakes fault. Unlike the Dawson Thrust, which forms the boundary between Windermere Supergroup rocks and Selwyn Basin assemblages to the south, the nature of the Kathleen Lakes fault remains poorly constrained, but likely represents a long-lived basement structure possibly undergoing structural reactivation as recently as the Tertiary period (Pyle and Bennett, 2018).

Pyle and Bennett (2018) have categorized the sediment-hosted gold occurrences held by ATAC Resources as hosted by Neoproterozoic to Cambrian slope facies stratigraphic units of the Windermere Supergroup. Another essential component of this style of sediment-hosted mineralization is the presence of a “fluid corridor” to allow for transport of mineralizing fluids, and a favourable or chemically reactive host for mineral emplacement.

In order to obtain a better understanding of the mineral potential of the CL and HJ claims, a detailed analysis of the local Osiris luster stratigraphy was compiled by Coulter (2017) and Ristorcelli (2018) and included in the 2018 report by Pyle and Bennett (Figure 15). The stratigraphic table in Figure 15 was also used as a comparison of stratigraphic units on the CL and HJ claims to those in the Osiris area.

At the Osiris area, the basal unit is called the NONAD unit, referring to “North of Nadaleen” mudstone, and interpreted as part of the Ice Brook formation (uPIB, Figure 5). This comprises green to maroon and brown mudstone with minor quartz pebble conglomerate (Coulter et al., 2017). The NONAD unit is separated by the overlying upper Nadaleen Formation (uPN) by a north-dipping cataclastic shear zone (NFZ). The basal unit of the Nadaleen Formation comprises the Conrad limestone-1 (C-LST1) consisting of light grey, silty laminated limestone. This unit is overlain by the Conrad Siliciclastic Unit (C-SLC), comprising grey-green pyritic siltstone and mudstone and interbedded sandstone and conglomerate. Much of the auriferous mineralization correlates with the Conrad limestone-1 and lower Conrad Siliciclastic units. The Conrad Siliciclastics are overlain by the Conrad Shale (C-SHL) comprising black, laminated siltstone to shale, also part of the Nadaleen Formation (Coulter et al, 2017). The Conrad Shale is successively overlain by Conrad limestone-2 (C-LST2) comprising black, coarsely crystalline limestone, then by Osiris greenish-grey mudstone (O-MST1), the latter representing the uppermost sequence of the Nadaleen Formation. Overlying this is the Gametrail Formation (uPG), comprising a succession of Osiris limestone-1 (O-LST-1) consisting of well bedded limestone with monolithic rudstone layers, Osiris dolostone (O-DST), a diagenetic dolostone, and Osiris diamictite (O-DMT), a carbonate debris flow (debrite) unit. Most of the remaining auriferous zones at the Osiris cluster are located within the Gametrail Formation, particularly the Osiris limestone-1 units. The Gametrail succession is overlain by the Osiris Limestone (O-LST2) unit of the Blueflower Formation (uPB), and comprising dark grey to black limestone and floatstone (Pyle and Bennett, 2018, after Coulter et al, 2017).

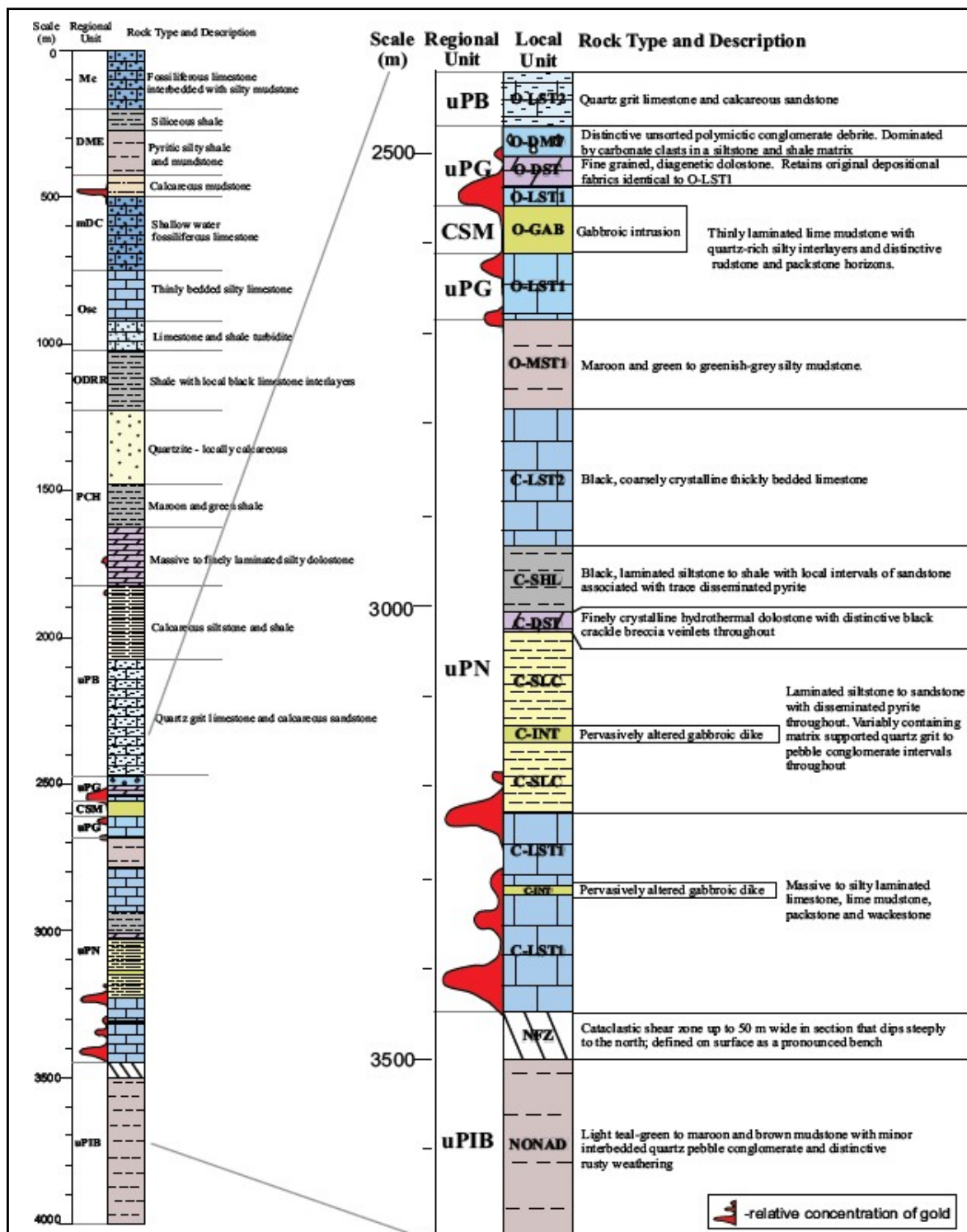


Figure 15: Local and regional stratigraphy and detailed sections of the Osiris cluster local stratigraphic units (Coulter et al., 2017; Ristorcelli et al., 2018)

8 2018 WORK PROGRAM

Pyle and Bennett, through Aurora Geosciences Ltd. selected two subareas of the CL and HJ properties for an evaluation of their stratigraphic / structural setting to facilitate assessment of mineral potential. The program targeted four stratigraphic successions and comprised three transects: two, the Area 1 NW and Area 1 SE transects in the southeastern part of CL claims (Area 1); and one, Area 2 NW, within the northwest corner of the HJ claims. The fieldwork, focusing on stratigraphic sections exposed along ridges and outcrop exposure in gullies, was done from July 22 to July 30, 2018. Stratigraphic observations were designed to:

- 1) Examine the lithostratigraphic framework/succession of units and estimate thicknesses;
- 2) Describe vertical and lateral stratigraphic relationships, unit compositions, grain characteristics, bedding and sedimentary structures, and;
- 3) Collect a suite of geochemical samples from representative lithologies from each section (n=45) and carbonate samples through the Ediacaran part of the upper Windermere Supergroup succession for potential carbon isotopic record analysis (n=19) (Pyle and Bennett, 2018).

The full Pyle and Bennett report (Appendix VII) includes a summary of stratigraphic results for each of the four successions covered in the three transects: Northwest (NW) part of Area 2, Southeast (SE) part of Area 1, SE2 part of Area 1, and NW part of Area 1. This is followed by a comparison of the interpreted stratigraphic setting with that of the Osiris area of the ATAC properties, and a summary of the structural settings of the two study areas.

Pyle and Bennett also collected 44 rock samples from the three transect areas to better define geochemical trends within basinal environments, and determine which basins may have distinctly different or similar geochemical settings. A total of 59 samples were listed as submitted in 2018, although only 44 rock samples were received. These comprise 16 from Area 2, 8 from Area 1 SE and 20 from Area 1 NW.

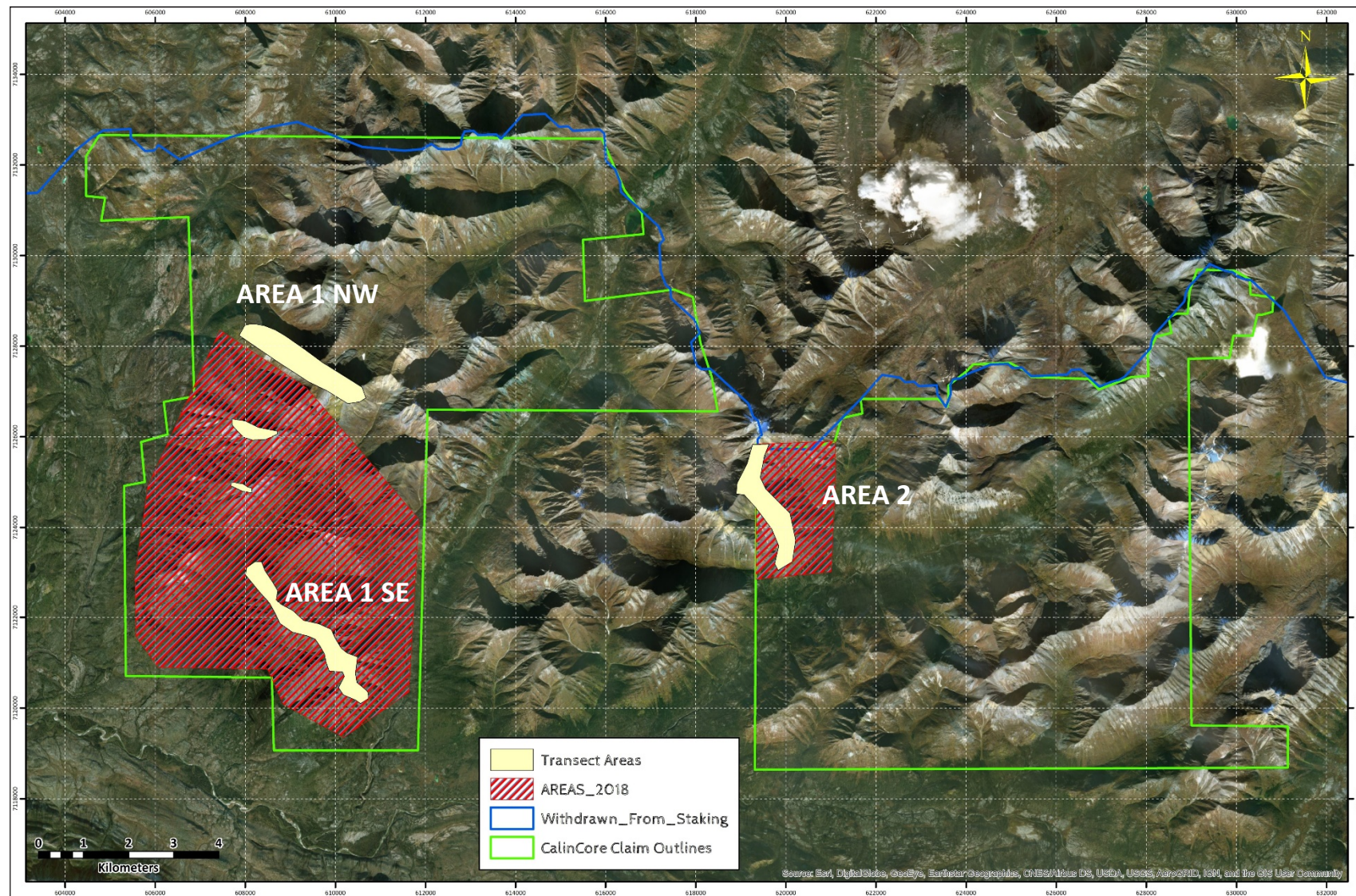


Figure 16: Location of transects, CL and HJ blocks (Pyle and Bennett, 2018)

8.1 NORTHWEST (NW) PART OF AREA 2 (HJ BLOCK)

This section is taken verbatim with minor edits from the report titled: “**Yukon Gold Project East Central Yukon, Canada, Report On the Stratigraphy and Structure of the CL and HJ Claims**” by Pyle and Bennett, 2018. The full report is included as Appendix VII.

A ridge section, about 220 m to 330 m thick, contains a heterolithic package of mudrock (shale, mudstone and siltstone), sandstone, and conglomeratic sandstone with rare cm-scale to dm- scale dolostone beds (about 5 m total carbonate or 0.02% of the total section). The siliciclastic succession contains thin-bedded to thick-bedded, fine-grained to coarse-grained sandstone with poorly sorted quartz pebbles and granules, that alternate with fine-grained packages.

Fine-grained units contain graded beds of fine sandstone with conglomeratic lenses or beds of quartz pebble-rich sandstone with scoured bed bases that grade into laminations of mudstone and siltstone. Stratigraphy at this locality remains poorly understood and requires further work to determine age and stratigraphic position.

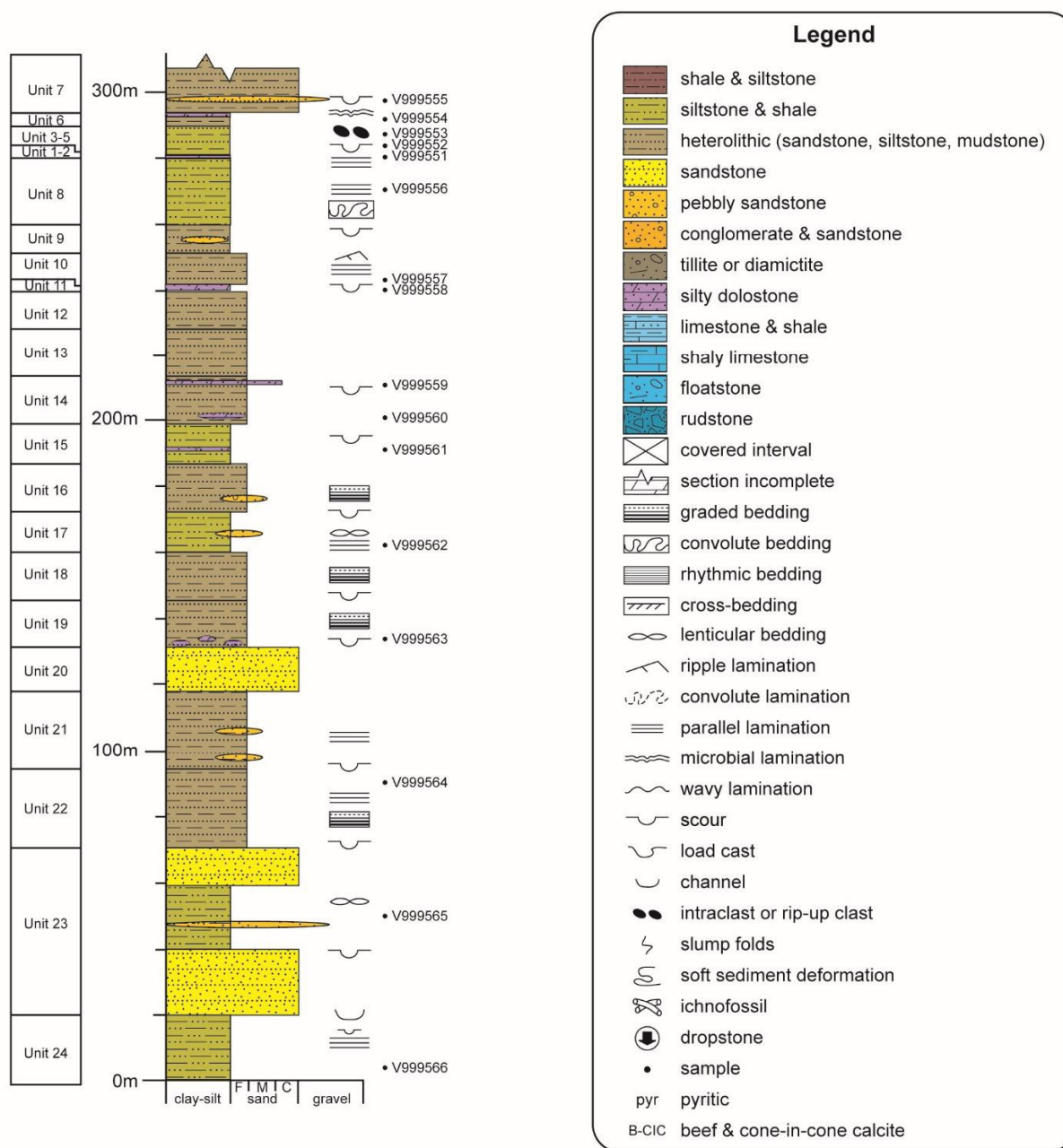


Figure 17: Stratigraphic log of the section in the northwest part of Area 2

8.2 SOUTHEAST (SE) PART OF AREA 1 (CL BLOCK)

Section 8.2 is taken verbatim with minor edits from the report titled: “**Yukon Gold Project East Central Yukon, Canada, Report on the Stratigraphy and Structure of the CL and HJ Claims**” by Pyle and Bennett, 2018”. The full report is included as Appendix VII.

8.2.1 *Southeast (SE) part of Area 1 (CL block)*

This ridgeline traverse, including partially vegetation-covered “rubble-crop”, exposes about 250 m to 350 m of 100% heterolithic siliciclastics. Lithologies range from mudrock to sandstone, and pebble to boulder conglomerate interbedded with tillite containing dropstones. The reddish-brown or maroon weathering mudrock facies contains innumerable layers of olive green or brown mudstone and siltstone, with minor fine-grained sandstone in thin beds. Laminae and beds are planar and commonly contorted due to soft sediment deformation. Dropstones, which range in size from pebbles to boulders, made impact depressions within the encasing mudstone layers that were squeezed around the dropstone. Thick beds of polymictic conglomerate with erosive bed bases are interbedded with the mudstone.

Stratigraphy along this transect is interpreted to represent part of the Rapitan Group (lower Windermere Supergroup).

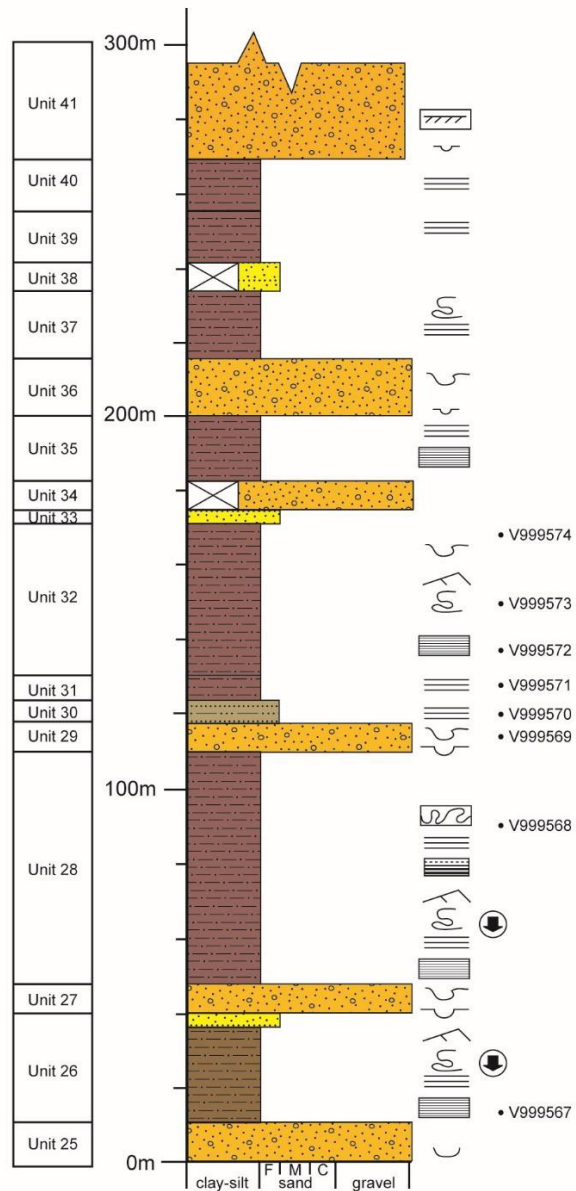


Figure 18: Stratigraphic log of the section in the SE part of Area 1 (Pyle and Bennett, 2018)

8.2.2 Southeast 2 (SE2) part of Area 1 (CL Block)

A second 100% heterolithic siliciclastic succession, estimated to be 150 m to 200 m thick, is exposed within a gully to ridge to partially vegetation-covered “rubble-crop” traverse. It is a heterolithic package with facies similar to those in the southeast part of Area 1. The section begins in a tillite unit containing boulder-sized dropstones. Red-brown weathering mudstone units commonly exhibit convolute lamination and soft sediment deformation. Conglomerate units occur in basal areas and near the top of the section.

Stratigraphy is interpreted to represent part of the Rapitan Group (lower Windermere Supergroup) and possibly the overlying Ice Brook/Keele Formation.

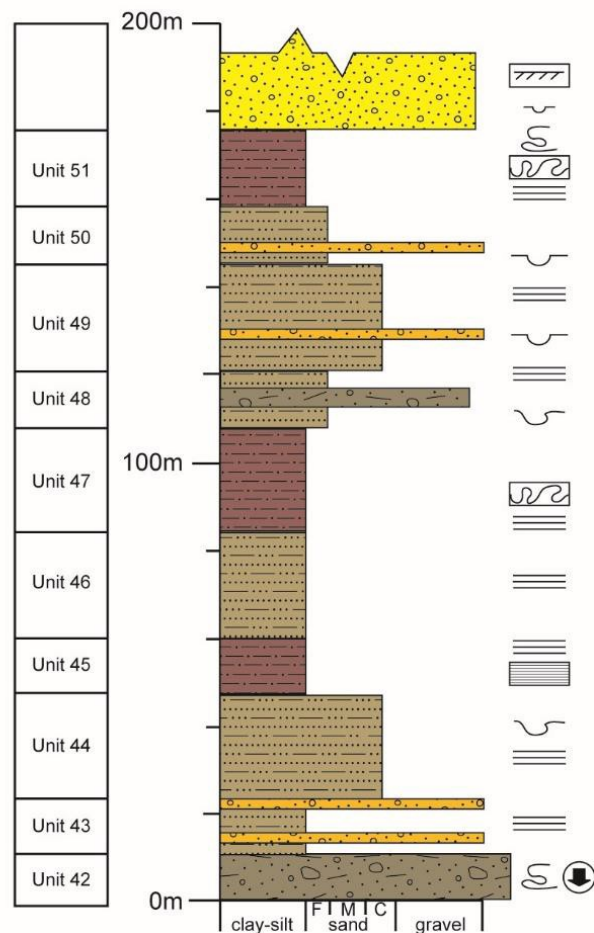


Figure 19: Stratigraphic log of the section in the SE2 part of Area 1.

8.2.3 Northwest (NW) part of Area 1 (CL Block)

This comprises a composite of three ridge sections, 1,300 m to 1,400 m thick, containing about 20% carbonate and 80% heterolithic siliciclastics. The oldest part of the succession is exposed on the face of a structurally complicated ridge, overlain unconformably by about 400 m of a yellowish-brown to grey weathering, upward-coarsening package of thin bedded siltstone and medium to thick bedded, cross-bedded sandstone and conglomerate. The oldest part of the succession contains a mixed package of maroon weathering mudrock and olive green tillite. The overlying siliciclastic succession contains channelized conglomerate beds that are predominant in the upper part of the unit.

A distinct dark yellowish orange weathering, finely laminated dolostone unit (less than 5 m thick) gradationally overlies the siliciclastic succession and is a prominent marker bed. The dolostone is abruptly overlain by a carbonate-dominated unit that is at least 340 m thick and contains black shale and siltstone at the base and top of the unit. This unit consists mainly of wavy, thin bedded, shaly limestone to limemudstone cycles with intervals of erosive-based and slump-folded, medium to thick bedded floatstone. The floatstone intervals contain angular clasts up to pebble-size that weather a variety of colours and resemble confetti within the light grey limemudstone matrix. A second prominent marker bed is a medium bedded to massive rudstone and limemudstone succession, at least 50 m thick, that contains matrix-supported intraformational, cobble sized intraclasts in beds with erosive bases interbedded with thin bedded dololimemudstone. A heterolithic siliciclastic succession, at least 200 m thick, overlies the marker carbonate. It is dominated by dark grey and brown weathering, thin bedded siltstone, mudstone, fine-grained sandstone, and minor conglomerate. A complimentary section to the south exposes at least 200 m of this uppermost unit and contains a 5 m thick interval of dolomitic rudstone.

This section is interpreted to contain seven formations of the Windermere Supergroup. The basal tillite and mudrock is likely part of the Rapitan Group, in turn part of the lower Windermere Supergroup. It is abruptly overlain by mixed siliciclastics of the Ice Brook/Keele Formation, which grades upward into the distinct dark yellowish orange weathering dolostone comprising the Ravensthorpe Formation carbonate cap. The mixed fine siliciclastics and limemudstone succession is equivalent to the Sheepbed Formation, which thickens upward to the light grey marker bed of carbonate debrites equivalent to the Gametrail Formation. The upper recessive part of the succession is equivalent to the Blueflower Formation, which may contain an upper carbonate unit. The upper rudstone may be equivalent to the Risky Formation.

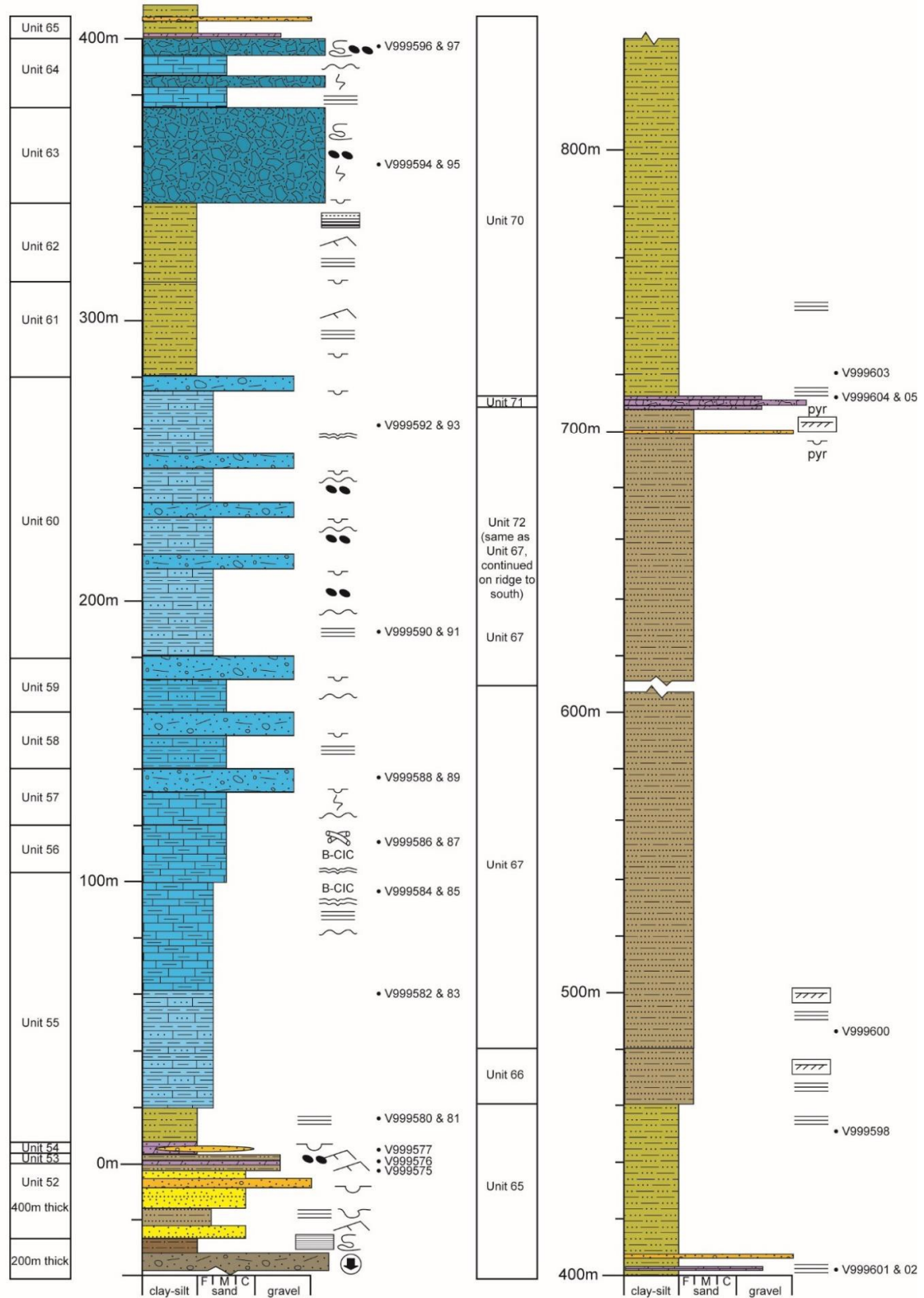


Figure 20: Composite stratigraphic log of the sections in the northwest part of Area 1.

9 Sampling Methodology, Analysis and Security

9.1 ROCK SAMPLES

Rock grab samples were collected in the field utilizing Geotool rock hammers, and placed in a poly bag with a tag containing a unique Sample ID number, and the same sample number written on the outside of the bag. Sample locations were marked in the field utilizing flagging tape with the sample number written on the tape. All samples were identified using the following criteria: Sample ID, Easting (NAD 83, Zone 8), Northing (NAD 83, Zone 8), lithology, transect area, and detailed description of each sample.

Individual samples were sealed with a cable tie, then placed into a rice bag with the sample sequence written on it, and also sealed with a cable tie. Sealed rice bags were delivered by Pyle and Bennett directly to the Aurora Geosciences Ltd. compound in Whitehorse, then Aurora personnel transported them directly to the Whitehorse prep lab of ALS Canada Ltd.

At the prep lab, all samples were crushed so that 70% could pass through a 2 mm screen (prep code CRU-21). The samples were then split utilizing a riffle splitter (prep code SPL-21). The split then underwent pulverization so that 85% of the sample was <75 µm.

The pulps were then sent to the North Vancouver lab of ALS Canada Ltd. for 48-element four acid “Inductively coupled plasma mass spectrometry” (ICP-MS) analysis utilizing a 0.5-gram portion of the pulp. The ICP-MS analysis tested for abundances for Ag, Al, As, Ba, Be, Bi, Ca, Cd, Ce, Co, Cr, Cs, Cu, Fe, Ga, Ge, Hf, In, K, La, Li, Mg, Mn, Mo, Nb, Ni, P, Pb, Rb, S, Sb, Sc, Sn, Sr, Ta, Te, Th, Ti, Tl, U, V, W, Y, Zn, Zr. No fire assay analysis was done for Au.

9.2 CARBON ISOTOPE CHEMOSTRATIGRAPHY

Carbonate samples were slabbed, and then microdrilled with a Dremel drill press (1 mm diameter). The most finely grained fabrics were targeted, and late stage carbonate units and veins were avoided. Carbonate powders (~500 micrograms) were analyzed using a Sercon 20-22 continuous flow mass spectrometer at the University of Victoria. Samples were weighed into individual borosilicate vials. Next, vial head space was flushed with He gas to remove atmosphere, and samples were reacted with 100% phosphoric acid at 85°C. Reaction time was 40 minutes. Precision of $\delta^{13}\text{C}$ is 0.15 permil (1 S.D.), based on measurements of the internal laboratory monitoring standard (Pyle and Bennett, after Dr. J. Husson, University of Victoria, personal communication, 2018).

10 Discussion: Structural Evolution of the CL and HJ Claims

This section is based with minor edits from the report titled: “**Yukon Gold Project East Central Yukon, Canada, Report on the Stratigraphy and Structure of the CL and HJ Claims**” by Pyle and Bennett, 2018. The full report is included as Appendix VII.

10.1 OVERVIEW

The CL and HJ properties are located north of both the regional-scale Dawson thrust and Kathleen Lakes fault (Figure 4). Both fault structures are key controls for mobilizing fluids from depth, and for localizing mineralization in the vicinity of the Osiris and Anubis clusters, held by ATAC, and the Venus occurrence, held by Anthill Resources (Yukon) Ltd.

Favourable mineralizing structures associated with gold deposition within the Rackla belt area include low-angle SW- and W-vergent thrust faults, high-angle NNE-trending strike-slip and dip-slip faults and ESE-trending high-angle strike slip faults. The overall structural setting associated with sediment-hosted gold mineralization consists of a transpressional deformation regime with larger gold accumulations occurring in ENE plunging fold hinges.

The dominant structural grain varies from NNE to NE within Area 1 to predominantly E and ESE within Area 2. No major shear zones or thrust faults were observed within the transect areas. The most prevalent structures present in all transect areas are late brittle N, NE-ENE and NW fault systems which are associated with localized folding. No mineralization was observed in any of the structures examined within the claim blocks in 2018.

Drone imagery was flown over the three main transects to better understand the structural setting in each of the areas reviewed. High resolution orthophotos (5 – 10 cm spatial resolution), digital elevation models (10 – 20 cm) and a suite of hillshade models were generated for each area and used in final map interpretations. An outline of drone data acquisition and data products is provided in Appendix 2 of the attached Pyle and Bennett report.

10.2 AREA 2 TRANSECT (HJ BLOCK)

The mapping transect can broadly be divided into the three structural domains (Figure 21):

- i) A northern domain (structural domain 1) characterized by north trending structural grain which is oblique to the dominant trend of stratigraphy in the area (off claims).
- ii) A domain (structural domain 2) of folding characterized by steep NW trending fold axes and constrained within a single map unit. This domain is bounded to the NW and SE by ENE trending fault zones (Figure 21).
- iii) Structural domain 3 represents the majority of the mapping transect and is characterized by NE and ENE brittle faults and associated localized folding (Figure 21). Stereonet analysis of bedding within this domain indicate the presence of shallow to moderately ENE plunging folds.

The NW-trending tight folding occurring in structural domain 2 is interpreted to predate the ENE open fault-related folding in structural domain 3 which is the oldest deformation event observed in Area 2.

No mineralization was observed within any of the three structural domains.

A 1:2500 scale structural/stratigraphic map interpretation is presented in Figure 46 of the full report in the Appendix VII. The stratigraphy within the area is poorly understood. No major marker horizons are present, and no analytical data is available to help identify possible stratigraphic positions. Stratigraphic units as outlined in Section 8.1 have been simplified into five map units (Figure 46 of Appendix VII). Stratigraphy containing carbonate lenses are shown as separate map units. Carbonates are more prospective host rocks than siliciclastics in the majority of sediment-hosted gold deposits. Other map unit subdivisions are based on the dominance of siltstone and shale over coarser siliciclastics and vice versa.

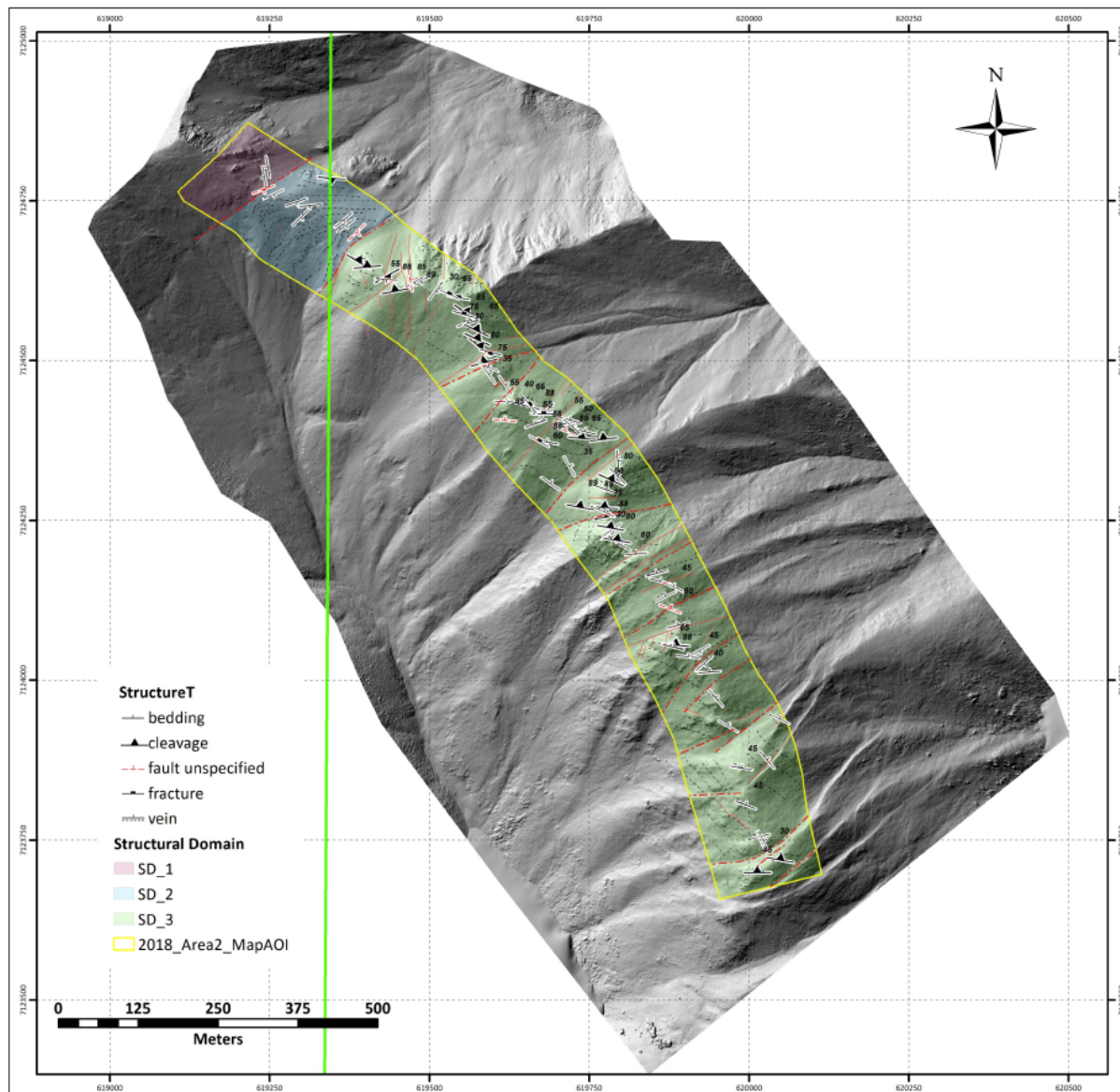


Figure 21: Interpreted structural domains for Area 2 transect, superimposed on hillshade model (Pyle and Bennett, 2018)

10.3 AREA 1 SE TRANSECT (CL BLOCK)

Two structural domains are present within the transect area (Fig. 48 in Appendix VII):

- i) Structural domain 1 consists of predominantly NNE striking and west dipping stratigraphy overprinted by NE – ENE late brittle faults. Similar to Area 2, this late generation of faulting is characterized by decimetre-scale ENE-plunging open folding.
- ii) Structural domain 2 is characterized by NNE striking and east dipping stratigraphy. A synclinal hinge is interpreted to exist between the two domains. Stereonet analysis of bedding in this transect indicates the syncline is a shallow, SSW plunging fold structure (Figure 49 in Appendix VII).

Folding within structural domain 2 is interpreted as an early generation (F1) fold and is overprinted by N, NE and NW-trending brittle faulting. These have commonly localized F2 folding in close proximity to these faults. Late brittle NE and NW fault are often associated with significant oxidation (limonite- carbonate alteration) in brecciated faults zones. No significant gold values were returned, and no other mineralization was observed in this transect area.

A 1:3000 scale structural/stratigraphic map interpretation is presented in Fig. 51 of the attached report. The stratigraphy is interpreted to belong to the Rapitan Group and the Ice Brook/ Keele Formations.

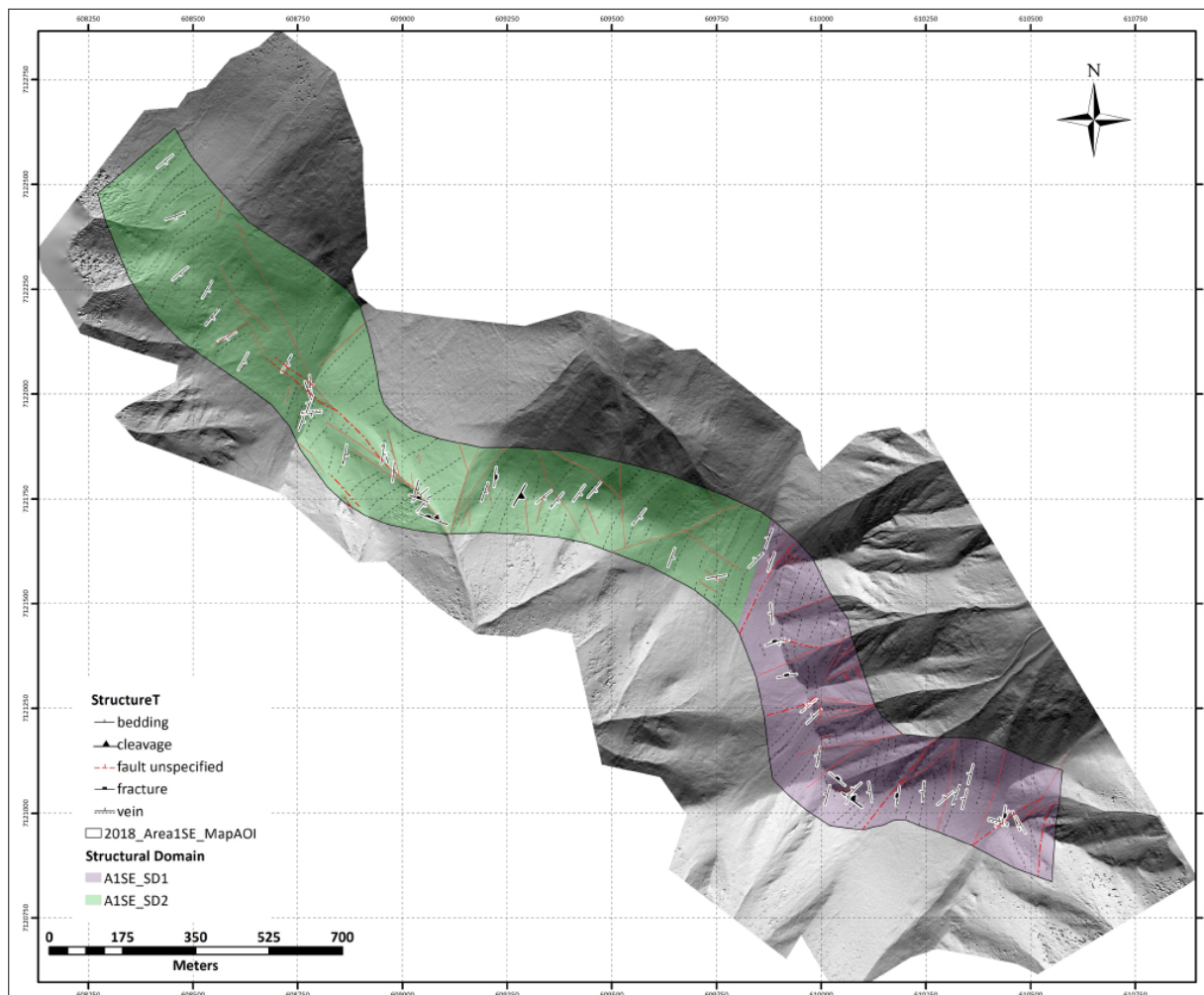


Figure 22: Interpreted structural domains for Area 1SE transect (Pyle and Bennett, 2018)

10.4 AREA 1 NW TRANSECT (CL CLAIMS)

Reconnaissance work was carried out only within the eastern third of the mapping transect. This area was not subdivided into structural domains. The dominant structural grain is NNE-trending and west-dipping. The transect represents a reasonably structurally intact stratigraphic sequence, younging to the west. No thrust faults were observed.

Bedding reversals occur in association with a series of N, NE-ENE and NW brittle faults. A major NNW trending structure occurs approximately midway through the transect (Figure 23). The NW and NE- ENE faults are not observed to offset the NNW faults and are interpreted as either coeval with the NNW faults (potential Riedel shear geometry?) or predating them. No mineralization was observed within any late brittle structures.

The late brittle NE faults are associated with localized open ENE trending folding similar to Area 2 and Area 1 SE, suggesting the presence of a regional deformation event. No mineralization was observed associated with this generation of folding.

A 1:5,000 scale structural/stratigraphic map interpretation is presented in Fig. 55 of Appendix VII. The stratigraphy represents six groups/formations of the Windermere Supergroup: the Rapitan Group, Ice Brook/Keele Formation, Ravenstthroat Formation, Sheepbed Formation, Gametrail Formation and the Blueflower Formation.

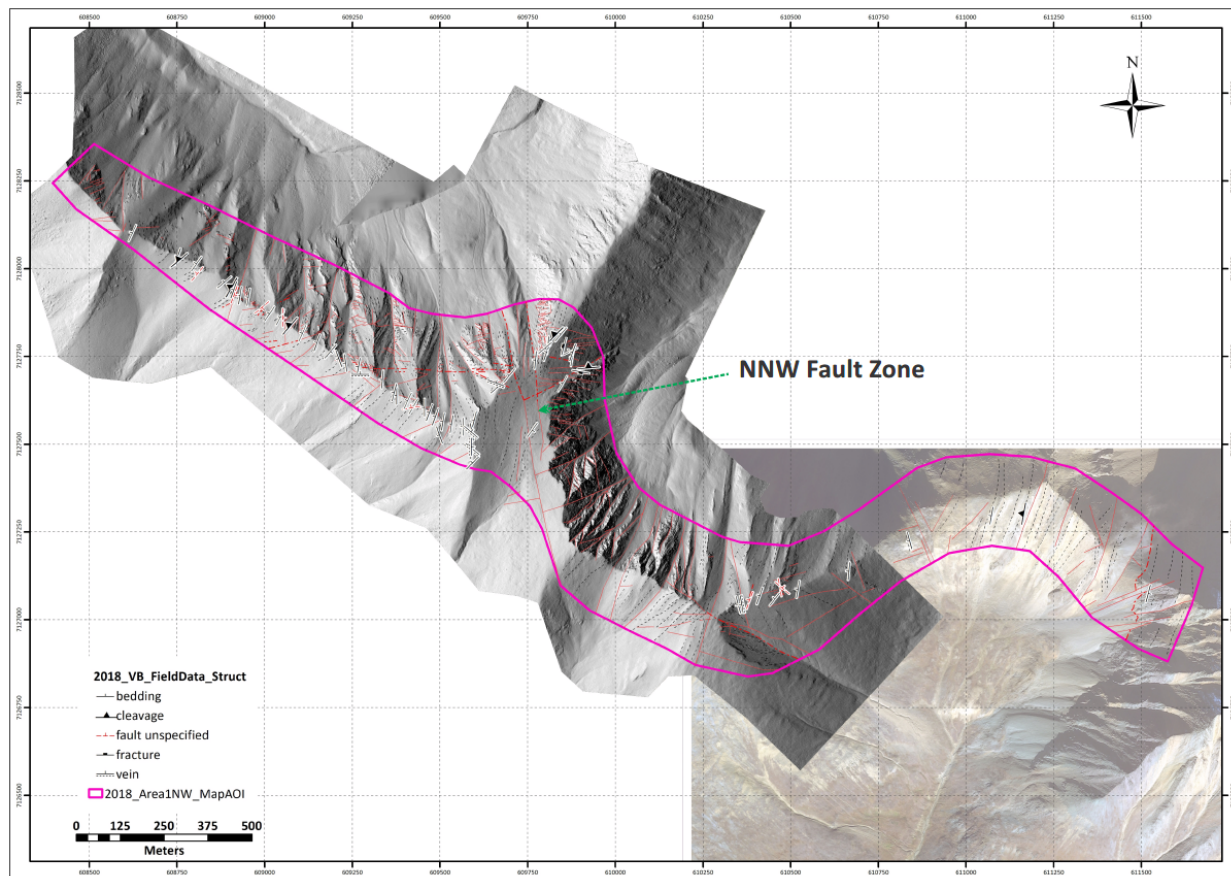


Figure 23: NNW trending late brittle fault zone within Area 1 NW (Pyle and Bennett, 2018).

10.5 CARBON ISOTOPE CHEMOSTRATIGRAPHY

The $\delta^{13}\text{C}$ chemostratigraphy of the mixed carbonate- siliciclastic succession of the Ice Brook Formation to Risky Formation (unconfirmed stratigraphic unit) portion of the Ediacaran Windermere Supergroup shows a range of carbonate carbon isotope values from 9.30 to -9.15 ‰. This is consistent with trends interpreted from studies of this succession adjacent to the study area (e.g., James et al., 2001; Hoffman and Halverson, 2011; Macdonald et al., 2013). Negative carbon isotope values characterize the Ravenstthroat Formation, whereas values in the Sheepbed Formation are enriched (up to 9.30‰), perhaps

indicating correlation with the June beds (described by Macdonald et al., 2013). Strong negative carbon isotope anomalies characterize the Gametrail Formation. Samples are sparse through the Blueflower Formation but yielded a negative excursion in the base, and positive values in the middle of the unit. Another large negative carbon isotope anomaly (down to -9.15 ‰) is present in the uppermost carbonate unit which is likely correlative to the Risky Formation (Figure 24).

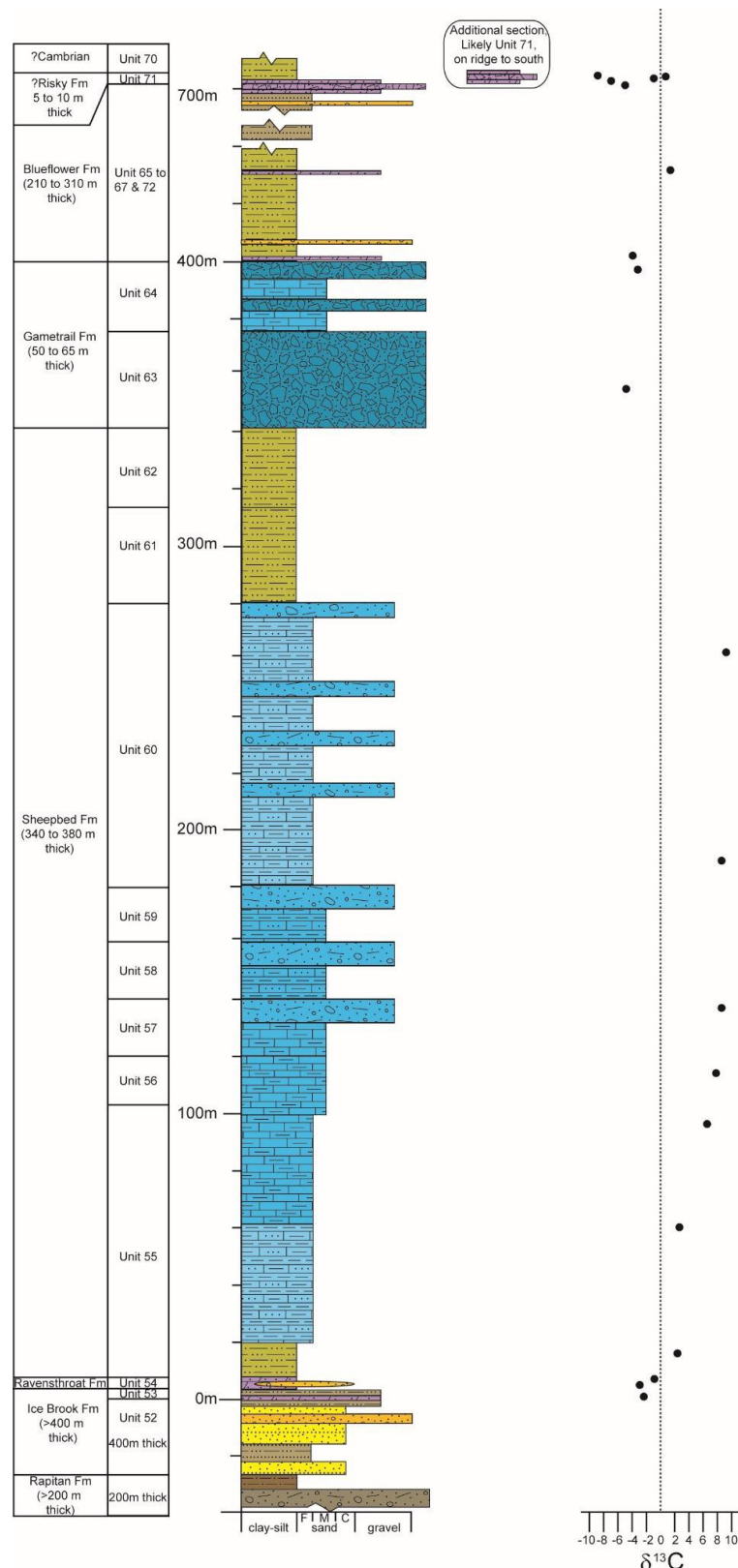


Figure 24: Carbon isotope chemostratigraphy of the Edicaran Windermere Supergroup, through the composite section in the NW part of Area 1 (Pyle and Bennett, 2018).

10.6 2018 ROCK SAMPLING

A total of 44 rock samples were received by ALS Global Laboratories; 16 from Area 2, 8 from Area 1 SE and 20 from Area 1 NW. The samples were not analyzed for Au, although were analyzed for 48-element four-acid ICP-MS. A review of the main pathfinder elements for Carlin-style mineralization (As, Cu, Sb, Sn, Te and Ti) revealed few anomalous values. The highest As value, of 20.4 ppm, was taken from a siltstone bed within a conglomerate unit in Area 1 SE. Elevated Cu values from 96.7 to 192.5 ppm were returned from brown mudrock and lesser olive green mudrock within Area 1 SE.

The main purpose of rock sample collection was to use the data to prepare X-Y scatterplots utilizing element ratios that profile resistive mineral phases (e.g. zircon, ilmenite, rutile). These provide a better representation of source material. Two significant findings are:

1. Sedimentary material that formed in the Rapitan basinal environment, which are elevated in Fe, Ti, Zr, Sc and Nb, has a distinct geochemical signature from that of younger overlying stratigraphy and the unknown stratigraphy of Area 2.
2. The poorly constrained Area 2 stratigraphy is geochemically more similar to that of the Ravenstthroat Formation and younger strata (Pyle and Bennett, 2018). The Ravenstthroat Formation directly overlies the Ice Brook formation and underlies the Hayhook and Sheepbed formations (Hoffman and Halverson, 2011).

Figures 25 and 26 show the Niobium: Zirconium scatter plots, and indicate fairly discrete geochemical signatures for the Rapitan, Area 2, and Ravenstthroat and younger stratigraphy.

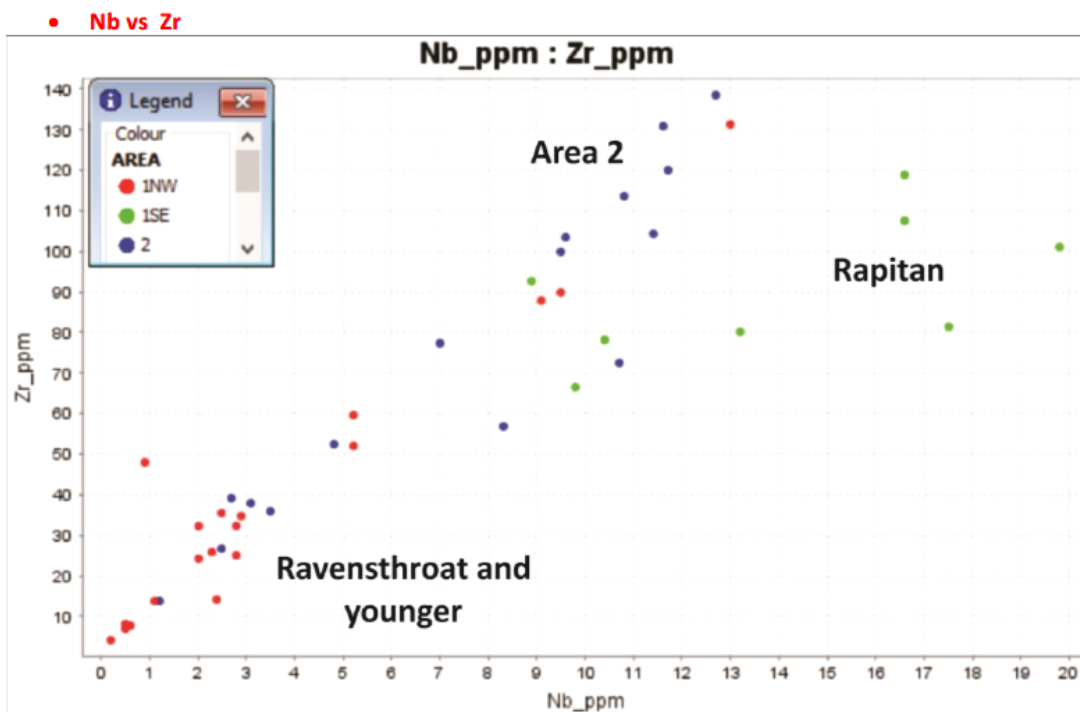


Figure 25: Scatter plot of Niobium versus Zirconium.

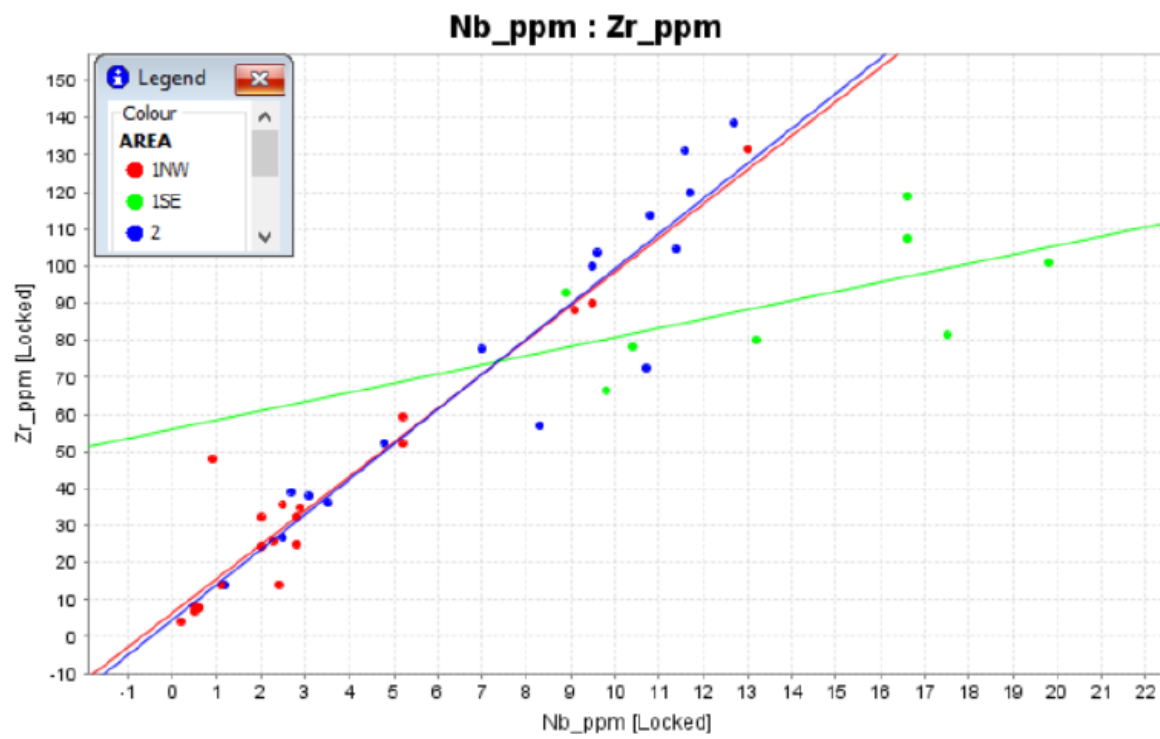
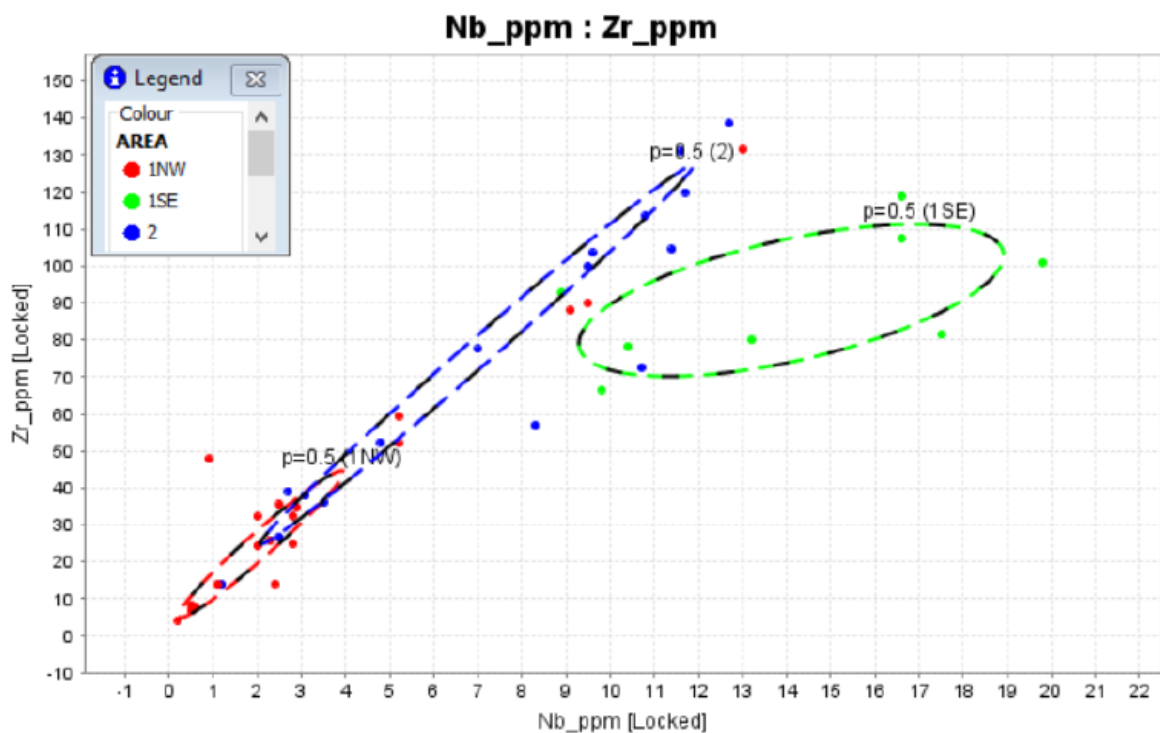
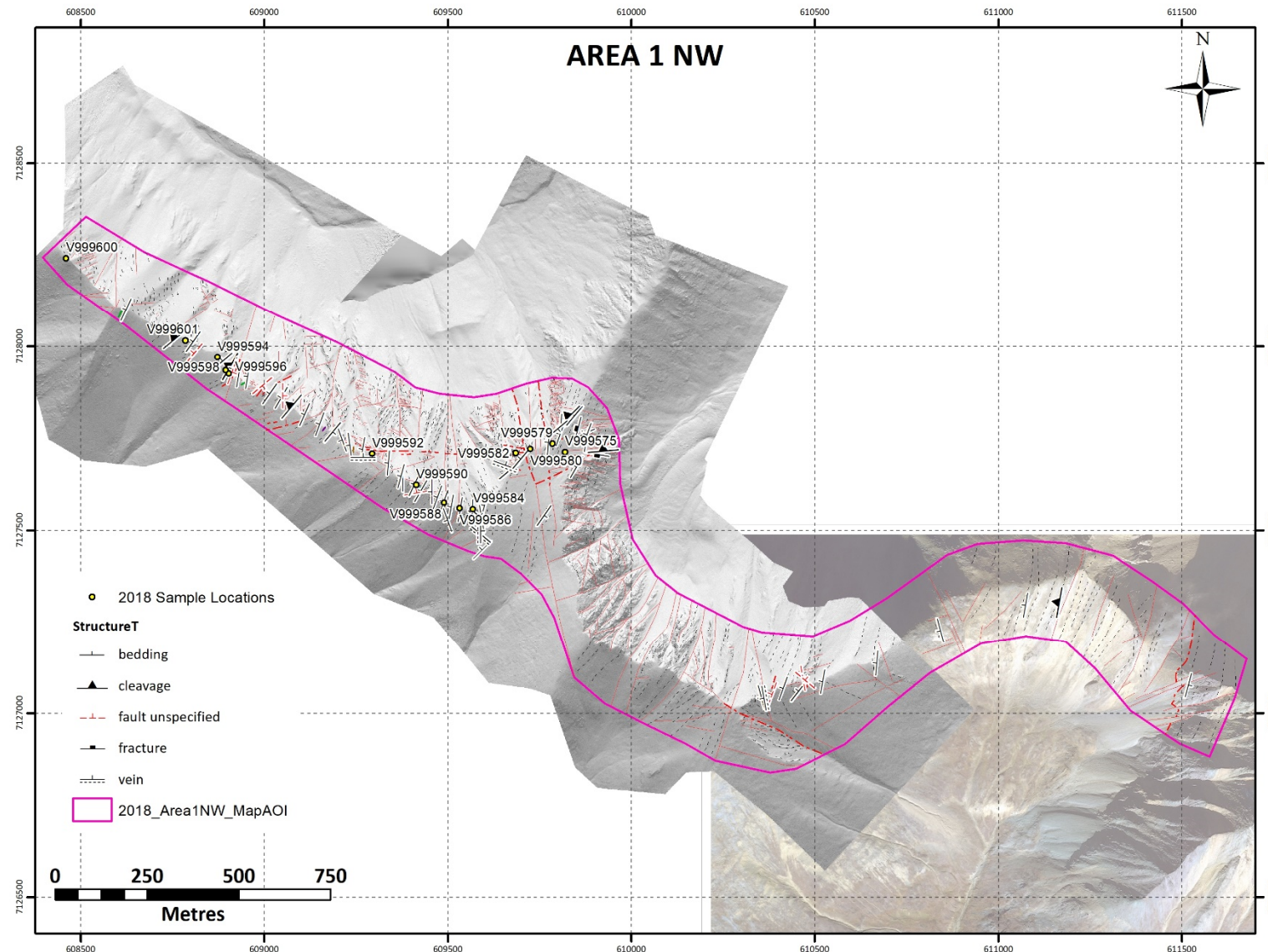


Figure 26: Groupings of geochemical data and median line plots for Areas 1 NW, 1 SE and 2

Further geochemical plots are located within “Appendix 3: Geochemical Sampling Results” of the full Pyle and Bennett report (Appendix VII).

**Figure 27: Rock sample locations, Area 1 NW**

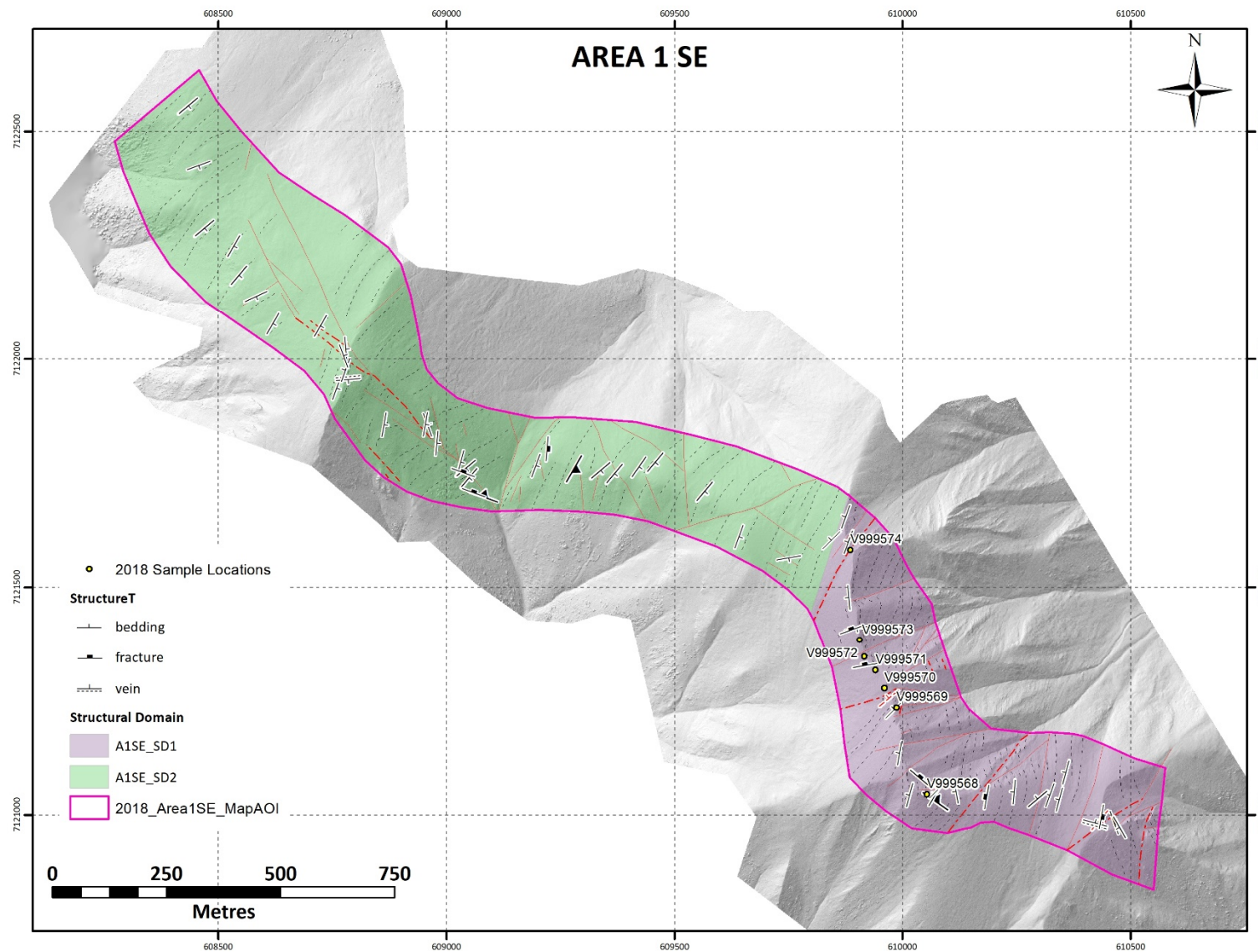
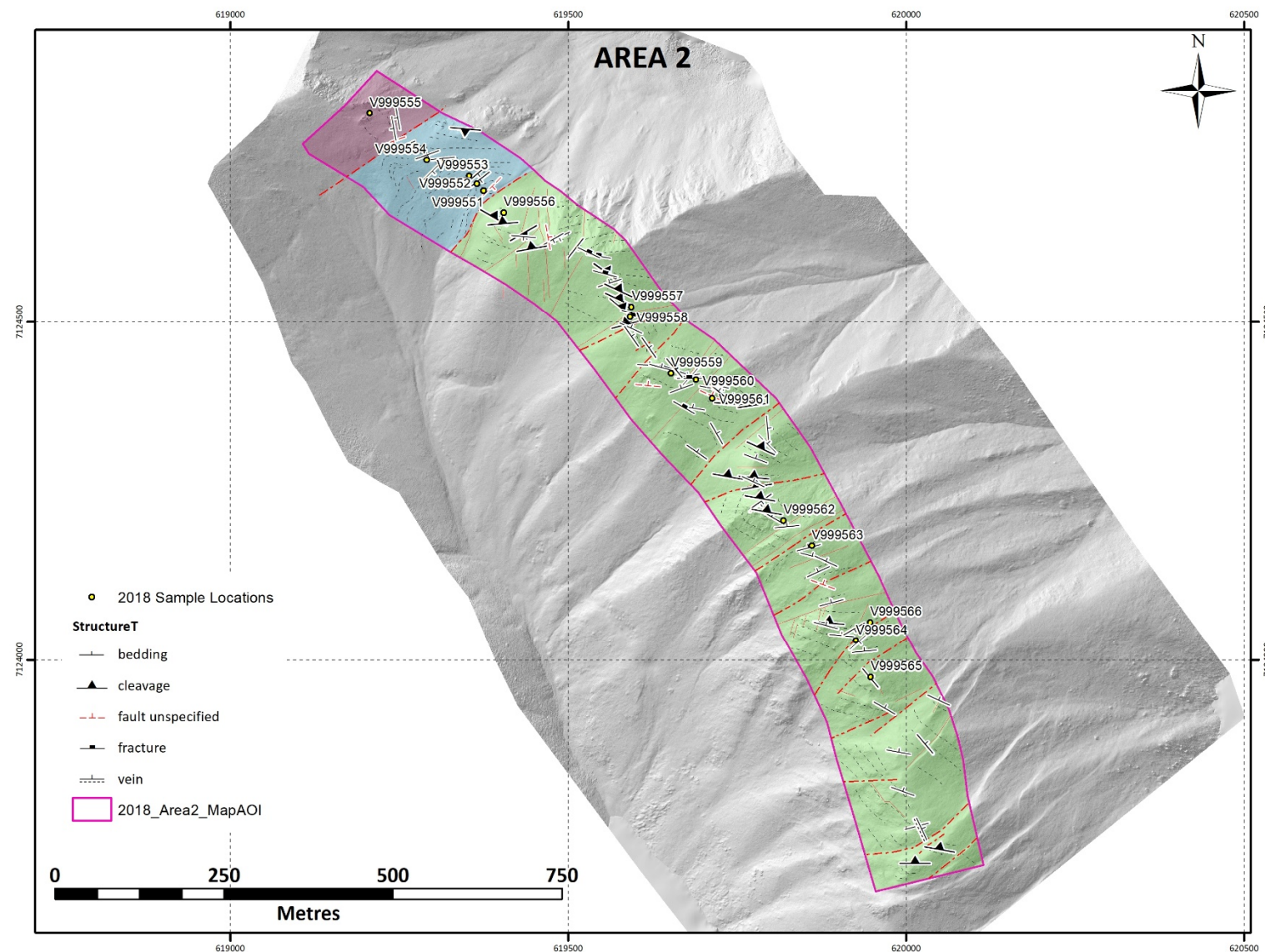


Figure 28: Rock sample locations, Area 1 SE

**Figure 29: Rock sample locations, Figure 2**

11 Conclusions

This section is based with minor edits from the report titled: “**Yukon Gold Project East Central Yukon, Canada, Report On the Stratigraphy and Structure of the CL and HJ Claims**” by Pyle and Bennett, 2018. The full report is included as Appendix VII.

Three detailed transects were completed on the CL and HJ blocks of Carlincore Resources Ltd. The Area 2 Transect was done across the northwest corner of the HJ claim block, and the Area 1 SE and the Area 1 NW transects were done across the southeastern portion of the CL block. The main objective of these traverses was to place the rocks in a regional stratigraphic and structural context to better assess the potential for sediment hosted gold mineralization.

An important component of sediment hosted gold deposits is the presence of well-established, long-lived fault systems. Reactivated basement structures are excellent conduits to facilitate fluid flow.

11.1.1 AREA 2 NW (HJ Block)

Stratigraphy in Area 2 requires further work to determine age and stratigraphic position of the 220 m to 330 m thick heterolithic package examined in 2018. Strata consist of mudrock (shale, mudstone and siltstone), sandstone, and conglomeratic sandstone with rare dolostone beds.

The stratigraphy in Area 2 remains unconstrained in a regional context. However, the predominance of siliciclastics over carbonate lithologies lowers potential for this to be a prospective target area for sediment-hosted gold.

Area 2 consists of three structural domains, the largest of which is characterized by late NE and ENE brittle faults and associated shallow to moderate ENE plunging folds. A second structural domain is associated with a localized area of NW trending folds that predate the late ENE plunging folds. No major thrust faults or shear zones, features that play an important role in mineral emplacement at the Osiris cluster, occur in Area 2. The area is characterized by late brittle NE-ENE faults with only minor amounts of displacement.

No mineralization was observed in this area.

11.1.2 AREA 1 SE (CL Block)

The southeastern portion of Area 1 (Area 1 SE) comprises two stratigraphic units, the Rapitan Group and Ice Brook/ Keele Formation of the Windermere Supergroup. Strata comprises two 100% siliciclastic successions, consisting of mudrock, sandstone, conglomerate, and tillite containing dropstones. Although these stratigraphic units are present within the Osiris cluster (as the NONAD succession), they are not mineralized hosts.

The structural setting of Area 1 SE comprises an early generation of SSW shallow plunging tight to open folds within the Rapitan Group that is overprinted by a later generation of fault-related folding. The Oxidized fluids (limonite – carbonate) are typically associated with these late faults. No mineralization was observed associated with these faults.

No major shear zones or thrust faults were observed in this transect area.

11.1.3 AREA 1 NW (CL Block)

Stratigraphy in Area 1 NW is represented by a composite section from 1,300 m to 1,400 m thick comprising about 20% carbonate and 80% heterolithic siliciclastics interpreted as units of the Windermere Supergroup. The basal unit is the Rapitan Group (siliciclastics), successively overlain by the Ice Brook/Keele Formation (siliciclastics), Ravenstthroat Formation (cap carbonates), Sheepbed Formation (mixed fine siliciclastics and carbonate), Gametrail Formation (dominated by carbonate debrites), Blueflower Formation (siliciclastics), and possibly the Risky Formation (carbonates). The Sheepbed and Gametrail formations have stratigraphic equivalents within the Osiris cluster stratigraphy of the Rackla Gold Belt trend.

The northwestern portion of Area 1 (Area 1 NW) hosts the most intact section of prospective carbonate host rocks. The eastern half of the area is underlain by the Rapitan Group and the Ice Brook/ Keele Formation. The lack of carbonates within this succession renders this section of the Windermere Supergroup as unprospective for sediment-hosted gold. However, the carbonate units located stratigraphically above the Ice Brook / Keele Formation represent the widest section of carbonate stratigraphy within the three transects. Carbonate rocks include dolostone within the Ravenstthroat Formation and limestones within the Sheepbed, Gametrail, Blueflower formations, and possibly the Risky formation. No mineralization was observed in these units in the traverse areas; however, mineralization within the Osiris cluster occurs within the Nadaleen and Gametrail formations which are the stratigraphic equivalents of the Sheepbed and Gametrail formations.

The dominant structural grain is NNE-trending and west-dipping. No major brittle- ductile shear zones or thrust faults where observed. The area is characterized by a suite of N, NE-ENE and NW late brittle structures that may be coeval and may represent part of a Riedel shear system. Late NE-ENE faults are associated with open folding with ENE- trending steep axial planes.

Rock geochemical results for the three transects revealed distinct Nb:Zr signatures for each of the Area 2, Rapitan, and Ravenstthroat and younger strata. The poorly constrained stratigraphy of Area 2 is more geochemically similar to that of the Ravenstthroat formation rather than the Rapitan Group.

No work plan or budget is provided at this time, due to low potential for significant zones of sediment-hosted gold at the CL and HJ properties.

Respectfully Submitted
On behalf of AURORA GEOSCIENCES LTD.

____ "signed" _____
Carl Schulze, B.Sc. P.Geo.

12 REFERENCES

- Abbott, G., 1990.** Geological map of Mt. Westman map area (106D/1). Yukon Geological Survey, Open File 1990-1, 1:50 000.
- Aitken, J.D., 1991.** The Ice Brook Formation and post-Rapitan, late Proterozoic glaciation, Mackenzie Mountains, Northwest Territories, Geological Survey of Canada. Bulletin 404, 43 p.
- Abbott, G., 1997.** Geology of the upper Hart River area, eastern Ogilvie Mountains, Yukon Territory (116A/10, 116A/11); Exploration and Geological Services Division, Yukon, Indian and Northern Affairs Canada, Bulletin, 9, 92p.
- ATAC Resources Limited, 2016.** Web site retrieved 22 October 2016.
<http://www.atacresources.com/projects/rackla/nadaleen-trend>
- Bennett, V., 2016.** Yukon Gold Project, East Central Yukon, Canada, internal report for Carlincore Resources Ltd.
- Birkeland, A.O., 1975.** 1975 Geological and Geochemical Report on the Tara Claim Group; prepared for McIntyre Mines Ltd. Assessment Report 090169.
- Blusson, S.L., 1974.** Five geological maps of northern Selwyn Basin (Operation Stewart), Yukon Territory and District of Mackenzie, N.W.T. Geological Survey of Canada, Open File 205, 1:250 000.
- Chakungal, J., 2014.** CL & HJ Prospects, Field Summary of 2014 Mapping, TransTerritorial Bedrock Mapping & Consulting Inc., internal report for Carlincore Resources Ltd.
- Chakungal, J. and Bennett, V., 2011.** New bedrock geology of Mount Mervyn map sheet (106C/04) and mineral potential for the South Wernecke mapping project. *in:* Yukon Exploration and Geology 2010, K.E. MacFarlane, L.H. Weston and C. Relf (eds.), Yukon Geological Survey, p. 55-87.
- Colpron, M., 2012.** Preliminary geological map of the Mount Ferrell area (106C/3), central Yukon. Yukon Geological Survey, Open File 2012-11, 1:50 000.
- Colpron, M., Moynihan, D., Israel, S., and Abbott, G., 2013.** Geological map of the Rackla belt, east-central Yukon (NTS 106C/1-4, 106D/1). Yukon Geological Survey, Energy, Mines and Resources, Government of Yukon, Open File 2013-13, 1:50 000 scale, 5 maps and legend.
- Coulter, A.B., Lane, J. and Steiner, A., 2018.** Osiris cluster Carlin-type gold, east-central Yukon. *In:* Yukon Exploration and Geology Overview 2017, K.E. MacFarlane (ed.), Yukon Geological Survey, p. 65-74.
- Ecological Stratification Working Group. 1995.** A National Ecological Framework for Canada, Agriculture and Agri-Food Canada. Research Branch, Centre for Land and Biological Resources Research and Environment Canada, State of the Environment Directorate, Ecozone Analysis Branch, Ottawa/Hull. p. 2-4.
- Eisbacher, G.H., 1978.** Re-definition and subdivision of the Rapitan Group, Mackenzie Mountains. Geological Survey of Canada, Paper 77-35, 21 p.
- Floyd, A. and Arnold, R., 1977.** Summary Report on the Jam Claims; prepared for McIntyre Mines Ltd. Yukon Assessment Report 090308.

Green, L.H., 1972. Geology of Nash Creek, Larsen Creek, and Dawson map-areas, Yukon Territory. Geological Survey of Canada, Memoir 364, 157 p.

Gordey, S.P. and Anderson, R.G., 1993. Evolution of the northern Cordilleran miogeocline, Nahanni map area (105I), Yukon and Northwest Territories. Geological Survey of Canada Memoir 428, 127 p.

Gordey, S.P. and Makepeace, A.J. (comp.), 1999: Yukon bedrock geology *in*: Yukon digital geology, S.P. Gordey and A.J. Makepeace (comp.); Geological Survey of Canada Open File D3826 and Exploration and Geological Services Division, Yukon, Indian and Northern Affairs Canada, Open File 1999-1(D).

Héon, D. (compiler), 2003. Yukon Regional Geochemical Database 2003 - Stream sediment analyses. Exploration and Geological Services Division, Yukon Region, Indian and Northern Affairs Canada.

Hoffman, P.F., and Halverson, G.P., 2011. Neoproterozoic glacial record in the Mackenzie Mountains, northern Canadian Cordillera. In: Arnaud, E., Halverson, G.P., Shields- Zhou, G. (Eds.), *The Geological Record of Neoproterozoic Glaciations*. The Geological Society, London, pp. 397–412.

Hoffman, P.F., and Halverson, G.P., 2011. “Chapter 36: Neoproterozoic glacial record in the Mackenzie Mountains, northern Canadian Cordillera”. In Arnaud, E., Halverson, G.P., Shields- Zhou, G. (Eds.), *The Geological Record of Neoproterozoic Glaciations*. The Geological Society, London, pp. 397–411.

Hornbrook, E.H.W., Friske, P.W.B., Lynch, J.J., McCurdy, M.W., Gross, H., Galletta, A.C., Durham, C.C. (1990). National Geochemical Reconnaissance stream sediment and water geochemical data, east central Yukon (106D; parts of 106C, 106E and 106F). Geological Survey of Canada, Open File 2175.

James, N.P., Narbonne, G.M., Kyser, T.K., 2001. Late Neoproterozoic cap carbonates: Mackenzie Mountains, northwestern Canada: precipitation and global glacial meltdown. Canadian Journal of Earth Sciences, v. 38, p. 1229–1262.

Kalkowski, T., 2014. Technical Report describing Geochemical Sampling, Mapping and Prospecting at the CL and HJ properties by Aurora Geosciences Ltd. Yukon Assessment Report.

Kiss, F. and Coyle, M., 2008. Total field magnetic, Werneck Mountain Aeromagnetic Survey, NTS 106C (south half), Yukon. Yukon Geological Survey, Open File 2008-08.

Macdonald, F.A., Strauss, J.V., Sperling, E.A., Halverson, G.P., Narbonne, G.M., Johnston, D.T., Kunzmann, M., Schrag, D.P., and Higgins, J.A., 2013. The stratigraphic relationship between the Shuram carbon isotope excursion, the oxygenation of Neoproterozoic oceans, and the first appearance of the Ediacara biota and bilaterian trace fossils in northwestern Canada; *Chemical Geology*, v. 362, p. 250-272.

Mair, J.L., Hart, C.J.R., and Stephens, J.R., 2006. Deformation history of the northwestern Selwyn Basin, Yukon, Canada: Implications of orogeny evolution and mid Cretaceous magmatism. *Geological Society of America Bulletin*, vol. 118, p. 304-323.

Mitchell, A., 2015. Assessment Report describing soil and rock geochemical sampling, CL and HJ properties, Mayo Mining District. Carlincore Resources Ltd. Yukon Assessment Report.

Moynihan, D.P., 2016. Bedrock geology compilation of the eastern Rackla belt, NTS 105N/15, 105N/16, 105O/13, 106B/4, 106C/1, 106C/2, east-central Yukon. Yukon Geological Survey, Open File 2016-2, scale 1:75000, 2 sheets.

Moynihan, D.P., Strauss, J.V., Colpron, M., Israel, S.A., and Abbott, G, 2015. Stratigraphic ties between the Windermere Supergroup and the Hyland Group in the Rackla Belt of East-Central Yukon: Implications for Age of the Selwyn Basin; Geological Society of America Abstracts with Programs. vol. 47, no. 4, p.19.

Narbonne, G.M. and Aitken, J.D., 1995. Neoproterozoic of the Mackenzie Mountains, northwestern Canada. Precambrian Research, v. 73, p. 101-121.

Pyle, L., and Bennett, V., 2018: "**Yukon Gold Project East Central Yukon, Canada: Report On the Stratigraphy and Structure of the CL and HJ Claims.**" Report for Carlincore Resources Ltd.

Ristorcelli, S., Ronning, P., Martin, C., and Christensen, O., 2018. Technical report and estimate of mineral resources for the Osiris Project, Yukon, Canada. Mining Development Associates, Mine Engineering Services, 118 p.

Appendix I

Statement of Qualifications

STATEMENT OF QUALIFICATIONS

I, Carl Schulze, BSc, with business and residence addresses in Whitehorse, Yukon Territory, do hereby certify that:

1. I am a graduate of Lakehead University with a B.Sc. degree in Geology obtained in 1984.
2. I am a Professional Geoscientist registered with the Association of Professional Engineers and Geoscientists of British Columbia (registration number 25393), Association of Professional Geoscientists of Ontario (registration no. 1966) and with the Northwest Territories and Nunavut Association of Professional Engineers and Geoscientists (NAPEG, registration number L3359).
3. I have been employed in mineral exploration as a geologist since 1984, primarily on projects in the Yukon Territory, Northwest Territories, Nunavut, Alaska and British Columbia.
4. I supervised the work described in this report, reviewed, edited and contributed sections to this report.
5. I have no interest, direct or indirect, nor do I hope to receive any interest, direct or indirect, from Carlincore Resources Ltd. or any of its properties.

Dated this 24th day of January, 2019 in Whitehorse, Yukon Territory.

Respectfully Submitted,

Carl Schulze

Carl M. Schulze, BSc. P. Geo.

Appendix II

Claim Information

CL Claims:

Grant No	Claim Name	Claim Owner	Recording Date	Staking Date	Expiry Date	NTS Map
YD156278	CL 494	Carlincore Resources Ltd. - 100%	2014-07-04	2014-06-17	2024-05-07	106C07
YD156279	CL 495	Carlincore Resources Ltd. - 100%	2014-07-04	2014-06-17	2024-05-07	106C07
YD156280	CL 496	Carlincore Resources Ltd. - 100%	2014-07-04	2014-06-17	2024-05-07	106C07
YD156281	CL 497	Carlincore Resources Ltd. - 100%	2014-07-04	2014-06-17	2024-05-07	106C07
YD156282	CL 498	Carlincore Resources Ltd. - 100%	2014-07-04	2014-06-17	2024-05-07	106C07
YD156283	CL 499	Carlincore Resources Ltd. - 100%	2014-07-04	2014-06-17	2024-05-07	106C07
YD156284	CL 500	Carlincore Resources Ltd. - 100%	2014-07-04	2014-06-17	2024-05-07	106C07
YD156285	CL 501	Carlincore Resources Ltd. - 100%	2014-07-04	2014-06-17	2024-05-07	106C07
YF42001	CL 1	Carlincore Resources Ltd. - 100%	2012-11-07	2012-10-29	2021-05-07	106C02
YF42001	CL 1	Carlincore Resources Ltd. - 100%	2012-11-07	2012-10-29	2021-05-07	106C02
YF42002	CL 2	Carlincore Resources Ltd. - 100%	2012-11-07	2012-10-29	2021-05-07	106C02
YF42002	CL 2	Carlincore Resources Ltd. - 100%	2012-11-07	2012-10-29	2021-05-07	106C02
YF42003	CL 3	Carlincore Resources Ltd. - 100%	2012-11-07	2012-10-29	2021-05-07	106C02
YF42003	CL 3	Carlincore Resources Ltd. - 100%	2012-11-07	2012-10-29	2021-05-07	106C02
YF42004	CL 4	Carlincore Resources Ltd. - 100%	2012-11-07	2012-10-29	2021-05-07	106C02
YF42004	CL 4	Carlincore Resources Ltd. - 100%	2012-11-07	2012-10-29	2021-05-07	106C02
YF42005	CL 5	Carlincore Resources Ltd. - 100%	2012-11-07	2012-10-29	2021-05-07	106C02
YF42005	CL 5	Carlincore Resources Ltd. - 100%	2012-11-07	2012-10-29	2021-05-07	106C02
YF42006	CL 6	Carlincore Resources Ltd. - 100%	2012-11-07	2012-10-29	2021-05-07	106C02
YF42006	CL 6	Carlincore Resources Ltd. - 100%	2012-11-07	2012-10-29	2021-05-07	106C02
YF42007	CL 7	Carlincore Resources Ltd. - 100%	2012-11-07	2012-10-29	2021-05-07	106C02
YF42007	CL 7	Carlincore Resources Ltd. - 100%	2012-11-07	2012-10-29	2021-05-07	106C02
YF42008	CL 8	Carlincore Resources Ltd. - 100%	2012-11-07	2012-10-29	2021-05-07	106C02
YF42008	CL 8	Carlincore Resources Ltd. - 100%	2012-11-07	2012-10-29	2021-05-07	106C02
YF42009	CL 9	Carlincore Resources Ltd. - 100%	2012-11-07	2012-10-29	2021-05-07	106C02
YF42009	CL 9	Carlincore Resources Ltd. - 100%	2012-11-07	2012-10-29	2021-05-07	106C02
YF42010	CL 10	Carlincore Resources Ltd. - 100%	2012-11-07	2012-10-29	2021-05-07	106C02
YF42010	CL 10	Carlincore Resources Ltd. - 100%	2012-11-07	2012-10-29	2021-05-07	106C02
YF42011	CL 11	Carlincore Resources Ltd. - 100%	2012-11-07	2012-10-29	2021-05-07	106C02
YF42011	CL 11	Carlincore Resources Ltd. - 100%	2012-11-07	2012-10-29	2021-05-07	106C02
YF42012	CL 12	Carlincore Resources Ltd. - 100%	2012-11-07	2012-10-29	2021-05-07	106C02
YF42012	CL 12	Carlincore Resources Ltd. - 100%	2012-11-07	2012-10-29	2021-05-07	106C02
YF42013	CL 13	Carlincore Resources Ltd. - 100%	2012-11-07	2012-10-29	2021-05-07	106C02
YF42014	CL 14	Carlincore Resources Ltd. - 100%	2012-11-07	2012-10-29	2021-05-07	106C02
YF42015	CL 15	Carlincore Resources Ltd. - 100%	2012-11-07	2012-10-29	2021-05-07	106C02
YF42016	CL 16	Carlincore Resources Ltd. - 100%	2012-11-07	2012-10-29	2021-05-07	106C02
YF42017	CL 17	Carlincore Resources Ltd. - 100%	2012-11-07	2012-10-29	2021-05-07	106C02
YF42018	CL 18	Carlincore Resources Ltd. - 100%	2012-11-07	2012-10-29	2021-05-07	106C02
YF42019	CL 19	Carlincore Resources Ltd. - 100%	2012-11-07	2012-10-29	2021-05-07	106C02
YF42020	CL 20	Carlincore Resources Ltd. - 100%	2012-11-07	2012-10-29	2021-05-07	106C02
YF42021	CL 21	Carlincore Resources Ltd. - 100%	2012-11-07	2012-10-29	2021-05-07	106C02

YF42472	CL 472	Carlincore Resources Ltd. - 100%	2012-11-07	2012-10-31	2021-05-07	106C07
YF42473	CL 473	Carlincore Resources Ltd. - 100%	2012-11-07	2012-10-31	2021-05-07	106C07

HJ Claims

Grant No	Claim Name	Claim Owner	Recording Date	Staking Date	Expiry Date	NTS Map
YD156286	HJ 406	Carlincore Resources Ltd. - 100%	2014-07-04	2014-06-19	2026-05-07	106C02
YD156287	HJ 407	Carlincore Resources Ltd. - 100%	2014-07-04	2014-06-19	2026-05-07	106C02
YD156288	HJ 408	Carlincore Resources Ltd. - 100%	2014-07-04	2014-06-19	2026-05-07	106C02
YD156289	HJ 409	Carlincore Resources Ltd. - 100%	2014-07-04	2014-06-26	2026-05-07	106C01
YD156290	HJ 410	Carlincore Resources Ltd. - 100%	2014-07-04	2014-06-26	2026-05-07	106C01
YD156291	HJ 411	Carlincore Resources Ltd. - 100%	2014-07-04	2014-06-26	2026-05-07	106C01
YD156292	HJ 412	Carlincore Resources Ltd. - 100%	2014-07-04	2014-06-26	2026-05-07	106C01
YF41401	HJ 1	Carlincore Resources Ltd. - 100%	2012-11-07	2012-10-27	2026-05-07	106C01
YF41402	HJ 2	Carlincore Resources Ltd. - 100%	2012-11-07	2012-10-27	2026-05-07	106C01
YF41403	HJ 3	Carlincore Resources Ltd. - 100%	2012-11-07	2012-10-27	2026-05-07	106C01
YF41404	HJ 4	Carlincore Resources Ltd. - 100%	2012-11-07	2012-10-27	2026-05-07	106C01
YF41405	HJ 5	Carlincore Resources Ltd. - 100%	2012-11-07	2012-10-27	2026-05-07	106C01
YF41406	HJ 6	Carlincore Resources Ltd. - 100%	2012-11-07	2012-10-27	2026-05-07	106C01
YF41407	HJ 7	Carlincore Resources Ltd. - 100%	2012-11-07	2012-10-27	2026-05-07	106C01
YF41408	HJ 8	Carlincore Resources Ltd. - 100%	2012-11-07	2012-10-27	2026-05-07	106C01
YF41409	HJ 9	Carlincore Resources Ltd. - 100%	2012-11-07	2012-10-27	2026-05-07	106C01
YF41410	HJ 10	Carlincore Resources Ltd. - 100%	2012-11-07	2012-10-27	2026-05-07	106C01
YF41411	HJ 11	Carlincore Resources Ltd. - 100%	2012-11-07	2012-10-26	2026-05-07	106C01
YF41412	HJ 12	Carlincore Resources Ltd. - 100%	2012-11-07	2012-10-26	2026-05-07	106C01
YF41413	HJ 13	Carlincore Resources Ltd. - 100%	2012-11-07	2012-10-26	2026-05-07	106C01
YF41414	HJ 14	Carlincore Resources Ltd. - 100%	2012-11-07	2012-10-26	2026-05-07	106C01
YF41415	HJ 15	Carlincore Resources Ltd. - 100%	2012-11-07	2012-10-26	2026-05-07	106C01
YF41416	HJ 16	Carlincore Resources Ltd. - 100%	2012-11-07	2012-10-26	2026-05-07	106C01
YF41417	HJ 17	Carlincore Resources Ltd. - 100%	2012-11-07	2012-10-26	2026-05-07	106C01
YF41418	HJ 18	Carlincore Resources Ltd. - 100%	2012-11-07	2012-10-26	2026-05-07	106C01
YF41419	HJ 19	Carlincore Resources Ltd. - 100%	2012-11-07	2012-10-26	2026-05-07	106C01
YF41420	HJ 20	Carlincore Resources Ltd. - 100%	2012-11-07	2012-10-26	2026-05-07	106C01
YF41421	HJ 21	Carlincore Resources Ltd. - 100%	2012-11-07	2012-10-26	2026-05-07	106C01
YF41422	HJ 22	Carlincore Resources Ltd. - 100%	2012-11-07	2012-10-26	2026-05-07	106C01
YF41423	HJ 23	Carlincore Resources Ltd. - 100%	2012-11-07	2012-10-26	2026-05-07	106C01
YF41424	HJ 24	Carlincore Resources Ltd. - 100%	2012-11-07	2012-10-26	2026-05-07	106C01
YF41425	HJ 25	Carlincore Resources Ltd. - 100%	2012-11-07	2012-10-26	2026-05-07	106C01
YF41426	HJ 26	Carlincore Resources Ltd. - 100%	2012-11-07	2012-10-26	2026-05-07	106C01
YF41427	HJ 27	Carlincore Resources Ltd. - 100%	2012-11-07	2012-10-26	2026-05-07	106C01
YF41428	HJ 28	Carlincore Resources Ltd. - 100%	2012-11-07	2012-10-26	2026-05-07	106C01
YF41429	HJ 29	Carlincore Resources Ltd. - 100%	2012-11-07	2012-10-26	2026-05-07	106C01
YF41430	HJ 30	Carlincore Resources Ltd. - 100%	2012-11-07	2012-10-26	2026-05-07	106C01

YF41791	HJ 391	Carlincore Resources Ltd. - 100%	2012-11-07	2012-10-24	2026-05-07	106C02
YF41792	HJ 392	Carlincore Resources Ltd. - 100%	2012-11-07	2012-10-24	2026-05-07	106C02
YF41793	HJ 393	Carlincore Resources Ltd. - 100%	2012-11-07	2012-10-24	2026-05-07	106C02
YF41794	HJ 394	Carlincore Resources Ltd. - 100%	2012-11-07	2012-10-24	2026-05-07	106C02
YF41795	HJ 395	Carlincore Resources Ltd. - 100%	2012-11-07	2012-10-24	2026-05-07	106C02
YF41796	HJ 396	Carlincore Resources Ltd. - 100%	2012-11-07	2012-10-24	2026-05-07	106C02
YF41797	HJ 397	Carlincore Resources Ltd. - 100%	2012-11-07	2012-10-24	2026-05-07	106C02
YF41798	HJ 398	Carlincore Resources Ltd. - 100%	2012-11-07	2012-10-24	2026-05-07	106C02
YF41799	HJ 399	Carlincore Resources Ltd. - 100%	2012-11-07	2012-10-24	2026-05-07	106C02
YF41800	HJ 400	Carlincore Resources Ltd. - 100%	2012-11-07	2012-10-24	2026-05-07	106C02
YF41801	HJ 401	Carlincore Resources Ltd. - 100%	2012-11-07	2012-10-24	2026-05-07	106C02
YF41802	HJ 402	Carlincore Resources Ltd. - 100%	2012-11-07	2012-10-24	2026-05-07	106C02
YF41803	HJ 403	Carlincore Resources Ltd. - 100%	2012-11-07	2012-10-24	2026-05-07	106C02
YF41804	HJ 404	Carlincore Resources Ltd. - 100%	2012-11-07	2012-10-24	2026-05-07	106C02
YF41805	HJ 405	Carlincore Resources Ltd. - 100%	2012-11-07	2012-10-24	2026-05-07	106C02

Appendix III

2018 Fieldwork Log

Activity Summary for Project Personnel by Day		
Day	Venessa Bennett	Leanne Pyle
Sun 22-Jul-2018	Mobe in / Mapping/Drone Missions	mobe in/Reconnaissance
Mon 23-Jul-2018	Mapping/Drone Missions	Mapping
Tue 24-Jul-2018	Mapping	Mapping
Wed 25-Jul-2018	Mapping/Drone Missions	Mapping
Thu 26-Jul-2018	Mapping	Mapping
Fri 27-Jul-2018	Mapping/Drone Missions	Mapping
Sat 28-Jul-2018	Mapping	Mapping
Sun 29-Jul-2018	Mapping/Drone Missions	Mapping/Mobe Out day (PM)
Mon 30-Jul-2018	Half-day Mapping/Sampling/Drone Missions	

Date	Activity and Sample Production	Target	Production Day (Property)
Sun 22-Jul-2018	Reconnaissance and Drone Missions	Area 2	HJ
Mon 23-Jul-2018	Mapping and Drone Missions.	Area 2	HJ
Tue 24-Jul-2018	Mapping	Area 2	HJ
Wed 25-Jul-2018	Mapping and Drone Missions	Area 1 SE	CL
Thu 26-Jul-2018	Mapping	Area 1 SE	CL
Fri 27-Jul-2018	Mapping and Drone Missions	Area 1 NW	CL
Sat 28-Jul-2018	Mapping and Drone Missions	Area 1 NW	CL
Sun 29-Jul-2018	Mapping and Drone Missions	Area 1 SE	CL
Mon 30-Jul-2018	Mapping and Drone Missions;	Area 1 NW	CL

Appendix IV

Statement of Expenditures

	Act. Revenue
Service	
Geologic Report	7,500.00
Mapping Field Program	27,600.00
Geochemical Analysis	2,637.19
Project Management	240.00
Warehouse Labour	97.50
Fuel Expense	158.69
Accommodation and meals	3,560.00
Commercial Flights	1,153.73
Charter Fixed Wing	2,250.00
Charter Helicopter	28,340.00
Commercial Shipping (samples)	179.46
Expenses (consumables)	89.05
Expediting and Hotshots	2,962.50
Program Prep and Warehouse Labour	<u>2,757.50</u>
Total Service	79,525.62
Other Charges	
10% (10% Administration Fee)	<u>3,836.81</u>
Total Other Charges	<u>3,836.81</u>
TOTAL	<u><u>83,362.43</u></u>

Appendix V

Sample Descriptions.

SAMPLEID	Sample Type	NAD83Z8_E	NAD83Z8_N	Lithology	AREA	Description
V999551	geochemistry	619374.0991	7124695.346	Dolostone	2	finely crystalline, silty
V999552	geochemistry	619364.8714	7124705.562	Dolostone	2	finely crystalline, silty
V999553	geochemistry	619352.9161	7124716.999	Siltstone	2	siliceous
V999554	geochemistry	619290.3898	7124740.434	Dolostone	2	wavy laminated
V999555	geochemistry	619206.097	7124809.642	Mudstone	2	laminated
V999556	geochemistry	619403.9025	7124662.761	Mudstone	2	laminated, quartz clasts
V999557	geochemistry	619593.4441	7124523.007	Dolostone	2	finely crystalline, laminated
V999558	geochemistry	619591.1815	7124507.165	Dolostone	2	karstic, silty
V999559	geochemistry	619651.7253	7124424.005	Carbonate breccia	2	limestone clasts, matrix supported
V999560	geochemistry	619688.7768	7124414.445	Dolostone	2	finely crystalline
V999561	geochemistry	619713.1653	7124387.316	Dolostone	2	finely crystalline, silty
V999562	geochemistry	619818.053	7124206.728	Dolostone	2	concretion, finely laminated, finely crystalline
V999563	geochemistry	619860.1403	7124169.133	Siltstone	2	finely laminated, siliceous
V999564	geochemistry	619925.3776	7124028.76	Siltstone	2	finely laminated, siliceous
V999565	geochemistry	619947.1236	7123974.74	Siltstone	2	finely laminated, siliceous
V999566	geochemistry	619946.6117	7124055.967	Siltstone	2	finely laminated, siliceous
V999567	geochemistry	610478.2878	7120384.763	Siltstone	1SE	siltstone, base of olive green mudrock to tillite unit
V999568	geochemistry	610053.3613	7121044.739	Mudstone	1SE	olive green mudrock, convolute laminae
V999569	geochemistry	609986.4959	7121234.366	Siltstone	1SE	olive green, within conglomeratic unit
V999570	geochemistry	609959.6997	7121277.319	Mudstone	1SE	brown mudrock
V999571	geochemistry	609940.4396	7121317.046	Mudstone	1SE	olive green mudrock unit, convolute laminae
V999572	geochemistry	609915.7619	7121347.141	Mudstone	1SE	brown mudrock
V999573	geochemistry	609905.5308	7121383.858	Mudstone	1SE	brown mudrock
V999574	geochemistry	609885.0741	7121581.285	Mudstone	1SE	brown mudrock
V999575	geochemistry	609818.928	7127712.415	Mudstone	1NW	Ice Brook Fm, upper heterolithic clastic beds, interbedded with conglomerate
V999579	geochemistry	609785.371	7127735.529	Dolosiltstone	1NW	Ice Brook Fm, laminated, top cap carbonate beds?
V999580	geochemistry	609724.45	7127720.757	Lime mudstone	1NW	Sheepbed Fm lower, thin bed
V999582	geochemistry	609684.967	7127709.883	Lime mudstone	1NW	Sheepbed Fm middle, laminated

V999584	geochemistry	609567.527	7127556.927	Lime mudstone	1NW	Sheepbed Fm middle, wavy laminated
V999586	geochemistry	609532.491	7127559.92	Lime mudstone	1NW	Sheepbed Fm middle, platy weathering with ?trace fossils
V999588	geochemistry	609489.229	7127574.769	Floatstone	1NW	Sheepbed Fm top, angular to subround clasts float in carbonate matrix
V999590	geochemistry	609413.364	7127623.052	Lime mudstone	1NW	Sheepbed Fm top, platy weathering, argillaceous
V999592	geochemistry	609293.468	7127708.001	Lime mudstone	1NW	Sheepbed Fm top, wavy laminated
V999594	geochemistry	608872.966	7127970.583	Rudstone	1NW	Gametrail Fm, limestone clasts
V999596	geochemistry	608903.351	7127926.044	Rudstone	1NW	Gametrail Fm, limestone clasts
V999598	geochemistry	608894.974	7127935.345	Siltstone	1NW	middle Blueflower Fm, laminated
V999600	geochemistry	608459.756	7128241.943	Siltstone	1NW	upper Blueflower Fm, finely laminated
V999601	geochemistry	608785.183	7128016.211	Dolosiltstone	1NW	mid Blueflower Fm, finely laminated
V999603	geochemistry	608057.246	7126115.026	Siltstone	1NW	?Cambrian, finely laminated
V999604	geochemistry	608099.352	7126101.458	Dolostone	1NW	?Risky Fm, coarse crystalline
V999503	geochemistry	607815.289	7124941.622	Dolostone	1NW	Silty dolostone, Potential upper Blueflower?
V999504	geochemistry	607778.625	7125016.065	Dolostone	1NW	Silty dolostone, Potential upper Blueflower?
V999505	geochemistry	607752.731	7125021.71	Floatstone	1NW	Limestone clasts, matrix supported
V999506	geochemistry	607630.684	7125043.453	Dolostone	1NW	Silty dolostone, Potential upper Blueflower?

Title	Description	Lithology	Sed Type	Min	Max
2018CClp001	medium grey, weathers pale yellowish brown; thin bedded, finely laminated; subangular to subround quartz clasts; iron staining	siltstone	clastic	1	1
2018CClp002	light grey, weathers pale yellowish orange; thin bedded, laminated; silty, quartz veins up to 2 cm thick; folded	dolostone	carbonate	2	2
2018CClp003	medium grey, weathers yellowish brown; thin bedded; shale clasts up to cobble size; dark grey mudstone interbeds	siltstone	clastic	1	5
2018CClp004	70% sandstone, greyish orange, weathers pale orange; fine to coarse grained; coarse grained beds have erosive bases; clasts rounded; 30% siltstone as 2018CClp001, with quartz pebbles and rare dolostone clasts	sandstone and siltstone	clastic	1	5
2018CClp005	as 2018CClp004; planar bedded with some cross-beds; subangular to round clasts, fining upward to laminated siltstone; medium beds of sandstone at top of unit	sandstone and siltstone	clastic	1	5
2018CClp006	99% sandstone as 2018CClp004 with 1% dolostone in planar bed with wavy lamination (algal?), weathers pale brownish orange	sandstone and siltstone	clastic	1	5
2018CClp007	as 2018CClp004 but with massive beds of conglomeratic sandstone in base of unit that forms the upper part of the ridge to the northwest	sandstone and siltstone	clastic	10	15
2018CClp008	as 2018CClp001, including pyritic, silty mudstone in finely laminated beds that weather reddish brown; some beds contorted with small slump folds; unit has alternating lamination of medium grey and yellowish brown siltstone; common quartz pebble sandstone in bed bases with minor lithics, and disseminated quartz clasts	siltstone	clastic	15	20
2018CClp009	90% siltstone as 2018CClp001, weathers olive grey and platy; lenses of quartz pebbles; 10% sandstone beds are medium to thick, discontinuous, well cemented	siltstone and sandstone	clastic	5	10
2018CClp010	as 2018CClp001, weathers blocky, dense, siliceous, with dark grey and yellowish brown laminations; iron staining around clasts within dark grey siltstone; climbing ripples	siltstone and sandstone	clastic	5	10
2018CClp011	50% dolostone, 50% siltstone as above; in 3 alternations of lithologies; dolostone is medium grey; weathers yellowish brown, veined, upper bed is karst?, downcuts siltstone along erosive surface	dolostone and siltstone	clastic and carbonate	3	3
2018CClp012	50% sandstone, medium grey and greyish orange, lithic and quartz grains; thin to medium bedded; 50 % siltstone	sandstone and siltstone	clastic	5	10
2018CClp013	as 2018CClp012, 20% sandstone and 80% siltstone	sandstone and siltstone	clastic	10	15
2018CClp014	as 2018CClp013, with <1% dolostone: medium grey, weathers light grey and pale orange, thin bedded, discontinuous with irregular bed bases, finely crystalline; differential, rubbly weathering of carbonate breccia, 25 cm thick, with dissolved clasts up to cobble size. Some clasts contain algal laminae, and iron-alteration around clasts.	siltstone, sandstone and dolostone	clastic and carbonate	10	15
2018CClp015	medium grey, weathers pale olive; basal few metres covered; thin bedded; siliceous, rare lithics; 1% dolostone, light grey, weathers light grey and pale orange; 50 cm bed with irregular base; silty	siltstone and dolostone	clastic and carbonate	10	15
2018CClp016	50% sandstone, greyish orange, weathers light grey; thin to medium bedded with scoured bases; 80% quartz, 20% lithics; coarse sand to pebbles; moderate sorting; subangular to subround grains; thin beds of fine to medium sand; 50% siltstone interbeds, medium grey, weathers pale yellowish brown; finely laminated, siliceous, quartz pebbles; fining upward packages of quartz pebble sandstone to fine sandstone to siltstone	sandstone and siltstone	clastic	10	15
2018CClp017	medium dark grey, weathers medium grey and pale yellowish brown; thin to medium bedded, planar to irregular; laminated, recessive intervals are finely laminated; common quartz granules to pebbles, siliceous	siltstone	clastic	10	15
2018CClp018	as 2018CClp016	sandstone and siltstone	clastic	10	15
2018CClp019	as 2018CClp016 but rubbly weathering in top 2 m due to dolostone nodules, ellipsoidal up to 10 cm wide	siltstone	clastic and carbonate	10	15
2018CClp020	interval of pebbly sandstone, lithology as in as 2018CClp016	sandstone	clastic	10	15
2018CClp021	90% sandstone, 10% siltstone in thickening upward package; coarse, pebbly sandstone lenses in siltstone up to 1 m long	sandstone and siltstone	clastic	20	25
2018CClp022	90% sandstone in discontinuous, medium beds with erosive bases and thin, fine grained sandstone beds that are planar and with erosive bases; 10% siltstone is medium dark grey, finely laminated	sandstone and siltstone	clastic	20	25
2018CClp023	unit contains a 20 m thick, discontinuous coarse sandstone unit at the base, 20 m of siliceous siltstone with coarse pebble lenses and 10 m of thin to medium beds with erosive bases	sandstone and siltstone	clastic	40	50
2018CClp024	medium dark grey, weathers dark yellowish brown and flaggy; thin bedded, planar to irregular beds; finely laminated, siliceous, recessive and partially vegetation covered	siltstone	clastic	15	20
2018CClp025	light grey, weathers dark yellowish orange and blocky; medium to thick bedded, erosive bed bases; polymictic pebble to boulders; thin beds of conglomerate, poorly sorted, angular to subround clasts	conglomerate and sandstone	clastic	15	20
2018CClp026	pale olive green, weathers light to moderate brown; thin bedded, finely laminated, ripple cross-lamination; soft-sediment deformation; dropstones; minor sandstone interbeds, light grey; coarsens upward to fine-grained sandstone beds at top of unit	siltstone and sandstone	clastic	25	30
2018CClp027	light grey, weathers grayish orange and rubbly; thick discontinuous beds, erosive bed bases; polymictic, pebble to boulder clasts in fine grained matrix; pale olive mudstone interbeds; thin beds of fine-grained sandstone at top of unit with flute marks	conglomerate, sandstone, mudstone	clastic	5	10

2018CClp028	pale olive green, weathers dark yellowish brown to moderate brown; thin bedded, finely laminated, ripple cross-lamination; soft-sediment deformation, contortion of laminae; dropstones; minor thin sandstone interbeds and lenses, light grey, with climbing ripples and black laminae	siltstone	clastic	60	70
2018CClp029	light grey, weathers grayish orange and rubbly; medium to thick beds, loaded bed bases; polymictic, pebble to boulder clasts in fine grained matrix	conglomerate and sandstone	clastic	10	15
2018CClp030	medium grey, weathers light to moderate brown; thin bedded, finely laminated	mudstone and sandstone	clastic	5	10
2018CClp031	pale olive green, weathers light to moderate brown; thin bedded, finely laminated	mudstone and sandstone	clastic	5	10
2018CClp032	moderate brown, weathers brown and flaggy; finely laminated, fine grained sandstone interlaminae and beds; climbing ripples and soft sedimentary deformation such as contorted laminae; marker bed of sandstone, greyish orange, dolomitic with shale and sandstone clasts, load casts	mudstone and sandstone	clastic	30	40
2018CClp033	light grey, weathers greyish orange to light brown; thin beds, fine grained, siltstone interbeds	sandstone	clastic	5	5
2018CClp034	greyish orange, weathers rubbly on largely covered slope; thin beds of sandstone; polymictic with boulders of carbonate and sandstone	conglomerate and sandstone	clastic	10	15
2018CClp035	moderate brown, weathers brown and flaggy; finely laminated, fine grained sandstone interlaminae and beds	siltstone	clastic	15	20
2018CClp036	light grey, weathers grayish orange and rubbly; medium to thick beds, erosive and loaded bed bases; polymictic, pebble to boulder clasts in fine grained matrix	sandstone, conglomerate and siltstone	clastic	10	15
2018CClp037	moderate brown, weathers brown and flaggy; finely laminated, fine grained sandstone interlaminae and beds	mudstone and sandstone	clastic	15	20
2018CClp038	greyish orange, weathers rubbly on largely covered slope; thin beds	sandstone, conglomerate and siltstone	clastic	10	15
2018CClp039	pale olive green, weathers light to moderate brown; thin bedded, finely laminated; conglomeratic lenses	siltstone and sandstone	clastic	10	15
2018CClp040	pale olive green, weathers light to moderate brown; thin bedded, finely laminated	mudstone and sandstone	clastic	15	20
2018CClp041	greyish orange, weathers rubbly on largely covered slope; thin beds	conglomerate and siltstone	clastic	10	15
2018CClp042	greyish red, weathers pale yellowish brown to greyish red; thin to medium bedded; cleaved; matrix-supported clasts are pebble to cobble sized with common boulder dropstones within contorted strata; clasts angular to well-rounded, clastic and carbonate.	tillite	clastic	15	20
2018CClp043	pale greyish orange, weathers light to moderate brown and flaggy; thin bedded, finely laminated; thin beds of coarse-grained sandstone and conglomerate	siltstone and sandstone	clastic	20	25
2018CClp044	moderate brown, weathers brown and flaggy; thin bedded; fine grained to coarse grained; load structures; interbeds of olive green mudstone	heterolithic	clastic	20	25
2018CClp045	pale olive green, weathers olive green to light to moderate brown; thin bedded, finely laminated; thin siltstone and sandstone interbeds	heterolithic	clastic	10	15
2018CClp046	pale olive green, weathers light to moderate brown; thin bedded, finely laminated	mudstone and sandstone	clastic	20	25
2018CClp047	moderate brown, weathers brown and flaggy; thin bedded	siltstone	clastic	20	25
2018CClp048	pale olive green, weathers olive green; thin bedded; diamict in scree	heterolithic	clastic	10	15
2018CClp049	as 2018CClp044	heterolithic	clastic	20	25
2018CClp050	light grey, weathers grayish orange and rubbly; thick beds, erosive bed bases; polymictic, pebble to boulder clasts in fine grained matrix	heterolithic	clastic	10	15
2018CClp051	as 2018CClp047	siltstone	clastic	10	15
2018CClp052	light grey, weathers light grey, heterolithic package of mudstone with contorted laminae and intraclasts; conglomerate and sandstone in medium beds; conglomerate has granule to pebble sized clasts, poorly sorted, angular to subround, cross bedded	heterolithic	clastic	400	400
2018CClp053	medium light grey, weathers greyish orange; thin bedded, interbed of silty dolostone within conglomerate; finely laminated	dolostone	clastic and carbonate	1	1
2018CClp054	light grey, weathers dark yellowish orange; thin bedded, silty, finely laminated; erosive bed bases, coarse sandstone lenses	dolostone	carbonate	2	2
2018CClp055	medium grey, weathers greyish orange, basal Sheepbed Fm consists of black shale with interbeds of siltstone and rare thin fine grained sandstone with 5% lime mudstone	limestone	carbonate	100	100
2018CClp056	medium grey, weathers light to medium grey; thin to medium bedded, planar to wavy bedded, beef calcite and cone-in-cone structures, large spiral horizontal trace fossils up to 25 cm across on bedding planes	limestone	carbonate	20	25
2018CClp057	light grey, weathers medium grey; thin to medium bedded, planar to wavy bedded, slump-folded bedding near top of unit with thick-bedded floatstone containing polymictic, angular clasts up to pebble size; beds with erosive bases	floatstone and limestone	carbonate	20	25
2018CClp058	greyish orange, weathers medium light orange and platy; thin bedded to massive, planar bedded in cycles of shale to limestone that thicken up section; as 2018CClp057 with massive beds of floatstone near top of unit	shale and limestone	carbonate	20	25
2018CClp059	as 2018CClp058, massive beds of floatstone near top of unit	limemudstone	carbonate	20	25

2018CClp060	medium light grey, weathers yellowish grey and blocky; thin to medium bedded; argillaceous lime mudstone, finely laminated with black wavy laminae and black shale clasts; medium beds of floatstone have erosive bed bases, angular to subround polymictic clasts floating in structureless matrix	floatstone and shale	clastic	100	100
2018CClp061	light grey, weathers dark yellowish orange; thin bedded; finely interlaminated yellowish orange siltstone and dark grey mudstone; ripple cross-laminated; thin to medium siltstone beds have erosive bases and are laterally discontinuous	siltstone and shale	clastic	30	40
2018CClp062	greyish black, weathers greyish orange; thin bedded with olive green siltstone interbeds in fining upward beds	shale	clastic	30	40
2018CClp063	light grey, weathers medium and light grey, prominent marker bed that is folded; medium bedded to massive; bed bases scoured, sharp and erosive; truncated beds; matrix supported with randomly oriented, medium grey cobble sized intraclasts	rudstone and limemudstone	carbonate	30	40
2018CClp064	two cycles of thin bedded dololimemudstone to thick bedded rudstone; medium light grey, weathers greyish orange and medium light grey and rubbly; dololimemudstone is thin bedded, planar to wavy bedded, sharply overlain by medium bedded rudstone with intraformational intraclasts of laminated limemudstone chaotically arranged, matrix-supported, erosive bed bases with cm to dm downcutting; slumped beds	rudstone and limemudstone	carbonate	20	25
2018CClp065	dark grey, dark grey and light brown weathering; thin bedded, planar laminated siltstone with minor quartz to conglomeratic sandstone in thin beds with pebble sized clasts; silty dolostone in base of unit is thin-bedded and laminated	siltstone	clastic	50	60
2018CClp066	greyish orange and olive grey, weathers light brown; thin bedded; siltstone with fine grained quartz wacke interlaminae	siltstone	clastic	20	25
2018CClp067	resistant unit of siltstone and quartz wacke and sandstone, dark yellowish brown, weathers light to moderate brown overall; thin to medium bedded; increasing sandstone beds upsection; siltstone contains fine grained sandstone interbeds; cleaved; ?Aspidella Ediacaran fossil	sandstone and siltstone	clastic	140	150
2018CClp068	ridge forming unit of greyish orange, weathers dark yellowish orange to light brown; medium sand to boulders, polymictic clasts with dominant carbonate boulders in conglomerate; beds thin to massive and laterally discontinuous, cross-bedded quartzite intervals; siltstone interbeds more common in basal quarter of unit, laminated with sandstone interbeds.	conglomerate, sandstone and siltstone	clastic	400	400
2018CClp070	black shale, weathers dark grey; rare greyish orange weathering siltstone interbeds, thin bedded, planar lamination	shale and siltstone	clastic	200	200
2018CClp071	yellowish brown to greyish red weathering; thin to medium bedded, cross-bedded; fine to coarse crystalline; pyritic horizon at base of rudstone; clasts are tabular and finely laminated	dolostone and rudstone	clastic	5	5
2018CClp072	medium grey, weathers greyish orange, thickens upward with increase in sandstone beds and rare conglomerate with dolostone clasts near top; siltstone and shale interbeds are finely laminated; sandstone is cross-laminated	heterolithic	clastic	100	100

Title	Date Created	Latitude	Longitude	Northing (NAD 83)	Easting (NAD 83)	Lithology	Sed Type	Min	Max
2018CClp001	2018-07-23T09:14:48010:00	64.2276845	-132.5389067	7124695.346	619374.0991	siltstone	clastic	1	1
2018CClp002	2018-07-23T09:16:42010:00	64.2276845	-132.5389067	7124695.346	619374.0991	dolostone	carbonate	2	2
2018CClp003	2018-07-23T09:33:44010:00	64.22782666	-132.5391312	7124710.758	619362.6051	siltstone	clastic	1	5
2018CClp004	2018-07-23T10:09:00010:00	64.22788597	-132.5393257	7124716.999	619352.9161	sandstone and siltstone	clastic	1	5
2018CClp005	2018-07-23T10:35:09010:00	64.22810293	-132.5397094	7124740.442	619333.3761	sandstone and siltstone	clastic	1	5
2018CClp006	2018-07-23T11:05:22010:00	64.22814471	-132.5401087	7124744.346	619313.8367	sandstone and siltstone	clastic	1	5
2018CClp007	2018-07-23T11:30:54010:00	64.22876747	-132.5422756	7124809.642	619206.097	sandstone and siltstone	clastic	10	15
2018Cclp008	2018-07-23T12:10:07010:00	64.22809859	-132.5397291	7124739.922	619332.4403	siltstone	clastic	15	20
2018CClp009	2018-07-23T13:08:21010:00	64.22733056	-132.5386183	7124656.47	619389.6108	siltstone and sandstone	clastic	5	10
2018CClp010	2018-07-23T13:44:05010:00	64.22712534	-132.5380116	7124634.752	619419.9105	siltstone and sandstone	clastic	5	10
2018CClp011	2018-07-23T14:08:44010:00	64.22606322	-132.5345272	7124523.007	619593.4441	dolostone and siltstone	clastic and carbonate	3	3
2018CClp012	2018-07-23T15:37:02010:00	64.22592197	-132.5345865	7124507.165	619591.1815	sandstone and siltstone	clastic	5	10
2018CClp013	2018-07-23T16:15:42010:00	64.2254692	-132.5342121	7124457.443	619611.2908	sandstone and siltstone	clastic	10	15
2018CClp014	2018-07-23T17:21:07010:00	64.22515535	-132.5334062	7124424.005	619651.7253	siltstone, sandstone and dolostone	clastic and carbonate	10	15
2018CClp015	2018-07-24T08:38:30010:00	64.22505634	-132.5325052	7124414.672	619695.8424	siltstone and dolostone	clastic and carbonate	10	15
2018CClp016	2018-07-24T09:12:12010:00	64.2244951	-132.5305482	7124355.85	619793.1668	sandstone and siltstone	clastic	10	15
2018CClp017	2018-07-24T10:01:25010:00	64.22414195	-132.5308573	7124315.937	619779.7049	siltstone	clastic	10	15
2018CClp018	2018-07-24T10:22:54010:00	64.22371679	-132.5310446	7124268.234	619772.458	sandstone and siltstone	clastic	10	15
2018CClp019	2018-07-24T10:50:40010:00	64.22314353	-132.5301748	7124206.026	619817.1178	siltstone	clastic and carbonate	10	15
2018CClp020	2018-07-24T11:59:19010:00	64.22244153	-132.5291429	7124129.787	619870.1953	sandstone	clastic	10	15
2018CClp021	2018-07-24T11:52:54010:00	64.22229885	-132.5290255	7124114.119	619876.5086	sandstone and siltstone	clastic	20	25
2018CClp022	2018-07-24T12:34:27010:00	64.22181461	-132.5285769	7124061.034	619900.3589	sandstone and siltstone	clastic	20	25
2018CClp023	2018-07-24T13:05:49010:00	64.22126077	-132.5277392	7124000.931	619943.382	sandstone and siltstone	clastic	40	50
2018CClp024	2018-07-24T13:38:39010:00	64.22104772	-132.5276811	7123977.312	619947.1236	siltstone	clastic	15	20
2018CClp025	2018-07-25T08:42:31010:00	64.19871353	-132.7277285	7121127.755	610333.7949	conglomerate and sandstone	clastic	15	20
2018CClp026	2018-07-25T09:12:34010:00	64.19847318	-132.7283956	7121099.827	610302.3663	siltstone and sandstone	clastic	25	30
2018CClp027	2018-07-25T10:08:39010:00	64.1980831	-132.7315139	7121050.978	610152.5531	conglomerate, sandstone, mudstone	clastic	5	10
2018CClp028	2018-07-25T10:32:59010:00	64.19808197	-132.7323268	7121049.445	610113.0983	siltstone	clastic	60	70
2018CClp029	2018-07-25T11:59:44010:00	64.19969205	-132.7348835	7121224.356	609982.6032	conglomerate and sandstone	clastic	10	15
2018CClp030	2018-07-25T12:44:08010:00	64.20017427	-132.735316	7121277.319	609959.6997	mudstone and sandstone	clastic	5	10
2018CClp031	2018-07-25T13:05:35010:00	64.20043507	-132.7354062	7121306.211	609954.2836	mudstone and sandstone	clastic	5	10
2018Cclp032	2018-07-25T13:20:36010:00	64.20057672	-132.7358287	7121321.259	609933.2166	mudstone and sandstone	clastic	30	40
2018CClp033	2018-07-25T14:21:44010:00	64.20296223	-132.7366754	7121585.498	609882.6665	sandstone	clastic	5	5
2018CClp034	2018-07-25T15:28:50010:00	64.20342797	-132.7391798	7121633.051	609759.273	conglomerate and sandstone	clastic	10	15
2018Cclp035	2018-07-25T15:34:44010:00	64.20328848	-132.7396811	7121616.649	609735.496	siltstone	clastic	15	20
2018CClp036	2018-07-25T16:00:07010:00	64.20427113	-132.7434214	7121719.654	609550.0846	sandstone, conglomerate and siltstone	clastic	10	15
2018Cclp037	2018-07-25T16:31:01010:00	64.20428374	-132.7442365	7121719.654	609510.4786	mudstone and sandstone	clastic	15	20
2018Cclp038	2018-07-25T16:42:53010:00	64.20437881	-132.7460329	7121727.153	609422.9208	sandstone, conglomerate and siltstone	clastic	10	15
2018Cclp039	2018-07-25T17:08:00010:00	64.2045643	-132.7476993	7121744.949	609341.3166	siltstone and sandstone	clastic	10	15

2018CClp040	2018-07-25T17:19:08010:00	64.20466628	-132.7485011	7121754.929	609302.0003	mudstone and sandstone	clastic	15	20
2018CClp041	2018-07-25T17:24:20010:00	64.20473769	-132.7489004	7121762.198	609282.34	conglomerate and siltstone	clastic	10	15
2018CClp042	2018-07-26T11:22:14010:00	64.20474549	-132.7536676	64.20474549	-132.7536676	tilite	clastic	15	20
2018CClp043	2018-07-26T11:45:23010:00	64.20508956	-132.754652	64.20508956	-132.754652	siltstone and sandstone	clastic	20	25
2018CClp044	2018-07-26T12:32:52010:00	64.20569179	-132.7573094	64.20569179	-132.7573094	heterolithic	clastic	20	25
2018CClp045	2018-07-26T13:09:51010:00	64.20655863	-132.757724	64.20655863	-132.757724	heterolithic	clastic	10	15
2018CClp046	2018-07-26T15:34:25010:00	64.20806842	-132.7577273	64.20806842	-132.7577273	mudstone and sandstone	clastic	20	25
2018CClp047	2018-07-26T16:00:35010:00	64.20872083	-132.7574231	64.20872083	-132.7574231	siltstone	clastic	20	25
2018CClp048	2018-07-26T16:19:26010:00	64.20892136	-132.7571106	64.20892136	-132.7571106	heterolithic	clastic	10	15
2018CClp049	2018-07-26T16:26:56010:00	64.20899131	-132.7575897	64.20899131	-132.7575897	heterolithic	clastic	20	25
2018CClp050	2018-07-26T16:37:12010:00	64.20915477	-132.7577919	64.20915477	-132.7577919	heterolithic	clastic	10	15
2018CClp051	2018-07-26T16:44:57010:00	64.20934626	-132.7588	64.20934626	-132.7588	siltstone	clastic	10	15
2018CClp052		64.25792095	-132.7334931	609818.928	7127712.415	heterolithic	clastic	400	400
2018CClp053		64.25819704	-132.733821	609801.949	7127742.6	dolostone	clastic and carbonate	1	1
2018CClp054		64.25819704	-132.733821	609801.949	7127742.6	dolostone	carbonate	2	2
2018CClp055		64.25802594	-132.7354351	609724.45	7127720.757	limestone	carbonate	100	100
2018CClp056		64.25664502	-132.739511	609532.491	7127559.92	limestone	carbonate	20	25
2018CClp057		64.256749	-132.7402989	609493.914	7127570.145	floatstone and limestone	carbonate	20	25
2018CClp058		64.25687598	-132.7405718	609480.192	7127583.818	shale and limestone	carbonate	20	25
2018CClp059		64.25700806	-132.7419109	609414.805	7127596.225	limemudstone	carbonate	20	25
2018CClp060		64.25709005	-132.7418871	609415.633	7127605.398	floatstone and shale	clastic	100	100
2018CClp061		64.25825398	-132.745713	609225.717	7127728.463	siltstone and shale	clastic	30	40
2018CClp062		64.25871193	-132.746993	609161.906	7127777.274	shale	clastic	30	40
2018CClp063		64.25960395	-132.7501131	609007.266	7127871.277	rudstone and limemudstone	carbonate	30	40
2018CClp064		64.26016308	-132.752162	608905.827	7127930.045	rudstone and limemudstone	carbonate	20	25
2018CClp065		64.26026296	-132.752335	608897.055	7127940.874	siltstone	clastic	50	60
2018CClp066		64.26181303	-132.758094	608612.036	7128103.678	siltstone	clastic	20	25
2018CClp067		64.26427001	-132.7620889	608408.929	7128370.529	sandstone and siltstone	clastic	140	150
2018CClp068		64.25313205	-132.7146221	610752.157	7127211.743	conglomerate, sandstone and siltstone	clastic	400	400
2018CClp070	29-07-2018 12:44	64.24402104	-132.770115	608099.352	7126101.458	shale and siltstone	clastic	200	200
2018CClp071	29-07-2018 12:53	64.24402104	-132.770115	608099.352	7126101.458	dolostone and rudstone	clastic	5	5
2018CClp072	29-07-2018 13:12	64.24396495	-132.7698391	608112.944	7126095.679	heterolithic	clastic	100	100

SAMPLEID	Sample Type	NAD83Z8_E	NAD83Z8_N	Lithology	AREA	Description
V999551	geochemistry	619374.0991	7124695.346	Dolostone	2	finely crystalline, silty
V999552	geochemistry	619364.8714	7124705.562	Dolostone	2	finely crystalline, silty
V999553	geochemistry	619352.9161	7124716.999	Siltstone	2	siliceous
V999554	geochemistry	619290.3898	7124740.434	Dolostone	2	wavy laminated
V999555	geochemistry	619206.097	7124809.642	Mudstone	2	laminated
V999556	geochemistry	619403.9025	7124662.761	Mudstone	2	laminated, quartz clasts
V999557	geochemistry	619593.4441	7124523.007	Dolostone	2	finely crystalline, laminated
V999558	geochemistry	619591.1815	7124507.165	Dolostone	2	karstic, silty
V999559	geochemistry	619651.7253	7124424.005	Carbonate breccia	2	limestone clasts, matrix supported
V999560	geochemistry	619688.7768	7124414.445	Dolostone	2	finely crystalline
V999561	geochemistry	619713.1653	7124387.316	Dolostone	2	finely crystalline, silty
V999562	geochemistry	619818.053	7124206.728	Dolostone	2	concretion, finely laminated, finely crystalline
V999563	geochemistry	619860.1403	7124169.133	Siltstone	2	finely laminated, siliceous
V999564	geochemistry	619925.3776	7124028.76	Siltstone	2	finely laminated, siliceous
V999565	geochemistry	619947.1236	7123974.74	Siltstone	2	finely laminated, siliceous
V999566	geochemistry	619946.6117	7124055.967	Siltstone	2	finely laminated, siliceous
V999567	geochemistry	610478.2878	7120384.763	Siltstone	1SE	siltstone, base of olive green mudrock to tillite unit
V999568	geochemistry	610053.3613	7121044.739	Mudstone	1SE	olive green mudrock, convolute laminae
V999569	geochemistry	609986.4959	7121234.366	Siltstone	1SE	olive green, within conglomeratic unit
V999570	geochemistry	609959.6997	7121277.319	Mudstone	1SE	brown mudrock
V999571	geochemistry	609940.4396	7121317.046	Mudstone	1SE	olive green mudrock unit, convolute laminae
V999572	geochemistry	609915.7619	7121347.141	Mudstone	1SE	brown mudrock
V999573	geochemistry	609905.5308	7121383.858	Mudstone	1SE	brown mudrock
V999574	geochemistry	609885.0741	7121581.285	Mudstone	1SE	brown mudrock
V999575	geochemistry	609818.928	7127712.415	Mudstone	1NW	Ice Brook Fm, upper heterolithic clastic beds, interbedded with conglomerate
V999579	geochemistry	609785.371	7127735.529	Dolosiltstone	1NW	Ice Brook Fm, laminated, top cap carbonate beds?
V999580	geochemistry	609724.45	7127720.757	Lime mudstone	1NW	Sheepbed Fm lower, thin bed
V999582	geochemistry	609684.967	7127709.883	Lime mudstone	1NW	Sheepbed Fm middle, laminated
V999584	geochemistry	609567.527	7127556.927	Lime mudstone	1NW	Sheepbed Fm middle, wavy laminated
V999586	geochemistry	609532.491	7127559.92	Lime mudstone	1NW	Sheepbed Fm middle, platy weathering with ?trace fossils
V999588	geochemistry	609489.229	7127574.769	Floatstone	1NW	Sheepbed Fm top, angular to subround clasts float in carbonate matrix
V999590	geochemistry	609413.364	7127623.052	Lime mudstone	1NW	Sheepbed Fm top, platy weathering, argillaceous
V999592	geochemistry	609293.468	7127708.001	Lime mudstone	1NW	Sheepbed Fm top, wavy laminated
V999594	geochemistry	608872.966	7127970.583	Rudstone	1NW	Gametrail Fm, limestone clasts
V999596	geochemistry	608903.351	7127926.044	Rudstone	1NW	Gametrail Fm, limestone clasts
V999598	geochemistry	608894.974	7127935.345	Siltstone	1NW	middle Blueflower Fm, laminated
V999600	geochemistry	608459.756	7128241.943	Siltstone	1NW	upper Blueflower Fm, finely laminated
V999601	geochemistry	608785.183	7128016.211	Dolosiltstone	1NW	mid Blueflower Fm, finely laminated
V999603	geochemistry	608057.246	7126115.026	Siltstone	1NW	?Cambrian, finely laminated
V999604	geochemistry	608099.352	7126101.458	Dolostone	1NW	?Risky Fm, coarse crystalline
V999503	geochemistry	607815.289	7124941.622	Dolostone	1NW	Silty dolostone, Potential upper Blueflower?
V999504	geochemistry	607778.625	7125016.065	Dolostone	1NW	Silty dolostone, Potential upper Blueflower?
V999505	geochemistry	607752.731	7125021.71	Floatstone	1NW	Limestone clasts, matrix supported
V999506	geochemistry	607630.684	7125043.453	Dolostone	1NW	Silty dolostone, Potential upper Blueflower?

Appendix VI

Geochemical Assay Certificates

SAMPLEID	Sample Type	NAD83Z8	NAD83Z8	Lithology	AREA	Description
V999551	geochemistry	619374.1	7124695	Dolostone	2	finely crystalline, silty
V999552	geochemistry	619364.9	7124706	Dolostone	2	finely crystalline, silty
V999553	geochemistry	619352.9	7124717	Siltstone	2	siliceous
V999554	geochemistry	619290.4	7124740	Dolostone	2	wavy laminated
V999555	geochemistry	619206.1	7124810	Mudstone	2	laminated
V999556	geochemistry	619403.9	7124663	Mudstone	2	laminated, quartz clasts
V999557	geochemistry	619593.4	7124523	Dolostone	2	finely crystalline, laminated
V999558	geochemistry	619591.2	7124507	Dolostone	2	karstic, silty
V999559	geochemistry	619651.7	7124424	Carbonate breccia	2	limestone clasts, matrix supported
V999560	geochemistry	619688.8	7124414	Dolostone	2	finely crystalline
V999561	geochemistry	619713.2	7124387	Dolostone	2	finely crystalline, silty
V999562	geochemistry	619818.1	7124207	Dolostone	2	concretion, finely laminated, finely crystalline
V999563	geochemistry	619860.1	7124169	Siltstone	2	finely laminated, siliceous
V999564	geochemistry	619925.4	7124029	Siltstone	2	finely laminated, siliceous
V999565	geochemistry	619947.1	7123975	Siltstone	2	finely laminated, siliceous
V999566	geochemistry	619946.6	7124056	Siltstone	2	finely laminated, siliceous
V999567	geochemistry	610478.3	7120385	Siltstone	1SE	siltstone, base of olive green mudrock to tillite unit
V999568	geochemistry	610053.4	7121045	Mudstone	1SE	olive green mudrock, convolute laminae
V999569	geochemistry	609986.5	7121234	Siltstone	1SE	olive green, within conglomeratic unit
V999570	geochemistry	609959.7	7121277	Mudstone	1SE	brown mudrock
V999571	geochemistry	609940.4	7121317	Mudstone	1SE	olive green mudrock unit, convolute laminae
V999572	geochemistry	609915.8	7121347	Mudstone	1SE	brown mudrock
V999573	geochemistry	609905.5	7121384	Mudstone	1SE	brown mudrock
V999574	geochemistry	609885.1	7121581	Mudstone	1SE	brown mudrock
V999575	geochemistry	609818.9	7127712	Mudstone	1NW	Ice Brook Fm, upper heterolithic clastic beds, interbedded with conglomerate
V999579	geochemistry	609785.4	7127736	Dolosiltstone	1NW	Ice Brook Fm, laminated, top cap carbonate beds?
V999580	geochemistry	609724.5	7127721	Lime mudstone	1NW	Sheepbed Fm lower, thin bed
V999582	geochemistry	609685	7127710	Lime mudstone	1NW	Sheepbed Fm middle, laminated
V999584	geochemistry	609567.5	7127557	Lime mudstone	1NW	Sheepbed Fm middle, wavy laminated
V999586	geochemistry	609532.5	7127560	Lime mudstone	1NW	Sheepbed Fm middle, platy weathering with ?trace fossils
V999588	geochemistry	609489.2	7127575	Floatstone	1NW	Sheepbed Fm top, angular to subround clasts float in carbonate matrix
V999590	geochemistry	609413.4	7127623	Lime mudstone	1NW	Sheepbed Fm top, platy weathering, argillaceous
V999592	geochemistry	609293.5	7127708	Lime mudstone	1NW	Sheepbed Fm top, wavy laminated
V999594	geochemistry	608873	7127971	Rudstone	1NW	Gametrail Fm, limestone clasts
V999596	geochemistry	608903.4	7127926	Rudstone	1NW	Gametrail Fm, limestone clasts
V999598	geochemistry	608895	7127935	Siltstone	1NW	middle Blueflower Fm, laminated
V999600	geochemistry	608459.8	7128242	Siltstone	1NW	upper Blueflower Fm, finely laminated
V999601	geochemistry	608785.2	7128016	Dolosiltstone	1NW	mid Blueflower Fm, finely laminated
V999603	geochemistry	608057.2	7126115	Siltstone	1NW	?Cambrian, finely laminated
V999604	geochemistry	608099.4	7126101	Dolostone	1NW	?Risky Fm, coarse crystalline
V999503	geochemistry	607815.3	7124942	Dolostone	1NW	Silty dolostone, Potential upper Blueflower?
V999504	geochemistry	607778.6	7125016	Dolostone	1NW	Silty dolostone, Potential upper Blueflower?
V999505	geochemistry	607752.7	7125022	Floatstone	1NW	Limestone clasts, matrix supported
V999506	geochemistry	607630.7	7125043	Dolostone	1NW	Silty dolostone, Potential upper Blueflower?

SAMPLEID	Ag_ppm	Al_pct	As_ppm	Ba_ppm	Be_ppm	Bi_ppm	Ca_pct	Cd_ppm	Ce_ppm	Co_ppm	Cr_ppm	Cs_ppm	Cu_ppm	Fe_pct	Ga_ppm	Ge_ppm	Hf_ppm	In_ppm	K_pct	La_ppm	Li_ppm	Mg_pct	Mn_ppm	Mo_ppm
V999551	0.01	2	11.2	120	0.72	0.12	16.45	0.32	23.5	8.5	20	1.67	23.7	5.37	5.84	0.06	1	0.041	0.81	10.5	5.3	7.96	2500	0.18
V999552	0.02	3.02	2	180	1.19	0.16	13.6	0.25	35.6	5.5	23	2.96	16.7	5.86	9.48	0.08	1.4	0.055	1.2	16.9	15.9	6.46	2220	0.27
V999553	0.03	8.15	3.9	250	1.31	0.24	1.64	0.95	51.8	25.2	105	3.67	170.5	6.86	20.1	0.13	2.1	0.141	1.47	23.8	73.3	2.44	457	0.74
V999554	0.02	6.82	2.4	250	0.97	0.18	5.38	0.36	37.4	14.2	85	2.7	123.5	5.17	13.65	0.1	1.7	0.089	1.25	17	25.8	2.61	766	0.24
V999555	0.03	9.92	5.1	560	2.81	0.18	0.24	0.08	81.3	15	88	11.7	55.8	6.14	28.7	0.16	4.1	0.104	3.48	34.9	61.5	1.68	244	0.22
V999556	0.08	6.62	7.6	370	1.67	0.32	1.26	0.12	69.5	16.1	68	5.86	53.1	4.72	18.5	0.14	3	0.07	2.18	33.5	54.7	1.81	412	0.3
V999557	0.03	2.57	5	230	1.21	0.14	15.4	0.05	34.5	8.3	21	2.46	18.2	6.14	7.64	0.1	1.1	0.038	1.29	19.7	7.8	5.19	3320	0.61
V999558	0.01	1.05	3.1	80	0.36	0.05	31.8	0.03	21	3.1	9	0.62	7.6	1.79	2.27	0.07	0.4	0.012	0.27	10.6	5	0.49	1630	0.18
V999559	0.03	2.17	2.7	130	0.73	0.09	26.8	0.04	24.5	8.1	22	2.2	17.1	1.79	6.1	0.07	0.8	0.023	0.83	11.6	13.8	0.7	531	0.1
V999560	0.04	5.36	6.7	240	1.02	0.3	0.54	0.08	53.7	15.9	55	3.37	41.5	5.18	14.7	0.08	2.4	0.047	1.45	25.4	57.3	1.3	223	0.2
V999561	0.06	7.97	3.9	410	1.93	0.38	0.34	0.11	81.9	20.7	80	6.94	55.7	5.83	22.2	0.15	3.8	0.077	2.63	38.5	68.8	1.62	334	0.18
V999562	0.11	2.37	6.9	110	0.55	0.11	0.06	0.03	30	3.8	25	1.53	45.7	2.95	7.15	0.06	1.2	0.035	0.56	15.4	33.3	0.53	75	0.4
V999563	0.05	6.56	5.1	310	1.54	0.24	1.17	0.06	64.2	13	68	4.6	50	4.92	18.05	0.12	3	0.065	2.1	30.7	54.8	1.54	495	0.18
V999564	0.04	6.48	2	390	1.47	0.18	4.32	0.1	65.3	12.8	67	4.99	52.7	3.93	18.55	0.12	3.3	0.071	2.46	32.2	32.9	2.22	808	0.44
V999565	0.08	7.65	5.7	470	2.34	0.21	1.31	0.17	80.8	12.9	78	6.29	57.6	4.59	22.5	0.15	3.5	0.081	2.88	39.2	53.2	1.66	282	0.17
V999566	0.05	6.74	3.8	350	1.59	0.21	2.96	0.04	64.6	17	70	4.34	54.2	5.26	18.85	0.14	3.2	0.067	2.2	31	54.7	2.56	767	0.11
V999567	0.08	6.83	4.5	100	1.02	0.18	3.46	0.19	41.8	35.7	69	3.22	139.5	7.76	19.15	0.1	2.4	0.087	1.04	19.4	47.6	3.52	664	0.25
V999568	0.08	6.89	3.7	960	1.01	0.16	4.79	0.28	43	31.4	78	3.06	160	7.37	18.5	0.1	1.8	0.091	0.97	19.7	46.3	3.37	995	0.33
V999569	0.12	5.43	20.4	190	1.29	0.31	1.98	0.28	45.6	24.6	36	5.51	54.1	5.53	15.2	0.1	2.8	0.063	1.85	20.3	29.3	1.8	473	0.94
V999570	0.05	6.79	3.3	380	1.74	0.26	0.43	0.07	63.8	24.3	73	8.05	96.7	5.92	18.95	0.13	3.5	0.081	2.15	27.2	26.6	1.26	171	0.32
V999571	0.1	7.87	13	110	1.84	0.32	1.62	0.58	63.5	41.4	73	7.09	156	8.25	23.7	0.15	2.8	0.132	2.02	26.7	41.3	2.65	646	0.57
V999572	0.11	6.76	3.7	100	0.92	0.22	2.98	0.53	46.5	37.1	62	3.49	178	7.91	19.05	0.12	2.1	0.104	1.06	21.9	40.9	2.92	845	0.34
V999573	0.08	7.63	3.1	320	1.45	0.27	0.97	0.27	54.2	39.4	73	5.26	192.5	8.87	23.4	0.13	2.1	0.131	1.46	23.9	52.7	3.28	491	0.32
V999574	0.1	7.3	4.1	320	1.44	0.27	0.96	0.25	51.6	34.4	71	4.14	178.5	8.07	22.3	0.19	2.9	0.122	1.29	23.6	54.5	2.93	424	0.27
V999575	0.04	5.86	3.8	220	1.39	0.16	6.86	0.26	44.3	25.8	58	3.58	124.5	6.54	17.2	0.17	2.5	0.073	1.25	20.3	50.7	3.21	1060	0.17
V999579	0.01	1.54	1.1	90	0.8	0.07	15.35	0.17	23	7	12	1.68	11.2	4.43	4.8	0.07	0.9	0.022	0.68	10.9	6	6.59	1340	0.11
V999580	0.01	0.56	1.4	240	0.29	0.03	34.8	0.1	18.2	3.2	7	0.47	6.7	0.75	1.43	0.08	0.5	0.006	0.15	8.5	4.4	0.25	676	0.27
V999582	0.04	1.84	2.2	180	0.9	0.09	29.7	0.19	37.7	7.2	19	2.58	19.8	1.99	5.06	0.1	0.9	0.023	0.6	17.5	13	0.51	917	0.61
V999584	0.02	1.24	1.8	160	0.47	0.06	29.9	0.09	28.3	4.8	12	1.41	10.4	1.47	3.26	0.09	1	0.013	0.34	13.4	10.9	0.38	464	0.2
V999586	0.01	0.4	0.3	130	0.16	0.03	35.8	0.04	9.44	2	4	0.42	4.3	0.42	1.07	0.08	0.2	0.00249	0.11	4.3	3.3	0.31	334	0.1
V999588	0.01	0.28	1	40	0.12	0.02	34.1	0.0099	4	1.7	3	0.16	3.4	0.79	0.7	0.08	0.2	0.00249	0.05	2	1.6	1.26	153	0.14
V999590	0.01	1.44	0.8	110	0.38	0.08	32.3	0.04	28.6	5.7	12	1.06	9.8	1.06	3.33	0.1	0.7	0.016	0.33	15.3	10	0.3	428	0.13
V999592	0.0049	0.82	0.5	150	0.26	0.03	35.2	0.02	10.85	1.6	8	0.79	5.4	0.39	2.15	0.08	0.4	0.006	0.26	5.6	5	0.23	112	0.05
V999594	0.01	0.45	0.8	40	0.22	0.02	36.5	0.0099	15.75	2.3	6	0.41	5.5	0.31	1.32	0.12	0.2	0.01	0.18	7.1	3.5	0.21	43	0.13
V999596	0.0049	0.16	0.099	20	0.21	0.01	37.1	0.0099	2.63	1.4	2	0.08	2.3	0.36	0.39	0.11	0.1	0.00249	0.02	1.3	1.9	0.27	149	0.1
V999598	0.0049	0.3	0.099	30	0.4	0.02	35.9	0.0099	5.86	1.9	4	0.11	3.7	1.08	0.68	0.05	0.2	0.00249	0.04	2.6	2.4	0.34	415	0.13
V999600	0.07	7.65	4.5	370	2.06	0.27	2.66	0.04	69.5	18.4	73	5.91	72.6	5.69	20.5	0.15	3.7	0.078	2.18	33	63.1	2.43	778	0.26
V999601	0.0049	1.5	1.7	80	0.63	0.05	32.2	0.03	29.8	1.8	12	1.09	10	0.71	3.76	0.09	0.7	0.015	0.55	15.3	9	0.27	146	0.07
V999603	0.02	7.03	6.8	390	2.39	0.2	8.04	0.07	89.2	26	41	3.71	29.8	5.87	19.95	0.13	2.6	0.079	2.13	44.1	73	3.07	3390	0.18
V999604	0.06	1.42	7	150	0.69	0.09	18.1	0.48	16.6	12.4	6	0.61	58.3	4.13	3.61	0.06	0.4	0.035	0.38	6.2	21.1	7.13	4620	2.35
V999605	0.03	1.04	4	90	0.47	0.07	13.05	0.07	16.65	4.1	23	0.72	8.8	3.44	2.85	0.07	0.8	0.016	0.42	7.9	7	3.42	1150	0.32
V999606	0.31	2.9	5.1	170	0.92	0.14	14.1	0.26	48.3	8.2	22	2.53	19	3.17	7.59	0.07	1.4	0.034	1.06	21.4	12.6	6.78	2320	2.34
V999607	0.03	3.09	3.7	210	0.68	0.11	20.1	0.08	36.5	7.1	29	2.24	20.1	2.66	6.87	0.09	1.6	0.03	0.69	16.7	28	1.44	1310	0.45
V999608	0.05	1.63	3.9	130	0.52	0.07	16.5	0.02	17.95	4.2	10	1.11	8.6	2.24	3.91	0.06	0.7	0.017	0.53	9.4	7	9.08	2280	1.11

SAMPLEID	Na_pct	Nb_ppm	Ni_ppm	P_ppm	Pb_ppm	Rb_ppm	S_pct	Sb_ppm	Sc_ppm	Sn_ppm	Sr_ppm	Ta_ppm	Te_ppm	Th_ppm	Tl_pct	Tl_ppm	U_ppm	V_ppm	W_ppm	Y_ppm	Zn_ppm	Zr_ppm
V999551	0.33	3.5	17.1	530	1.6	37.6	0.03	0.3	8.7	0.7	602	0.22	0.09	2.76	0.15	0.21	0.6	52	1.5	16.1	38	36
V999552	0.27	4.8	14.4	1260	3.4	57.5	0.08	0.22	11.8	1.1	386	0.31	0.07	4.18	0.174	0.3	1	66	0.7	22.5	50	52.4
V999553	2.25	10.7	89	780	4.9	64.6	0.07	0.28	31.1	2	72.3	0.64	0.18	5.46	0.827	0.47	1.1	268	1.6	21.6	150	72.5
V999554	2.75	8.3	39.4	590	2.8	56.2	0.19	0.21	27.3	1.4	169.5	0.51	0.13	3.94	0.7	0.34	0.8	196	1.4	17	83	56.9
V999555	0.64	12.7	43.9	650	11.3	129.5	0.0049	0.31	25.9	3.3	37	0.94	0.025	12.85	0.532	0.79	2.5	174	1.5	26.5	110	138.5
V999556	0.59	9.6	36.8	480	18	102	0.13	0.46	18.2	2.2	67.5	0.67	0.06	10.35	0.46	0.53	1.9	137	1.2	18	91	103.5
V999557	0.12	3.1	14.1	270	10.9	62.8	0.3	0.74	8.3	0.9	567	0.23	0.025	3.75	0.128	0.3	1.1	44	0.6	21.4	36	37.9
V999558	0.37	1.2	4.8	140	3.1	12.6	0.12	0.27	3.7	0.3	1225	0.09	0.025	1.44	0.048	0.06	0.9	14	0.2	14.9	16	13.9
V999559	0.1	2.5	14.2	230	7.9	38.9	0.0049	0.52	6.8	0.7	651	0.18	0.025	2.81	0.11	0.19	1.4	38	0.3	8.3	26	26.7
V999560	0.28	7	39.2	410	31.9	69.1	0.01	0.44	10.4	1.4	38.1	0.5	0.11	7.36	0.34	0.34	1.4	97	0.9	12.9	121	77.5
V999561	0.45	11.6	45.1	600	25.5	125.5	0.03	0.4	19.7	2.5	39	0.84	0.11	12.3	0.525	0.62	2.4	148	1.4	24.3	116	131
V999562	0.07	2.7	14.1	70	19.9	26.8	0.04	1.04	5.4	0.6	11.5	0.19	0.025	3.21	0.117	0.13	0.7	41	0.5	8	56	39.2
V999563	0.61	9.5	35.4	450	18.6	98.8	0.01	0.33	17	2.2	38.7	0.69	0.05	10.25	0.476	0.48	1.8	140	1.1	18	84	100
V999564	0.85	10.8	29.8	570	13.2	115	0.01	0.29	17.1	2	117	0.75	0.025	10	0.508	0.56	1.9	140	1.1	19.5	75	113.5
V999565	0.71	11.7	39.1	560	17.3	137	0.01	0.55	20.4	2.5	46.4	0.82	0.06	11.6	0.533	0.67	2.1	153	1.2	22.7	88	120
V999566	0.86	11.4	39.9	530	14.7	103	0.07	0.38	17.9	2.1	118	0.78	0.06	9.81	0.52	0.51	1.7	140	1.2	18.6	85	104.5
V999567	1.39	10.4	64.1	610	8.5	44.8	0.33	0.36	28	1.8	33.4	0.68	0.17	4.22	0.748	0.27	1	240	0.7	22.6	116	78.3
V999568	1.72	9.8	57.8	560	11	43.8	0.11	0.36	28.7	1.8	91.3	0.63	0.12	3.94	0.786	0.26	1	221	0.7	22.9	99	66.6
V999569	0.13	8.9	41.3	410	24.7	73.9	0.14	0.95	11	1.9	18.2	0.61	0.07	7.47	0.324	0.42	1.7	89	0.9	18.6	95	92.8
V999570	0.62	16.6	49.4	440	6.4	91	0.05	0.4	18.2	2.1	28.8	1.04	0.26	7.47	0.639	0.55	1.7	176	1.1	22.6	94	119
V999571	0.88	19.8	61.1	710	13.1	85.6	0.67	0.61	29.3	2.9	22.3	1.2	0.37	6.59	0.745	0.6	1.4	239	1	26.8	114	101
V999572	1.39	13.2	59.7	570	11.1	47.9	0.21	0.36	26.4	2	46.1	0.84	0.26	4.24	0.693	0.34	1.1	198	1.2	22.2	114	80
V999573	1.12	17.5	63.3	760	9.5	60.8	0.1	0.35	31.2	2.5	31.7	1.01	0.35	4.86	0.806	0.41	1.1	262	0.8	26.3	120	81.4
V999574	1.01	16.6	64.5	760	9.1	54.9	0.02	0.38	29.4	2.3	30.9	1.07	0.37	4.87	0.765	0.33	1.2	252	0.7	25.8	115	107.5
V999575	0.74	9.1	46.8	470	4.8	57.5	0.15	0.28	24.6	1.7	186.5	0.62	0.13	4.67	0.59	0.28	1.1	202	0.8	22.4	91	88
V999579	0.03	2.8	12.6	190	2.1	30.9	0.03	0.18	4.6	0.5	207	0.21	0.025	2.48	0.102	0.14	0.5	35	0.3	11.6	38	32.5
V999580	0.08	0.9	4.3	4990	2	7.3	0.08	0.14	6.9	0.2	4540	0.07	0.025	0.94	0.034	0.05	2.5	14	0.2	18.2	12	47.8
V999582	0.1	2.9	12.1	1150	5.7	31.3	0.27	0.27	7.1	0.6	1690	0.2	0.025	2.96	0.121	0.16	1.9	37	0.4	18.9	38	34.9
V999584	0.23	2.5	6.5	250	4.1	18.3	0.29	0.25	4	0.4	2760	0.18	0.025	2.61	0.092	0.11	1.7	20	0.3	18.7	21	35.5
V999586	0.08	0.6	1.7	220	1.6	5.8	0.09	0.14	1.6	0.99	2390	0.0249	0.025	0.72	0.02	0.06	2.2	7	0.1	12.3	7	7.9
V999588	0.1	0.5	1	260	1.3	2.7	0.15	0.11	0.8	0.99	754	0.0249	0.025	0.47	0.017	0.04	1	5	0.1	3.1	2	6.9
V999590	0.43	2	7.6	200	5.1	17.5	0.01	0.2	4.1	0.4	1750	0.15	0.025	2.49	0.073	0.09	2.3	22	0.3	13.8	20	24.3
V999592	0.18	1.1	1	240	1.1	13.2	0.0049	0.12	2.6	0.2	1815	0.08	0.025	1.26	0.045	0.06	1.3	14	1	5.9	8	13.9
V999594	0.01	0.6	2.6	520	3.2	7.8	0.04	0.15	2.4	0.99	4510	0.0249	0.025	0.91	0.024	0.05	2.2	9	0.1	6.6	7	7.7
V999596	0.01	0.2	0.4	310	0.5	1.2	0.0049	0.13	0.6	0.99	1620	0.0249	0.025	0.24	0.009	0.099	0.7	3	0.2	1.5	3	4.2
V999598	0.01	0.5	1.1	260	1.2	2.1	0.05	0.11	1.1	0.99	1730	0.0249	0.025	0.52	0.02	0.02	0.8	6	0.1	3.9	4	8.3
V999600	0.7	13	40.6	630	15.3	101	0.03	0.49	19.6	2.3	60.5	0.95	0.06	11.15	0.577	0.47	2.2	147	1.5	23.6	91	131.5
V999601	0.3	2.3	2.4	230	3.1	25.4	0.01	0.15	3.8	0.4	2290	0.17	0.025	2.87	0.073	0.11	3.3	17	0.3	12.2	15	25.9
V999603	0.41	9.5	40.3	500	14.3	99.4	0.88	0.46	18.8	2.2	363	0.76	0.025	14.5	0.252	0.49	2	78	1.3	28.9	64	90
V999604	0.11	2.4	21.2	210	34.4	16.5	1.18	0.33	9.2	0.4	549	0.11	0.09	2.05	0.047	0.11	1.6	36	0.5	26.1	90	14.1
V999503	0.1	2	6.4	240	7.4	19.9	0.32	0.36	2.6	0.4	341	0.14	0.025	2.04	0.079	0.13	0.6	17	0.8	8.1	17	32.2
V999504	0.41	5.2	20.9	430	10.2	48.4	0.32	0.59	6.1	0.9	175	0.4	0.025	5.11	0.146	0.33	6.2	124	0.6	18.8	62	52
V999505	0.87	5.2	14.1	490	8.1	35	0.24	0.33	9	0.8	475	0.38	0.025	4.69	0.225	0.27	1.2	59	0.7	18.2	38	59.5
V999506	0.38	2.8	7.4	200	3.7	23.7	0.1	0.23	3.2	0.5	184.5	0.2	0.025	2.88	0.075	0.16	1.8	62	0.5	7.3	12	24.9

Appendix VII

Full Pyle/ Bennett Report

**Yukon Gold Project
East Central Yukon, Canada
Report On the Stratigraphy and Structure of the CL and HJ Claims.**

Summary Report

Prepared for:

**Carlincore Resources Ltd.
200-204 Lambert Street
Whitehorse YT
Y1A 3T2**

By:

Leanne Pyle (P.Geo., Ph.D.)
VI Geoscience Services Ltd.

And

Venessa Bennett (P.Geo., Ph.D, A.Dip (GIS/RS))
Geomantia Consulting

December 2018

KEY POINT SUMMARY

The CL, HJ and GY claim blocks of Carlincore Resources Ltd. area are located ca. 130 km, 145 km and 170 km northeast of Keno City in Central Yukon, respectively. Two subareas within the CL and HJ claim blocks of Carlincore Resources Ltd. were selected for an evaluation of the stratigraphic / structural setting to better assess mineral potential.

STRATIGRAPHIC INTERPRETATIONS

- ↗ Stratigraphy in Area 2 requires further work to determine age and stratigraphic position of the heterolithic package examined (220 to 330 m thick). Strata consist of mudrock (shale, mudstone and siltstone), sandstone, and conglomeratic sandstone with rare dolostone beds (about 5 m total carbonate or 0.02% of total section).
- ↗ Stratigraphy in the SE1 and 2 parts of Area 1 is interpreted to represent part of the Rapitan Group (lower Windermere Supergroup). Strata consist of mudrock, sandstone, conglomerate, and tillite containing dropstones, in two successions that are 100% siliciclastic (part 1, 250 to 350 m thick and part 2, 150 to 200 m thick).
- ↗ Stratigraphy in Area 1NW is represented by a composite section (1300 to 1400 m thick) of three ridge sections and contains about 20% carbonate and 80% heterolithic siliciclastics interpreted as units of the Windermere Supergroup. The lower part is the Rapitan Group (siliciclastic), overlain by the Ice Brook/Keele Formation (siliciclastic), Ravenstthroat Formation (cap carbonate), Sheepbed Formation (mixed fine siliciclastics and carbonate), Gametrail Formation (dominated by carbonate debrites), Blueflower Formation (siliciclastic), and possibly the Risky Formation (carbonate). The $\delta^{13}\text{C}$ chemostratigraphy of the Ravenstthroat Formation to ?Risky Formation succession shows a range of carbonate carbon isotope values from 9.30 to -9.15 ‰ in which carbon isotope anomalies are consistent with those defined for the succession elsewhere in the Wernecke and Mackenzie Mountains. The Sheepbed and Gametrail formations have stratigraphic equivalents within the Osiris cluster stratigraphy of the Rackla Gold Belt trend defined by ATAC Resources Ltd.

STRUCTURAL INTERPRETATIONS

- ↗ Area 2 consists of three structural domains, the largest of which is characterized by late NE and ENE brittle faults and associated shallow to moderate ENE plunging folds. A second structural domain is associated with a localized area of NW trending folds that predate the late ENE plunging folds. No mineralization was observed in this area.
- ↗ Area 1SE consists of an early generation of SSW shallow plunging tight to open folds within the Rapitan Group that is overprinted by a later generation of fault related folding. The later generation of folding is directly associated with a series of NE and ENE late brittle faults. Oxidized fluids (limonite – carbonate) are typically associated with these late faults. No mineralization was observed associated with these faults.
- ↗ Area 1NW represents a reasonably structurally intact stratigraphic section through the Windermere Supergroup. The dominant structural grain is NNE-trending and west-dipping. No major brittle-ductile shear zones or thrust faults where observed. The area is characterized by a suite of N, NE-ENE and NW late brittle structures that may be coeval and represent part of a Riedel shear system. Late NE-ENE faults are associated with open folding with ENE trending steep axial planes.

1.0 INTRODUCTION

The CL and HJ claim blocks of Carlincore Resources Ltd. area located ca. 130 km northeast of Keno City in Central Yukon (**Fig. 1**). The properties lie directly north of the Rackla Gold Belt trend recently defined by ATAC Resources Ltd., and have been the focus of exploration for sediment-hosted gold since 2014.

The CL and HJ claim blocks are located north the regional-scale Dawson thrust and Kathleen Lakes fault (**Fig. 1**). The Dawson thrust is interpreted to be a WNW-striking structure that demarcates the northern edge of Paleozoic Selwyn Basin. In contrast, the nature and significance of the Kathleen Lakes fault is poorly constrained, but is considered to represent a long-lived basement structure that may have seen structural reactivation as young as the Tertiary period.

Two subareas within the CL and HJ claim blocks of Carlincore Resources Ltd., were selected for an evaluation of the stratigraphic / structural setting to better assess mineral potential. A crucial component of sediment-hosted gold mineralization is the presence of both a favourable or chemically reactive host and a fluid corridor in which to transport mineralizing fluids.

Sediment-hosted gold occurrences on the ATAC Resources Ltd. property are considered to be hosted within Neoproterozoic to Cambrian slope facies stratigraphic units of the Windermere Supergroup. An important objective of the 2018 field program was to assess stratigraphic equivalencies between known Au-bearing stratigraphy on the ATAC property, and that present on CarlinCore Resources, CL and HJ claims. Publically available regional bedrock maps by (Yukon Geological Survey) indicate that the CL and HJ properties are underlain by Neoproterozoic Windermere Group strata or their equivalents.

Several detailed transects and two reconnaissance traverses were completed by Venessa Bennett and Leanne Pyle, through Aurora Geosciences Ltd., between July 22 and August 1st, 2018 (**Fig. 2**). Fieldwork focused on stratigraphic sections exposed along ridges and outcrop exposure in gullies within CarlinCore's CL (Area 1) and HJ (Area 2) properties.

The following report presents a summary of stratigraphic and structural observations for the CL and HJ claims across three main transects in Areas 1 and 2. A presentation of stratigraphic results is proceeded by a comparison to the proposed stratigraphic setting within the ATAC Resources Ltd. property and by a summary of the structural setting within the two focussed study areas. Four appendices are also provided including:

1. Summary of all stratigraphic observations
2. Outline of drone survey methodology and list of data products
3. Summary of geochemical sampling results
4. Overview of the Mappt™ digital data capture system

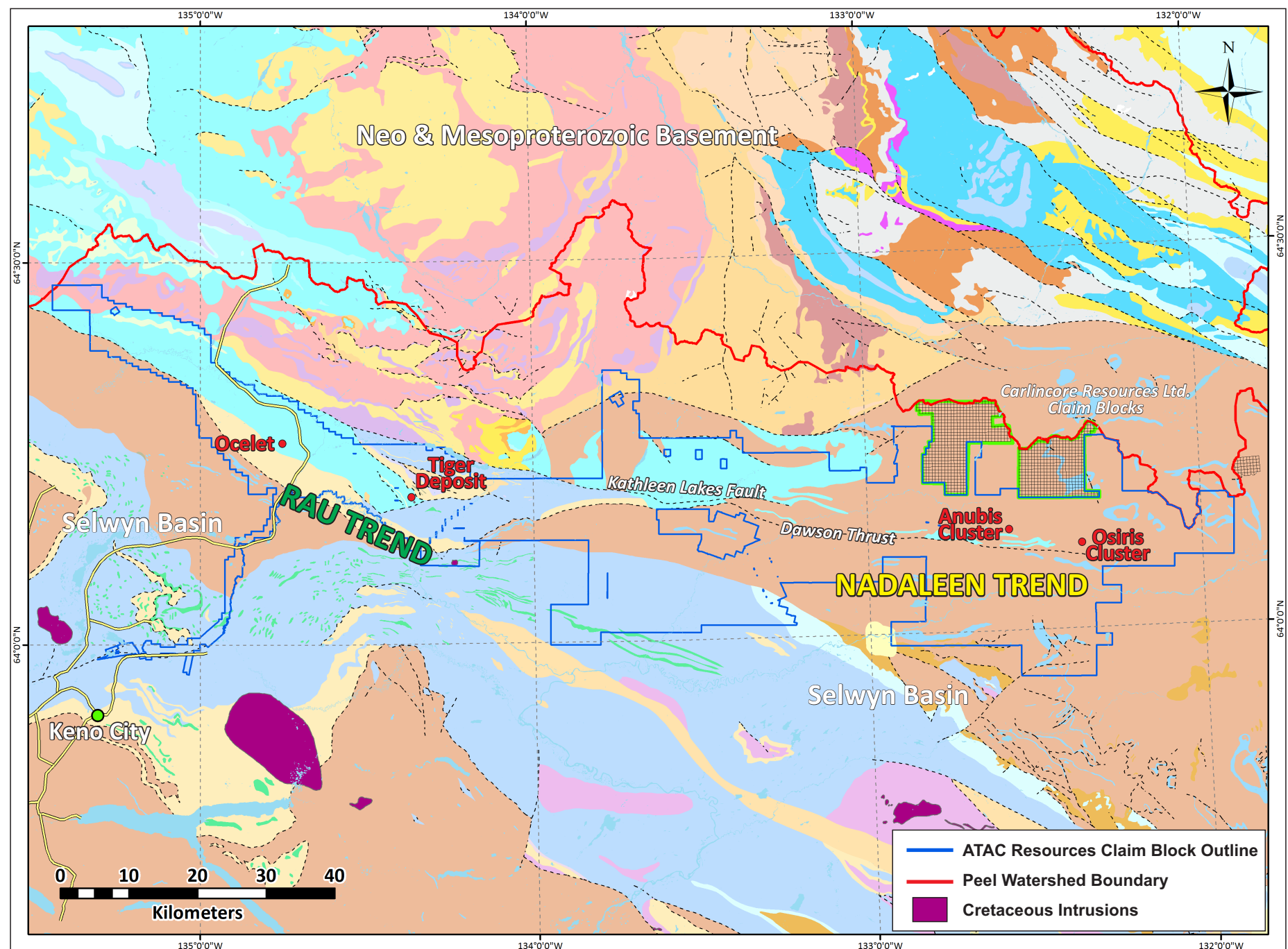


Figure 1: Regional geological setting of the Rackla Gold belt illustrating the distribution of Paleozoic basin, platform and Neo-& Mesoproterozoic basement rocks (Gordey and Makepeace, 1999; Yukon Digital Geology compilation). **Rau and Nadaleen Trends** marked in addition to location of Tiger Deposit, Ocelet and Osiris occurrences. Geographic Coordinate System - GCS North American1983

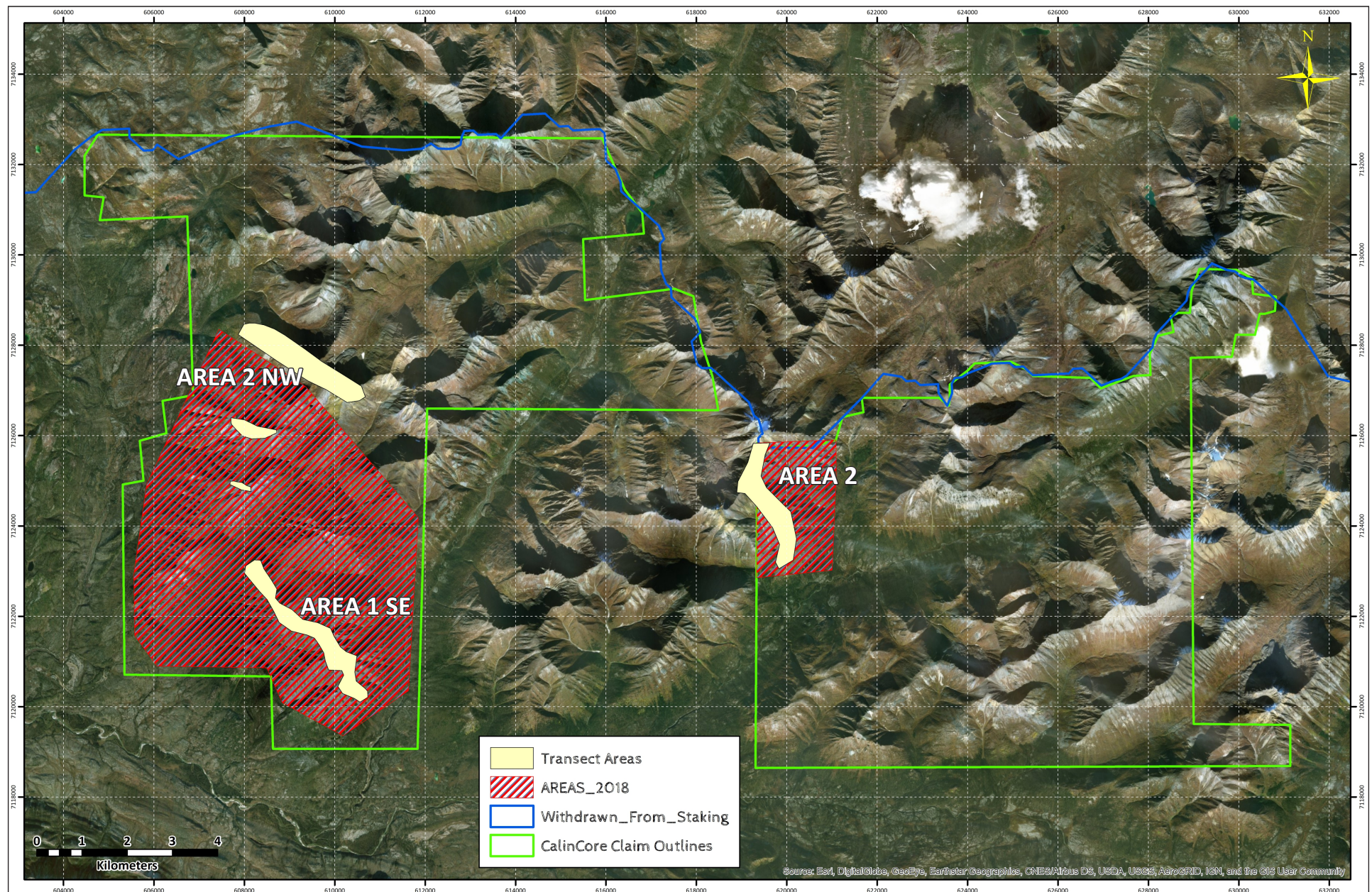


Figure 2: Location of Areas of Interest (AOI) and transects completed during the 2018 field season.

2.0 STRATIGRAPHIC EVALUATION OF THE CL AND HJ CLAIMS

Reconnaissance level stratigraphic studies were carried out within four stratigraphic successions, each with minor structural complications, in five transect areas during the 2018 fieldwork (**Fig. 2**): one in the NW part of Area 2, two within the SE part of Area 1, and three transects that make up a composite section for the NW part of Area 1. Stratigraphic observations, summarized in Appendix 1, aimed to:

- 1) Examine the lithostratigraphic framework/succession of units and estimate thicknesses;
- 2) Describe vertical and lateral stratal relationships, unit compositions, grain characteristics, bedding and sedimentary structures; and
- 3) Collect a suite of geochemical samples from representative lithologies from each section (n=45) and carbonate samples through the Ediacaran part of the upper Windermere Supergroup succession for potential carbon isotopic record analysis (n=19).

Northwest (NW) part of Area 2

A ridge section, about 220 to 330 m thick (**Fig. 3**), contains a heterolithic package of mudrock (shale, mudstone and siltstone), sandstone, and conglomeratic sandstone with rare cm-scale to dm-scale dolostone beds (about 5 m total carbonate or 0.02% of total section). The siliciclastic succession contains thin-bedded to thick-bedded, fine-grained to coarse-grained sandstone with poorly sorted quartz pebbles and granules, that alternates with fine-grained packages.

Fine-grained units contain graded beds of fine-grained sandstone with conglomeratic lenses or beds of quartz pebble-rich sandstone with scoured bed bases that grade into laminations of mudstone and siltstone (**Figs. 4 to 11**). Stratigraphy at this locality remains poorly understood and requires further work to determine age and stratigraphic position.

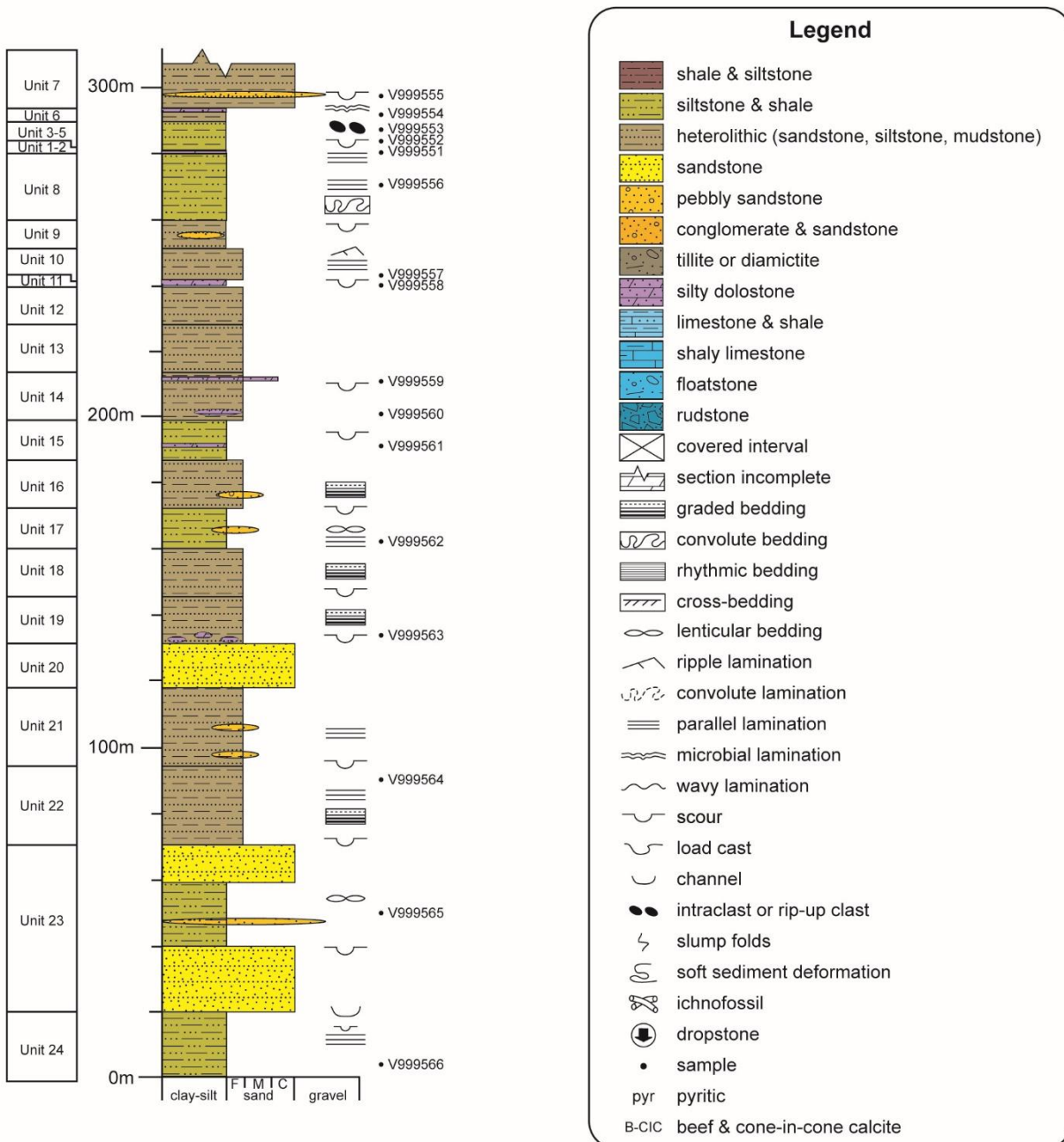
**Figure 3.** Stratigraphic log of the section in the NW part of Area 2, and legend for Figs. 12, 21, 27 and 39.



Figure 4. Siltstone (Unit 8) in foreground to heterolithic ridge-forming, massive beds of conglomeratic sandstone (Unit 7). Unit 2 dolostone at arrow (geologist for scale).



Figure 5. Yellowish-orange weathering, laminated, silty dolostone of Unit 2 (30 cm long hammer for scale).



Figure 6. Reddish-brown, pyritic, silty, finely laminated mudrock with pebbly sandstone interbeds containing angular to subround quartz pebbles (Unit 8).



Figure 7. Planar laminated to contorted beds at arrow (slump folds) in mudrock of Unit 8 (30 cm long hammer for scale).



Figure 8. Innumerable laminations of alternating mudrock and siltstone, with climbing ripples, at arrow (Unit 10).



Figure 9. Dolostone breccia interbed within siltstone (Unit 14) is differentially weathered, with scoured bed base, and rare algal laminated clasts.



Figure 10. Unit 24 in foreground to Unit 15 at ridge peak, contains sandstone in lower part of succession in NW part of Area 2 (at least 160 m thick for scale), compared to siltstone-dominated upper succession in background (at arrow).



Figure 11. Unit 24 contains siliceous, yellowish-brown and flaggy weathering siltstone in the base of the recessive part of the succession (30 cm long hammer for scale).

Southeast (SE) part of Area 1

The ridge to partially vegetation-covered “rubble-crop” traverse exposes about 250 to 350 m of 100% heterolithic siliciclastics (**Fig. 12**). Lithologies range from mudrock to sandstone and pebble to boulder conglomerate (**Figs. 13, 14**), interbedded with tillite containing dropstones (**Figs. 15, 16**). The reddish-brown or maroon weathering mudrock facies contains innumerable layers of olive green or brown mudstone and siltstone, with minor fine-grained sandstone in thin beds. Laminae and beds are planar and commonly contorted due to soft sediment deformation (**Figs. 17, 18**). Dropstones range in size from pebbles to boulders and make impact depressions within the encasing mudstone layers that were squeezed around the dropstone (**Figs. 15, 16**). Thick beds of polymictic conglomerate with erosive bed bases are interbedded with the mudstone (**Figs. 19, 20**).

Stratigraphy is interpreted to represent part of the Rapitan Group (lower Windermere Supergroup).

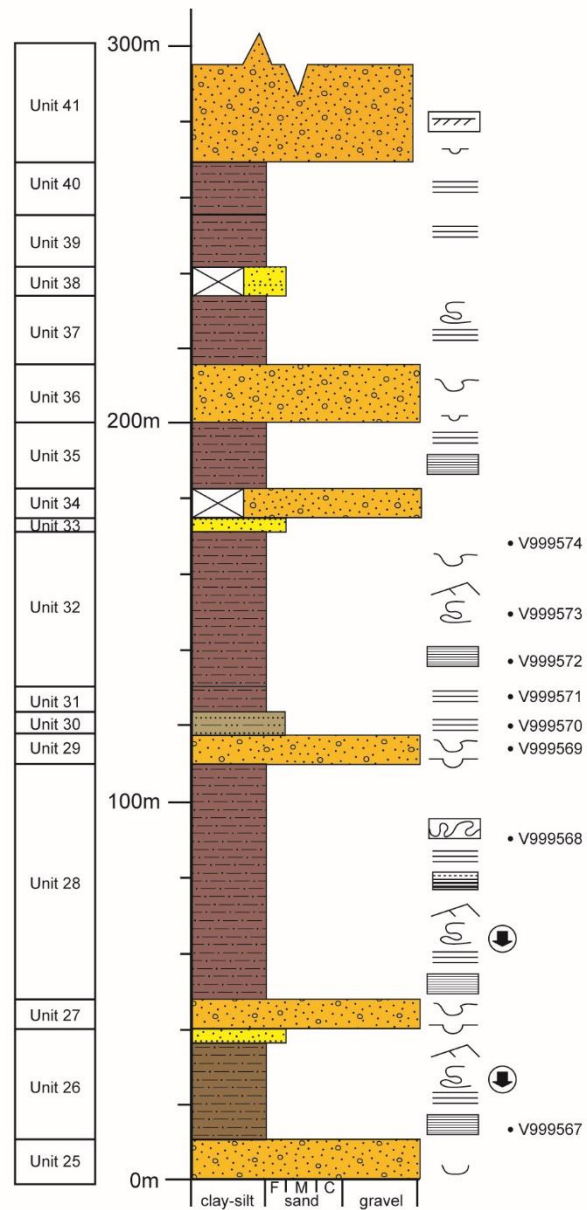


Figure 12. Stratigraphic log of the section in the SE part of Area 1.



Figure 13. Dark yellowish orange and blocky weathering conglomerate (Unit 25, foreground); view of SE part of Area 1 section, that consists of mainly reddish-brown (maroon) weathering mudrock (30 cm long hammer for scale).



Figure 14. Polymictic conglomerate in discontinuous beds with erosive bases (channelized) contains pebble to boulder sized clasts in fine-grained matrix, interbedded with pale olive mudstone and fine-grained sandstone (Unit 27; 30 cm long hammer for scale).

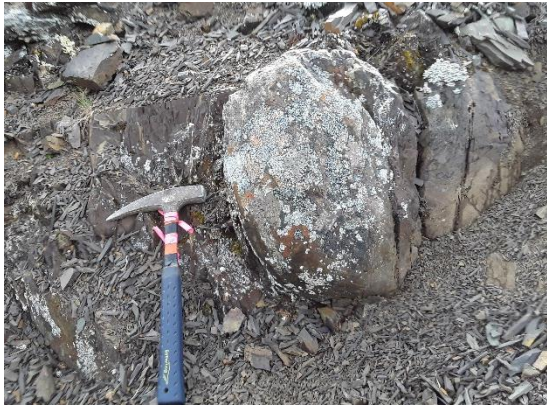


Figure 15. Boulder sized dropstone within reddish-brown weathering mudrock (Unit 28; 30 cm long hammer for scale at base of dropstone).



Figure 16. Dropstone (at arrow) with long axis perpendicular to bedding and impact depression in siltstone laminae that drape around clast (Unit 28).



Figure 17. Convolute bedding of siltstone (at 30 cm long hammer for scale) overlain by polymictic conglomerate (Unit 29).



Figure 18. Convolute laminae, soft-sediment deformation and flame structures (at arrow) in mudrock and fine-grained sandstone of Unit 32.



Figure 19. Discontinuous, thick polymictic conglomerate beds (Unit 36) have erosive bases (channelized; 30 cm long hammer for scale).



Figure 20. Conglomerate clasts are angular to subround, pebble to boulder sized, and matrix-supported in fine-grained sandstone (Unit 36).

SE2 part of Area 1

A second 100% heterolithic siliciclastic succession, estimated to be 150 to 200 m thick, is exposed within a gully to ridge to partially vegetation-covered “rubble-crop” traverse (Fig. 21). It is a heterolithic package with facies similar to those in the SE part of Area 1. The section begins in a tillite unit containing boulder-sized dropstones (Figs. 22, 23). Red-brown weathering mudstone units commonly exhibit convolute lamination and soft sediment deformation (Figs. 24, 25). Conglomerate units occur in the base and near the top of the section (Fig. 26).

Stratigraphy is interpreted to represent part of the Rapitan Group (lower Windermere Supergroup) and possibly the overlying Ice Brook/Keele Formation.

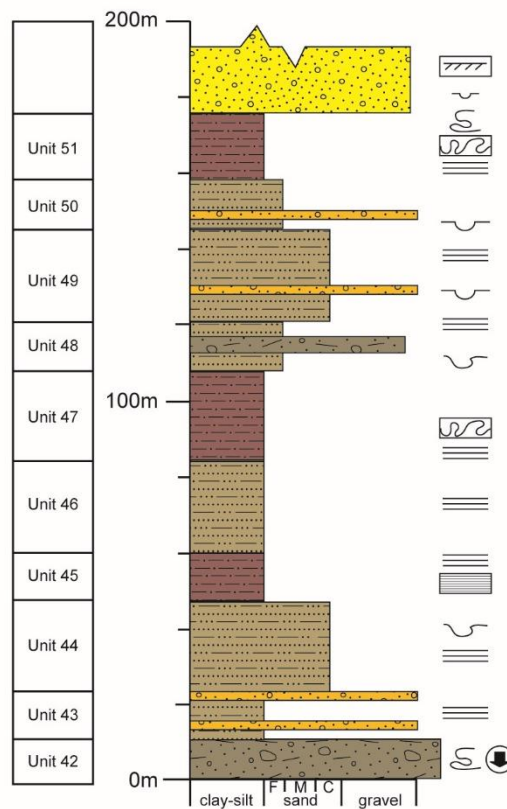


Figure 21. Stratigraphic log of the section in the SE2 part of Area 1.



Figure 22. Boulder-sized dropstone in cleaved, finely laminated mudrock that bends around dropstone (30 cm long hammer for scale; Unit 42).



Figure 23. Base of SE2 part of Area 1 section contains brown to greyish red weathering tillite containing common dropstones (30 cm long hammer for scale; Unit 42).



Figure 24. Interlaminated fine-grained sandstone and mudrock shows convolute laminae (above thumb for scale), and syn-sedimentary offsets of beds (at arrow; Unit 47).



Figure 25. Soft sedimentary deformation of thin bed of fine-grained sandstone (Unit 51; pen cap is 5 cm long for scale).



Figure 26. Discontinuous, polymictic conglomerate containing carbonate and ironstone clasts (at arrow; Unit 49; 30 cm long hammer for scale).

NW part of Area 1

A composite section of three ridge sections, 1300 to 1400 m thick, contains about 20% carbonate and 80% heterolithic siliciclastics (**Fig. 27**). The oldest part of the succession is exposed on the face of a structurally complicated ridge, overlain unconformably by about 400 m of a yellowish-brown to grey weathering, coarsening-upward package of thin bedded siltstone and medium to thick bedded, cross-bedded sandstone and conglomerate (**Fig. 28**). The oldest part of the succession contains a mixed package of maroon weathering mudrock and olive green tillite (**Fig. 29**). The overlying siliciclastic succession contains channelized conglomerate beds that are predominant in the upper part of the unit (**Fig. 30**).

A distinct dark yellowish orange weathering, finely laminated dolostone unit (less than 5 m thick) gradationally overlies the siliciclastic succession and is a prominent marker bed (**Figs. 31, 32**). The dolostone is abruptly overlain by a carbonate-dominated unit that is at least 340 m thick and contains black shale and siltstone at the base and top of the unit. This unit consists mainly of wavy, thin bedded, shaly limestone to lime mudstone cycles (**Fig. 33**) with intervals of erosive-based and slump-folded, medium to thick bedded floatstone that contains angular clasts up to pebble size that weather a variety of colours and resemble confetti within the light grey lime mudstone matrix (**Fig. 34**). A second prominent marker bed is a medium bedded to massive rudstone and limemudstone succession, at least 50 m thick, that contains matrix-supported intraformational, cobble sized intraclasts in beds with erosive bases interbedded with thin bedded dololimemudstone (**Fig. 35**). A heterolithic siliciclastic succession, at least 200 m thick, overlies the marker carbonate (**Fig. 36**). It is dominated by dark grey and brown weathering, thin bedded siltstone, mudstone, fine-grained sandstone, and minor conglomerate (**Fig. 37**). A complimentary section to the south exposes at least 200 m of this uppermost unit and contains a 5 m thick interval of dolomitic rudstone (**Fig. 38**).

This section is interpreted to contain seven formations of the Windermere Supergroup. The basal tillite and mudrock is likely the Rapitan Group, part of the lower Windermere Supergroup. It is abruptly overlain by mixed siliciclastics of the Ice Brook/Keele Formation, which grades upward into the distinct dark yellowish orange weathering dolostone that is the Ravensthorpe Formation cap carbonate. The mixed fine siliciclastics and limemudstone succession is equivalent to the Sheepbed Formation, which thickens upward to the light grey marker bed of carbonate debrites equivalent to the Gametrail Formation. The upper recessive part of the succession is equivalent to the Blueflower Formation, which may contain an upper carbonate unit, or this upper rudstone may be equivalent to the Risky Formation.

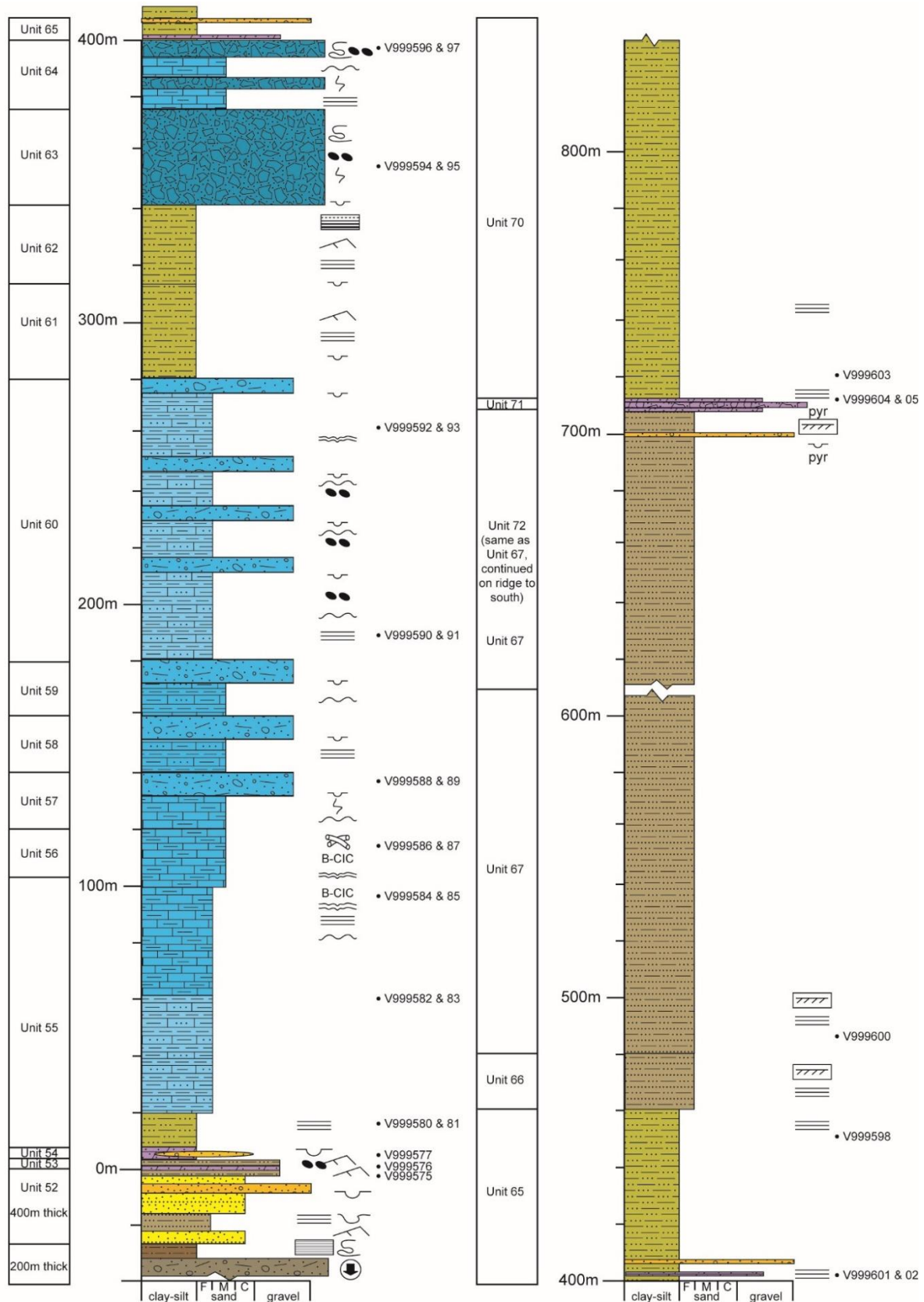


Figure 27. Composite stratigraphic log of the sections in the NW part of Area 1.



Figure 28. Face of a structurally complicated ridge, a mixed package of maroon weathering mudrock and olive green tillite interpreted as Rapitan Group (at arrow, cliff contains about 100 m thickness of strata for scale).



Figure 29. Unstratified greyish-green diamictite of dense mudstone containing unsorted, angular to subround, polymictic clasts, interbedded with maroon and olive green laminated mudrock of the Rapitan Group, basal part of NW part of Area 1 section.



Figure 30. Massive, clast-supported, polymictic boulder conglomerate of the Ice Brook Formation has an erosive base (in shadow) and weathers dark yellowish orange (Unit 68; 30 cm long hammer for scale).



Figure 31. Outcrop view of distinct orange weathering marker bed (Raventhroat Formation, at arrow, 3 m thick for scale), underlain by Ice Brook Formation (at least 400 m thick) and overlain by recessive basal Sheepbed Formation (foreground). This prominent marker bed can be traced northward (visible on distant ridge, top of photo).



Figure 32. Distinct dark yellowish orange weathering, finely laminated dolostone (Unit 54; hammer head is 15 cm wide for scale).



Figure 33. Basal Sheepbed Formation equivalent contains wavy bedded shaly lime mudstone and lime mudstone cycles (Unit 55; 30 cm long hammer for scale).



Figure 34. Upper Sheepbed Formation equivalent contains floatstone debrites with erosive bases and angular to subround clasts (Unit 57; 30 cm long hammer for scale).



Figure 35. Rudstone contains intraformational, cobble sized clasts in slump-folded beds with erosive bases (Unit 64; 30 cm long hammer for scale), likely the Gametrail Formation.



Figure 36. Light to medium grey marker bed of rudstone (debrites) and lime mudstone of Gametrail Formation equivalent (Units 63-64; helicopter for scale on Blueflower Formation).



Figure 37. Heterolithic package of shale and siltstone, with minor sandstone and conglomerate in resistant part of Unit 70 (about 100 m thick for scale), upper part of Blueflower Formation equivalent.



Figure 38. Orangish pink weathering rudstone with tabular clasts and laminated dolostone interbeds, ?Risky Formation equivalent (Unit 71).

Carbon Isotope Chemostratigraphy

Methods

Carbonate samples were slabbed, and then microdrilled with a Dremel drill press (1 mm diameter). Finest grained fabrics were targeted, and late stage carbonates/veins avoided. Carbonate powders (~500 micrograms) were analyzed using a Sercon 20-22 continuous flow mass spectrometer at the University of Victoria. Samples were weighed into individual borosilicate vials. Next, vial head space was flushed with He gas to remove atmosphere, and samples were reacted with 100% phosphoric acid at 85°C. Reaction time was 40 minutes. Precision of $\delta^{13}\text{C}$ is 0.15 permil (1 S.D.), based on measurements of internal laboratory monitoring standard (Dr. J. Husson, University of Victoria, personal communication, 2018).

Results

The $\delta^{13}\text{C}$ chemostratigraphy of the Ediacaran Windermere Supergroup mixed carbonate-siliciclastic succession (Ice Brook Formation to ?Risky Formation) shows a range of carbonate carbon isotope values from 9.30 to -9.15 ‰, consistent with trends from studies of this succession adjacent to the study area (e.g., James et al., 2001; Hoffman and Halverson, 2011; Macdonald et al., 2013). Negative carbon isotope values characterize the Ravensthorpe Formation, whereas values in the Sheepbed Formation are enriched (up to 9.30‰), perhaps indicating correlation with the June beds (described by Macdonald et al., 2013). Strong negative carbon isotope anomalies characterize the Gametrail Formation. Samples are sparse through the Blueflower Formation but yielded a negative excursion in the base, and positive value in the middle of the unit. Another large negative carbon isotope anomaly (down to -9.15 ‰) is present in the uppermost carbonate unit which is likely correlative to the Risky Formation (Fig. 39).

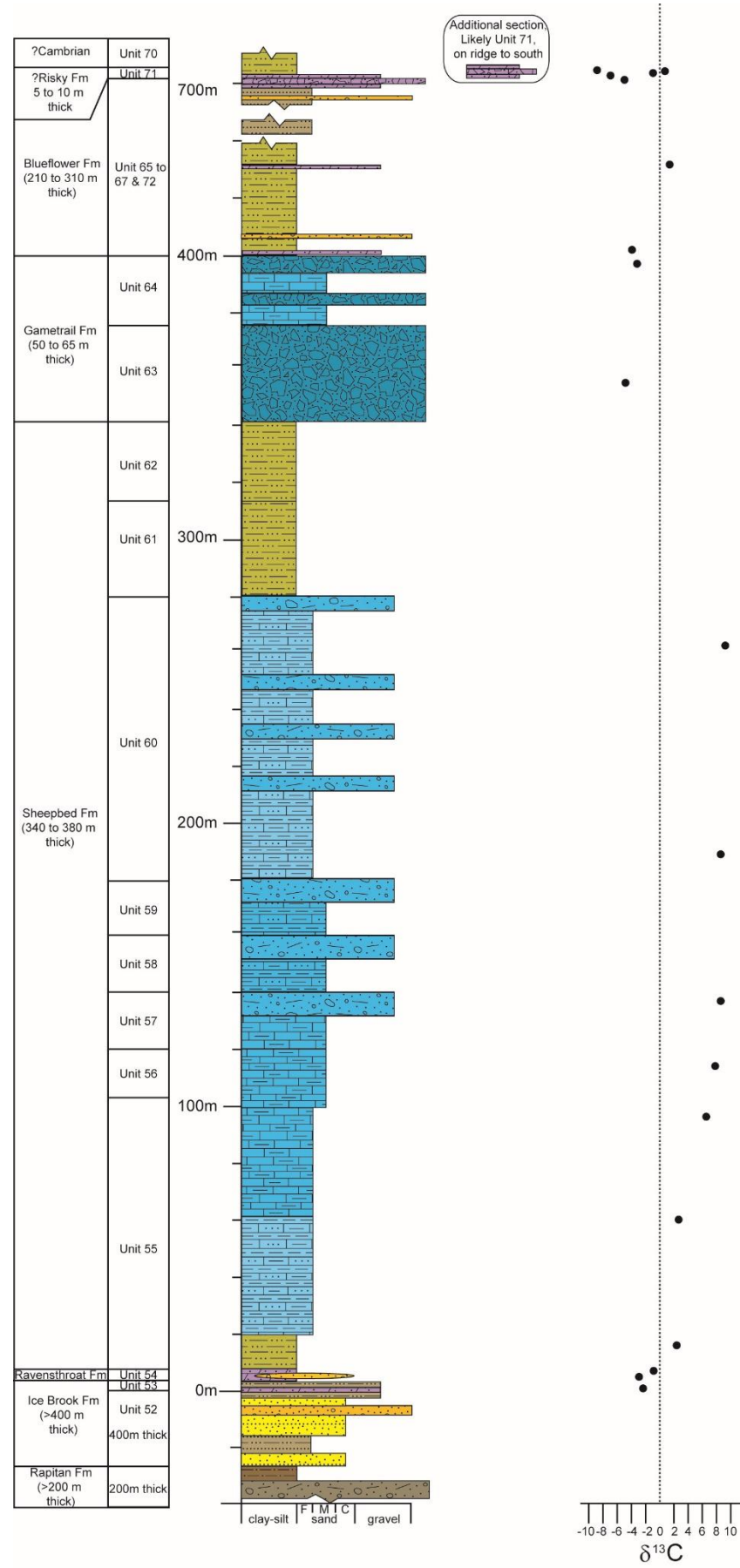


Figure 39. Carbon isotope chemostratigraphy of the Ediacaran Windermere Supergroup through the composite section in the NW part of Area 1.

Comparison of Property Stratigraphy to ATAC Osiris Cluster Stratigraphy and Regional Geology

Coulter et al. (2017) describe the Osiris cluster stratigraphy as a succession of Neoproterozoic to Cambrian slope facies of the Windermere Supergroup correlative to the regional formations mapped by the Yukon Geological Survey (Fig. 40; Colpron et al., 2013; Moynihan, 2016).

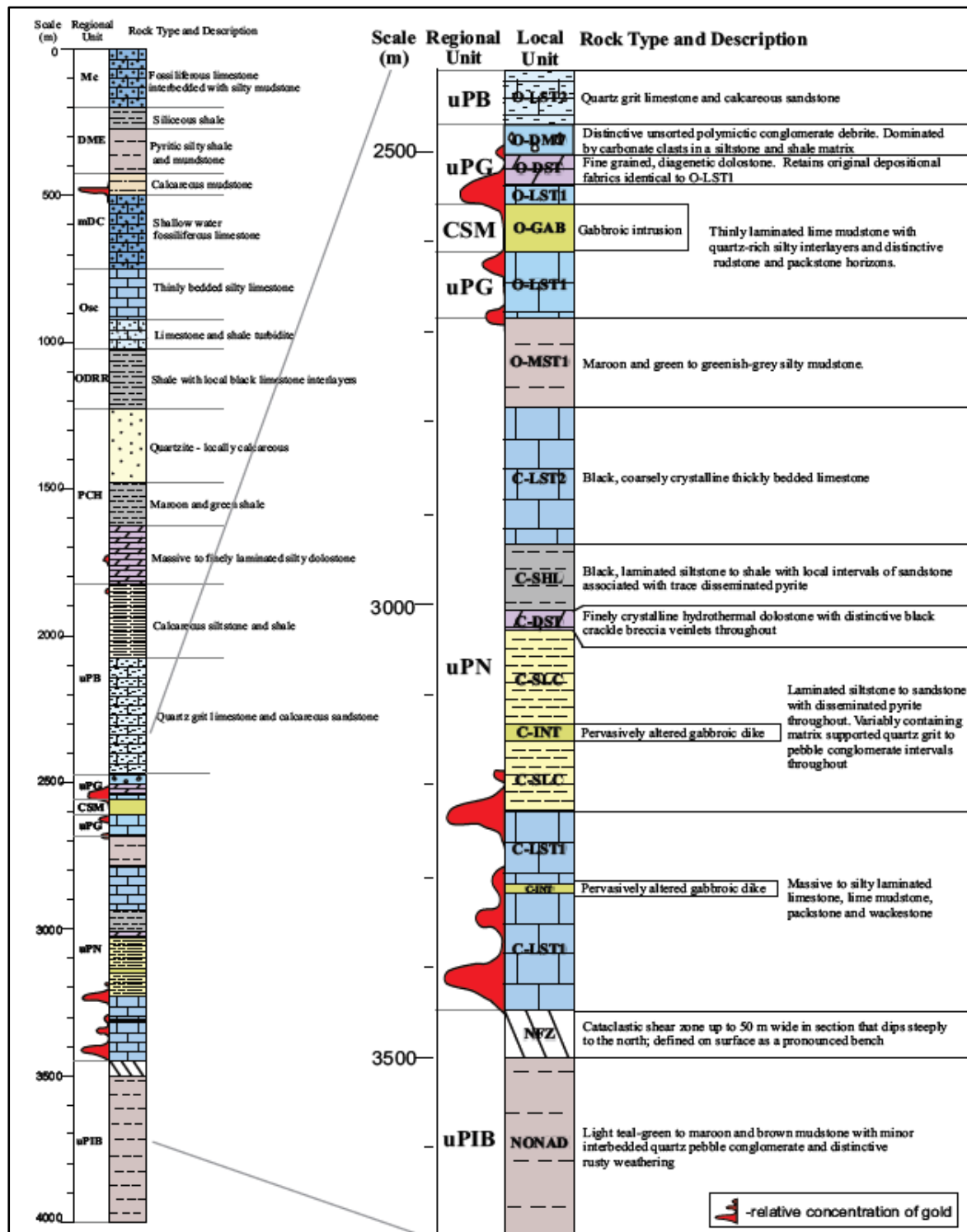


Figure 40. Local and regional stratigraphy and detailed sections of Osiris cluster local stratigraphic units (Coulter et al., 2017; Ristorcelli et al., 2018).

The lowest unit “NONAD” refers to North of Nadaleen mudstone, interpreted as part of the uPIB=Ice Brook Formation and described as green to maroon and brown mudstone with minor quartz pebble conglomerate (Coulter et al., 2017). A unit that fits this description was present at the composite section in the NW part of Area 1 but underlies 400 m of well bedded, orange-weathering, variable siliciclastic strata interpreted as correlatives to Ice Brook/Keele Formation. This mixed siliciclastic package directly underlies a “cap dolostone” with negative carbon isotope values characteristic of the Ravensthroat Formation regionally (e.g., MacDonald et al., 2013). It is therefore possible that the map units NONAD and UPIB are being used regionally to include two levels of glacial deposits related to the two Neoproterozoic glaciations (Rapitan Group and Ice Brook Formation of Aitken, 1991). In the SE and SE2 parts of Area 1 and possibly in the NW part of Area 2, the green and maroon to brown mudstone unit with dropstones and interstratified diamictite likely represent the older Rapitan Group (**Fig. 41**). Strata in these sections more closely fit the original descriptions of Rapitan Group units by Eisbacher (1978) to include dark red to maroon, green and grey, laminated siltstone-argillite couplets, diamictite and dropstones.

The C-LST1 Conrad limestone 1 is considered part of the uPN=Nadaleen Formation, described as light grey, silty laminated limestone with cone-in-cone and beef calcite. The C-SLC Conrad siliciclastic unit, described as grey-green pyritic siltstone and mudstone with conglomerate and sandstone interbeds, and C-SHL Conrad Shale, described as a black, laminated siltstone to shale, are also part of the Nadaleen Formation (Coulter et al., 2017). In the present study, these intervals possibly correlate with the lower carbonate-rich and upper siliciclastic-dominant parts of the Sheepbed Formation. Other units of the Nadaleen Formation at Osiris were not encountered at the NW part of Area 1 section such as the C-INT gabbroic dikes, C-DST Conrad dolostone, and O-MST Osiris mudstone.

The O-LST1 Osiris limestone (1) is described as well-bedded limestone with monolithic, intraclast rudstone layers. The O-DST Osiris dolostone is a diagenetic dolostone with depositional fabrics similar to those in O-LST1. The O-DMT Osiris diamictite is a carbonate debrite unit. These units represent the lower, middle, and upper Gametrail Formation=uPG unit (Coulter et al., 2017). In the present study, similar lithologies and depositional textures occur within the unit interpreted as the Gametrail Formation.

The O-LST2 Osiris limestone is considered part of the uPB=Blueflower Formation. This unit consists of very dark grey-black limestone and floatstone (Coulter et al., 2017). In the present study, a silty dolostone bed occurs at the base of the Blueflower Formation that may be correlative with this carbonate.

In summary, units with gold mineralization within the Osiris cluster stratigraphy include the C-LST1, C-SLC, O-LST1, O-DST, and O-DMT within the Nadaleen and Gametrail formations (Coulter et al., 2017). Stratigraphic equivalents in the Sheepbed and Gametrail formations are present in the NW part of Area 1.

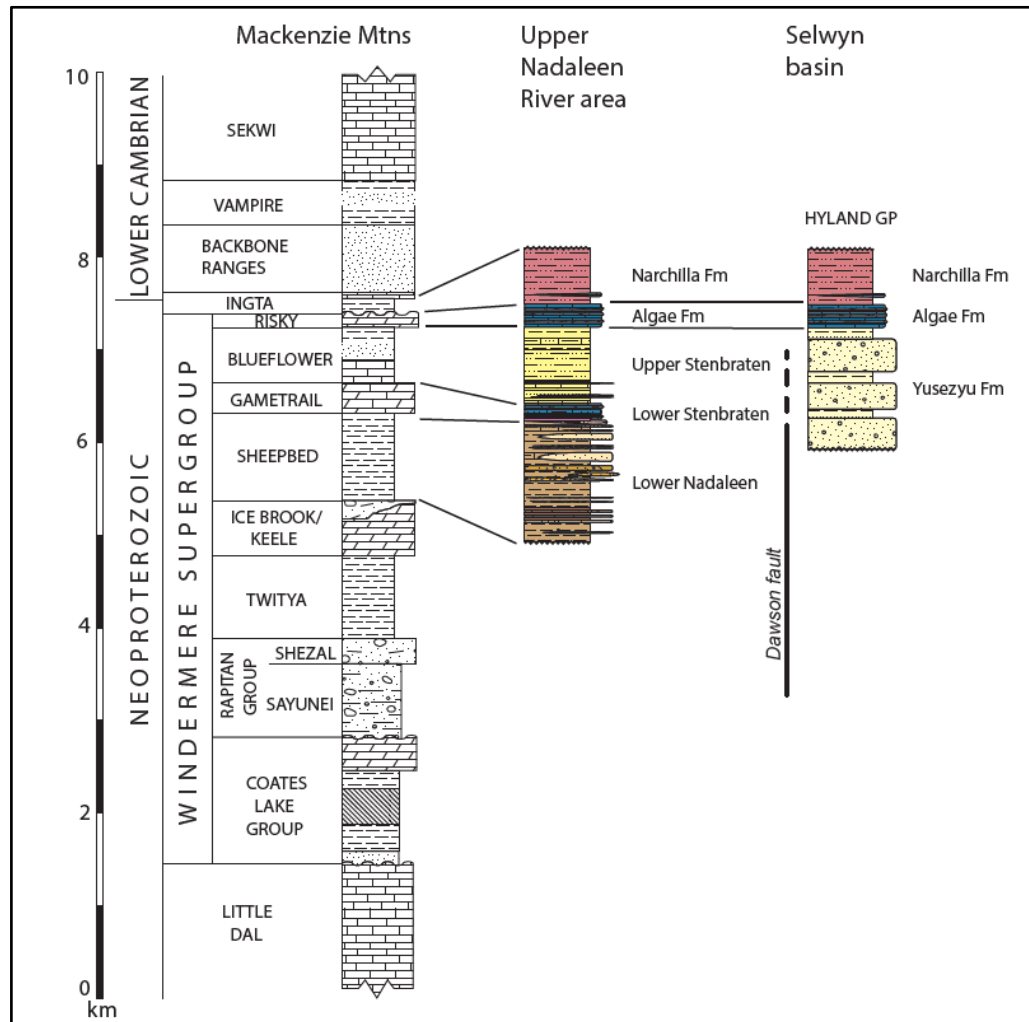


Figure 41. Neoproterozoic Windermere Supergroup stratigraphy (after Narbonne and Aitken, 1995), with proposed correlations to units along the Rackla belt (Colpron, 2013).

3.0 STRUCTURAL EVALUATION OF THE CL AND HJ CLAIMS

The CL and HJ claim blocks are located north of both the regional-scale Dawson thrust and Kathleen Lakes fault (**Fig. 1**). Both fault structures are considered key controls on mobilizing fluids from depth, and localizing mineralization in the vicinity of the Osiris and Anubis clusters and the Venus occurrence.

Favourable mineralizing structures associated with gold deposition within the Rackla belt area include low-angle SW- and W-vergent thrust faults, high-angle NNE-trending strike-slip and dip-slip faults and ESE-trending high-angle strike slip faults. The overall structural setting associated with sediment-hosted gold mineralization consists of a transpressional deformation regime with larger gold accumulations occurring in ENE plunging fold hinges.

The dominant structural grain varies from NNE to NE within Area 1 to predominantly E and ESE within area 2. No major shear zones or thrust faults were observed within the transect areas reviewed. The most prevalent structures present in all areas reviewed are late brittle N, NE-ENE and NW fault systems which are associated with localized folding. No mineralization was observed in any of the structures examined on the claim blocks during 2018.

Drone imagery was flown over the three main transects to better understand the structural setting in each of the areas reviewed. High resolution orthophotos (5 – 10cm spatial resolution), digital elevation models (10 – 20cm) and a suite of hillshade models were generated for each area and used in final map interpretations. An outline of drone data acquisition and data products is provided in Appendix 2.

AREA 2 Transect

Figure 42 illustrates the location of the mapping transect completed on newly acquired orthophoto and derivative hillshade model imagery. The mapping transect can broadly be divided into the three structural domains (**Fig. 43**):

- i) A northern domain characterized by north trending structural grain which is oblique to the dominant trend of stratigraphy in the area (off claims; **Fig. 44**).
- ii) A domain of folding characterized by steep NW trending fold axes and constrained within a single map unit. Structural domain 2 is bounded to the NW and SE by ENE trending fault zones (**Figs. 43, 44**).
- iii) Structural domain 3 represents the majority of the mapping transect and is characterized by NE and ENE brittle faults and associated localized folding (Fig. B). Stereonet analysis of bedding within this domain indicate the presence of shallow to moderately ENE plunging folds (**Fig. 45**).

The NW trending tight folding occurring in structural domain 2 is interpreted to predate the ENE open fault-related folding in structural domain 3 which is the oldest deformation event observed in Area 2. No mineralization was observed within any of the three structural domains.

A 1:2500 scale structural/stratigraphic map interpretation is presented in **Fig. 46**. The stratigraphy within the area is poorly understood as noted previously. No major marker horizons are present nor analytical data to help identify possible stratigraphic position. Stratigraphic units as outlined in section

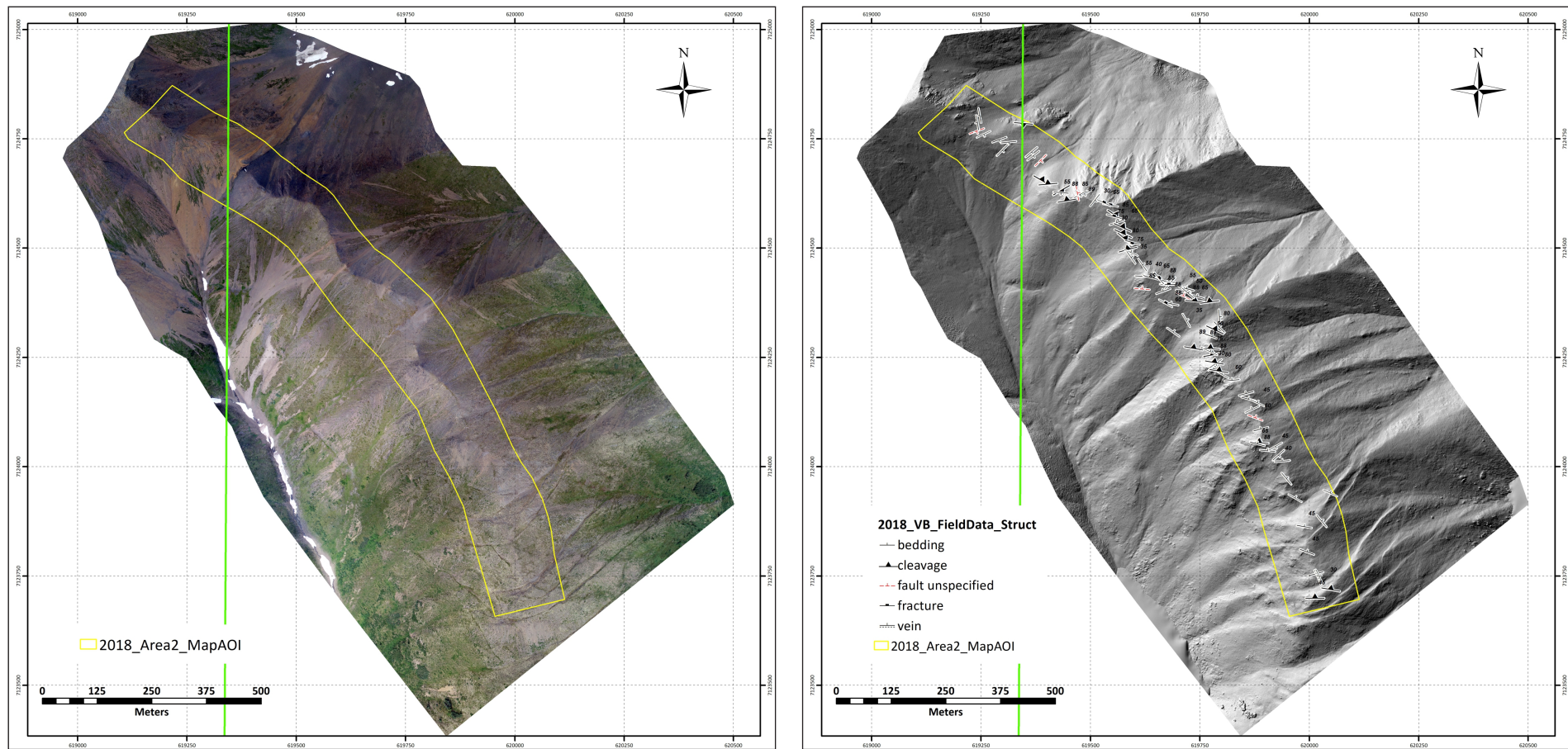


Figure 42: Orthophoto and hillshade model (illuminated from 315° azimuth) for Area 2 transect.

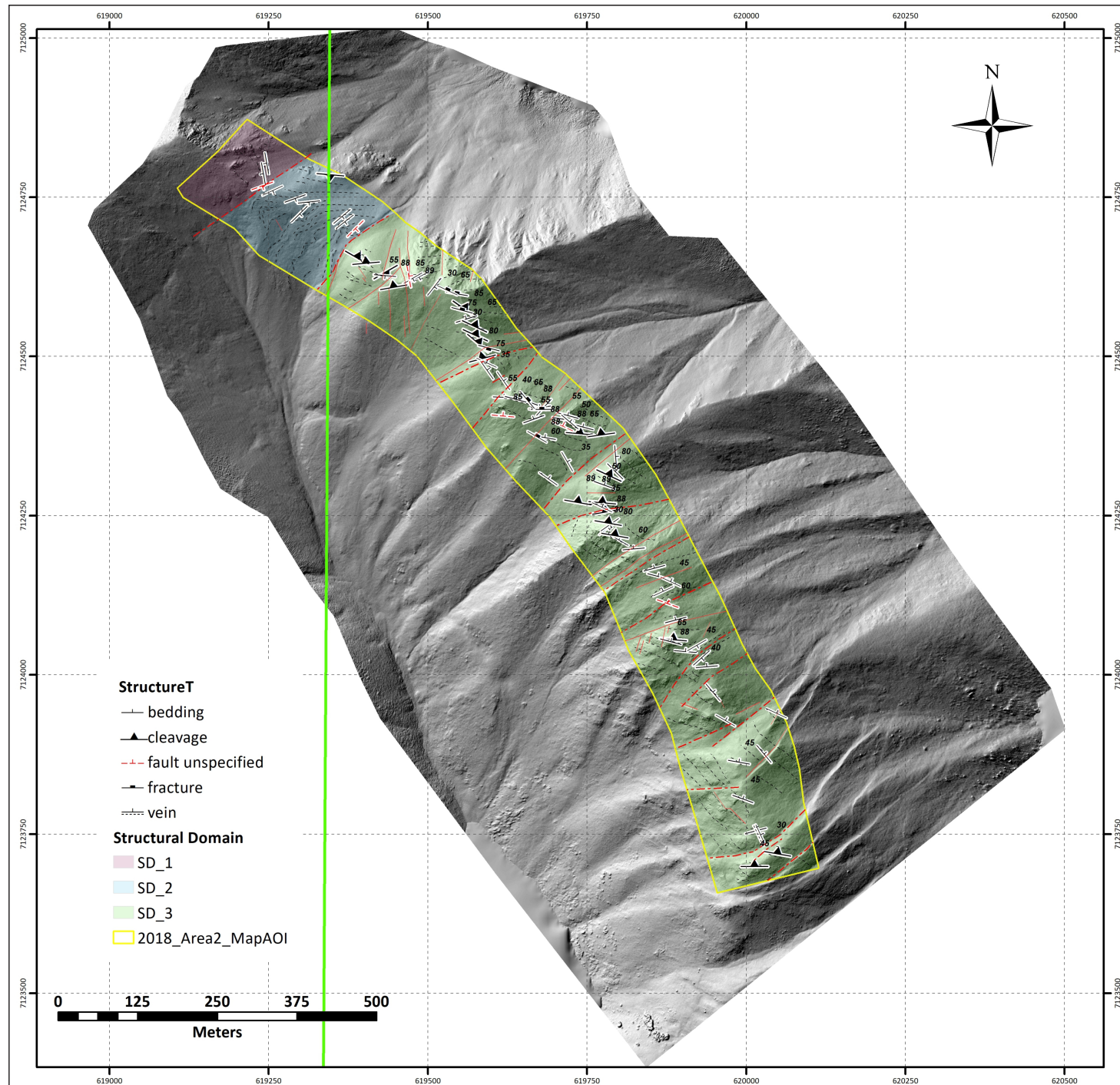


Figure 43: Interpreted structural domains for Area 2 transect superimposed on hillshade model

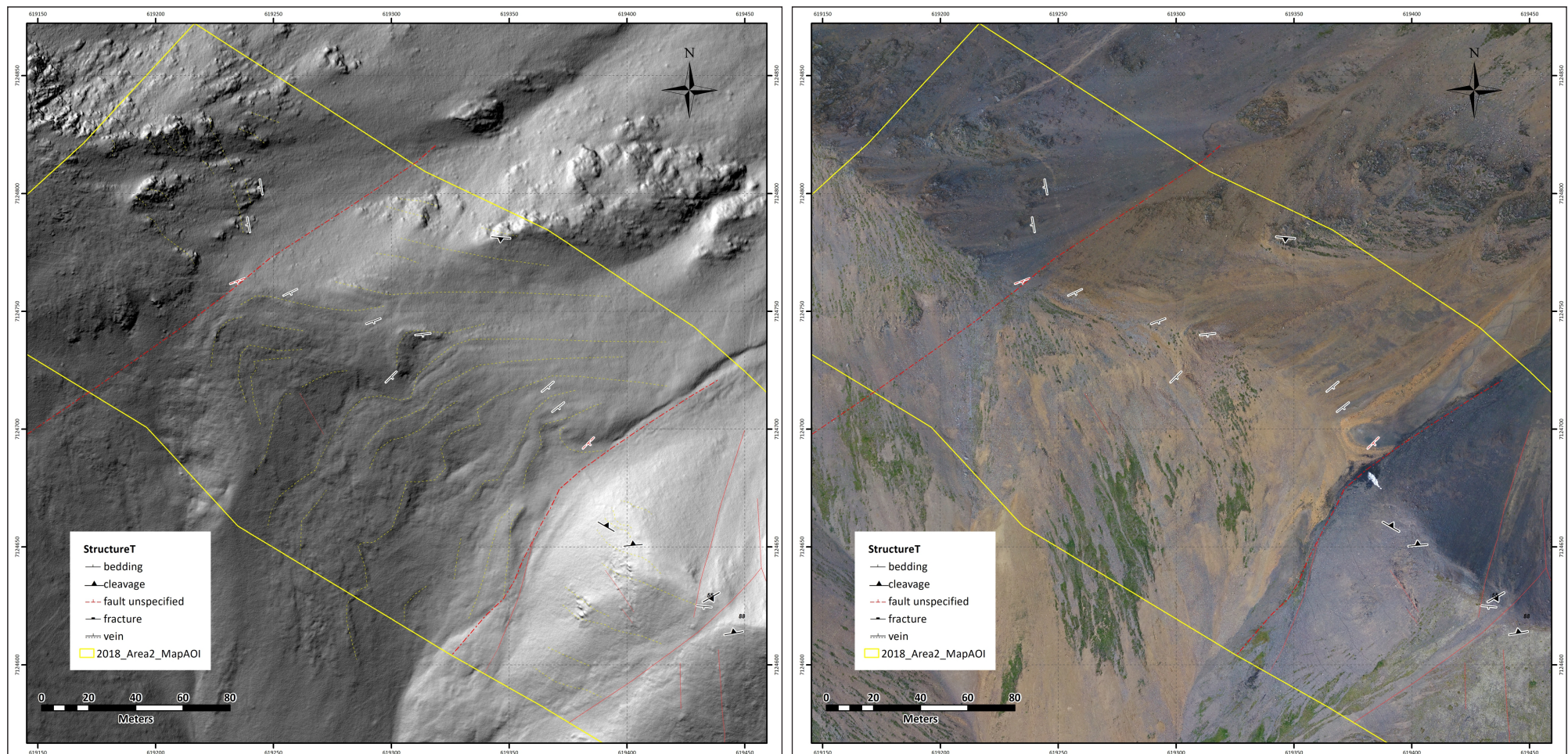


Figure 44: NW trending axial planes of folding with structural domain 2, Area 2 transect.

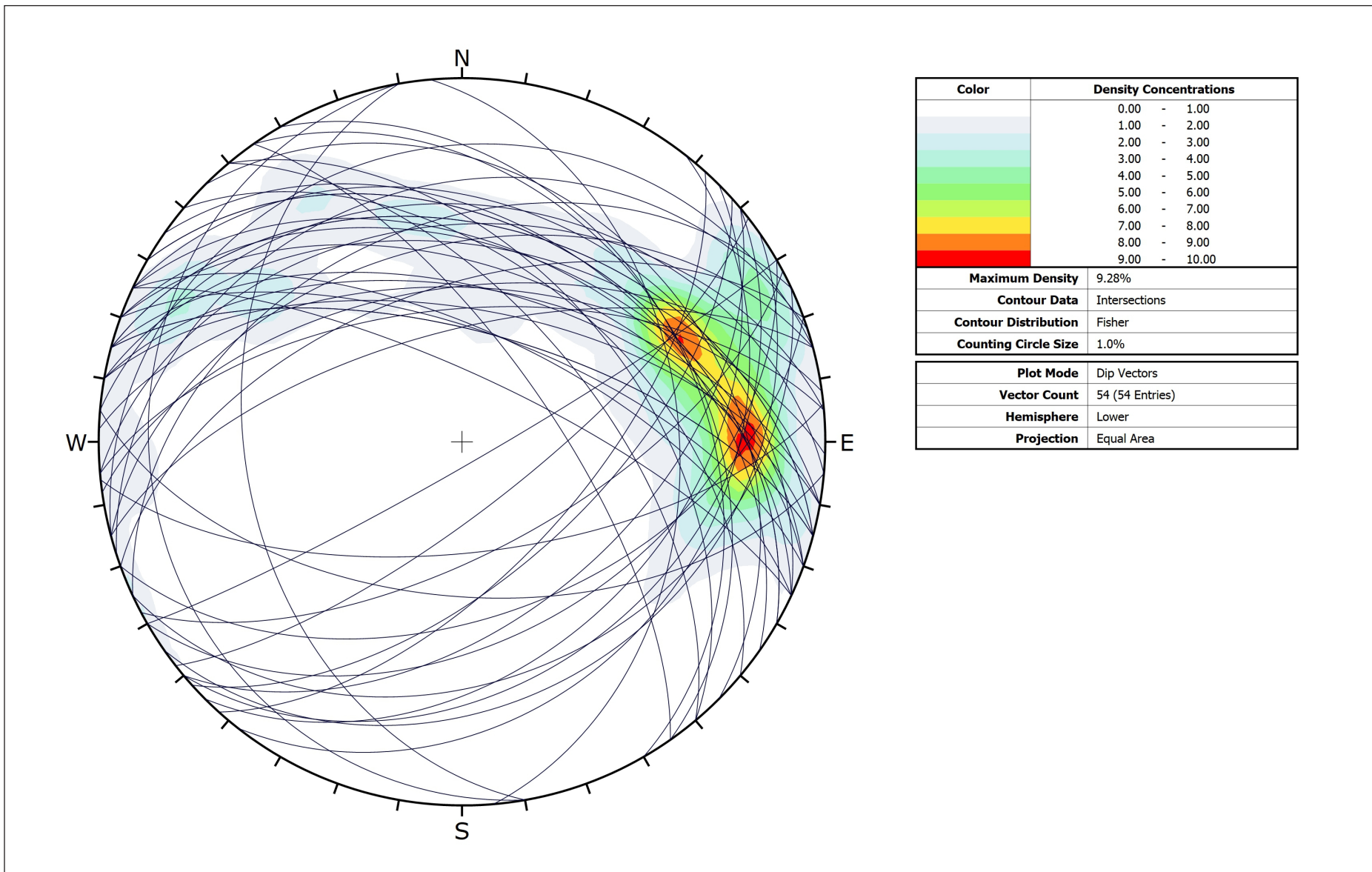
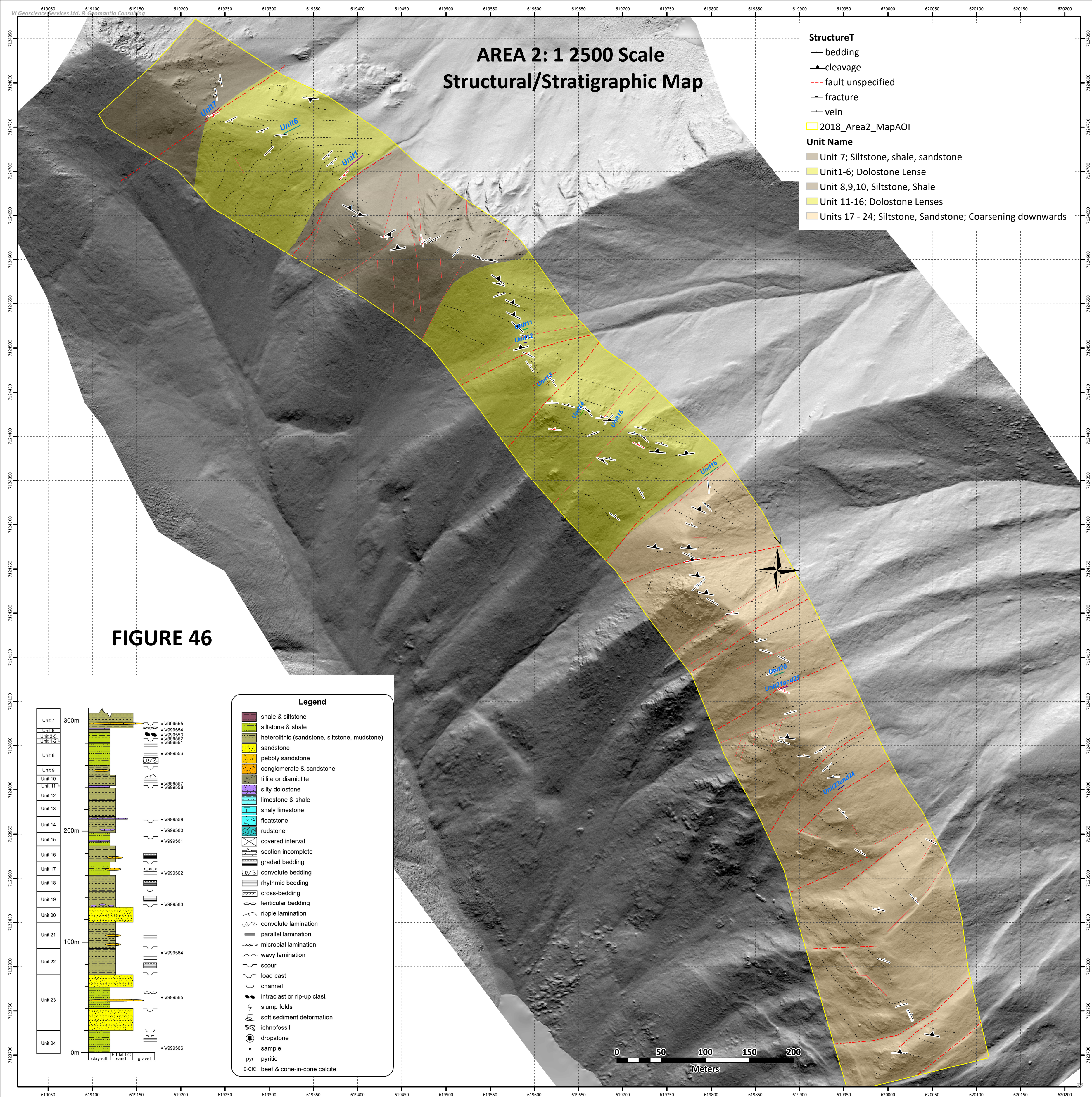


Figure 45: Intersection of bedding planes within structural domain 3, Area 2. Data indicate presence of shallow to moderately ENE plunging open folds



2.0 have been simplified into 5 map units (**Fig. 46**). Stratigraphy containing carbonate lenses are shown as separate map units. Carbonates are more prospective host rocks than siliciclastics in the majority of sediment-hosted gold deposits. Other map unit subdivisions are based on the dominance of siltstone and shale over coarser siliciclastics and vice versa. **Figure 46** is provided as a large format figure for plotting at 1:2500 scale if desired. The stratigraphic log and base of unit locations are also provided on the interpretation.

AREA 1 SE Transect

Figure 47 illustrates the location of the NW-SE mapping transect completed within the SE portion of Area 1. Two structural domains are present within the transect area (Fig. 48), including:

- i) Structural domain 1 consists of predominantly NNE striking and west dipping stratigraphy that is overprinted by NE – ENE late brittle faults. Similar to Area 2, this late generation of faulting is characterized by decimeter scale ENE plunging open folding.
- ii) Structural domain 2 is characterized by NNE striking and east dipping stratigraphy. A synclinal hinge is interpreted to exist between the two domains. Stereonet analysis of bedding in this transect indicates the syncline is a shallow, SSW plunging fold structure (**Fig. 49**).

Folding within structural domain 2 is considered to be an early generation of folding (F1) and is overprinted by N, NE and NW brittle faulting which often have localized F2 folding in close proximity to these faults. Late brittle NE and NW fault are often associated with significant oxidation (limonite-carbonate alteration) in brecciated faults zones (**Fig. 50**). Note that some of these oxidized vein faults had been sampled on previous prospecting programs. No significant gold values were returned. No other mineralization was observed in this transect area.

A 1:3000 scale structural/stratigraphic map interpretation is presented in **Fig. 51**. The stratigraphy is interpreted to be Rapitan Group and Ice Brook / Keele Formation. **Figure 51** is provided as a large format figure for plotting purposes. Stratigraphic logs and base of unit locations are also provided on the map to better visualize the stratigraphic log in map space.

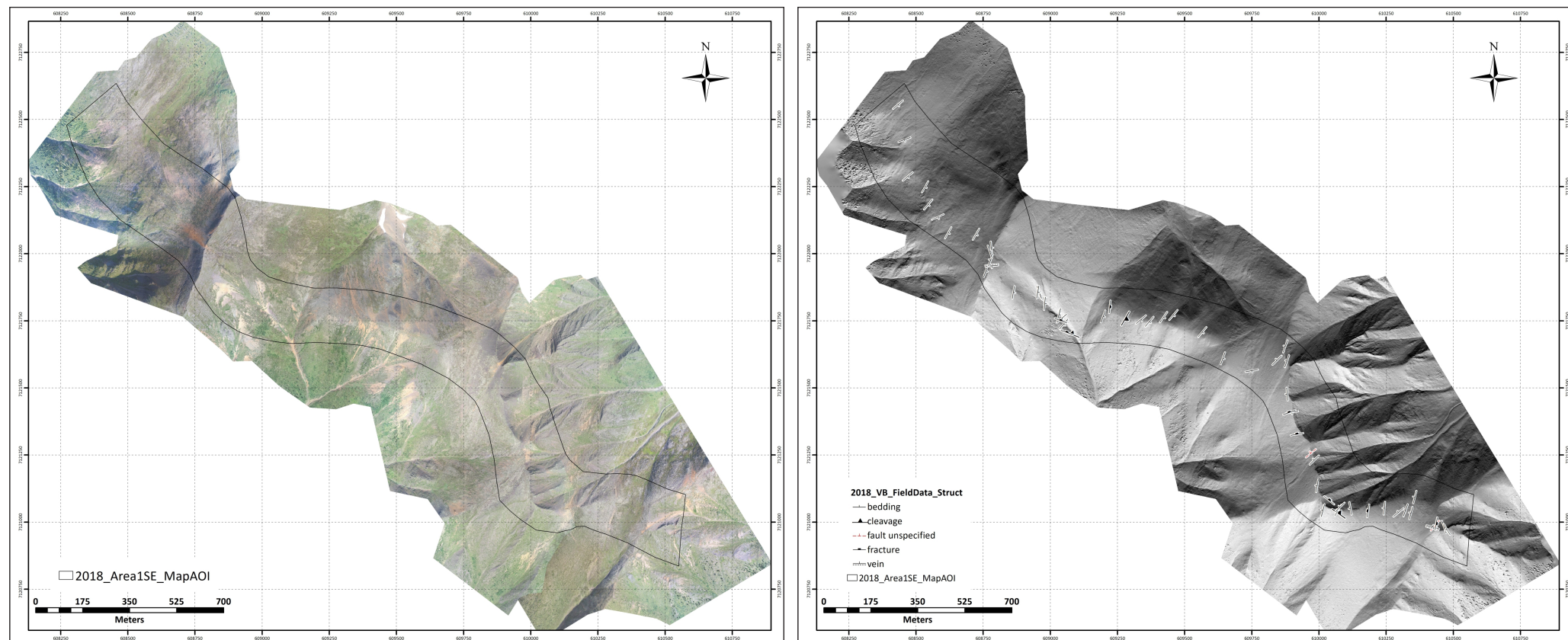


Figure 47: Orthophoto and hillshade model (illuminated from 180° azimuth) for Area 1SE transect.

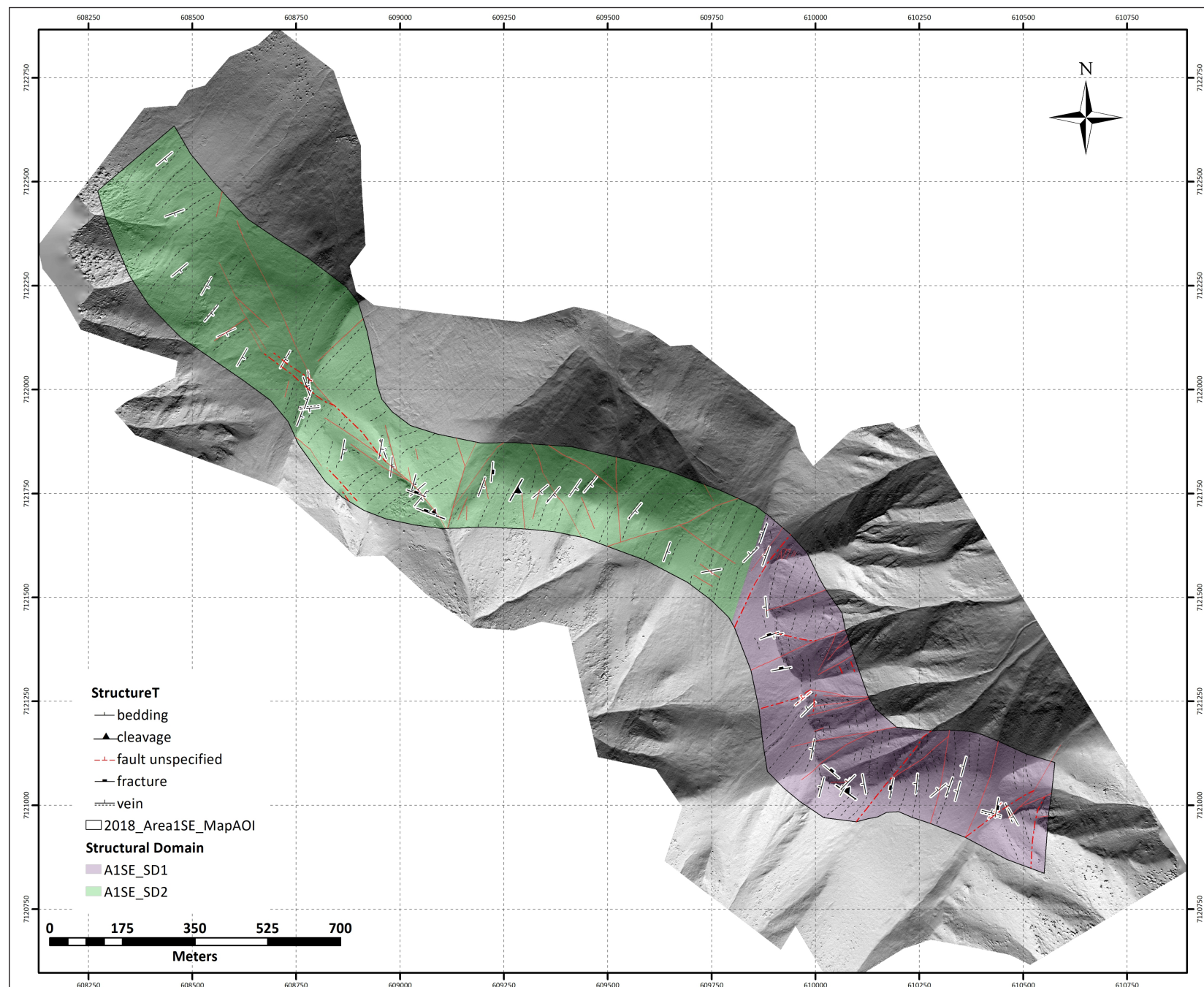


Figure 48: Interpreted structural domains for Area 1SE transect superimposed on hillshade model

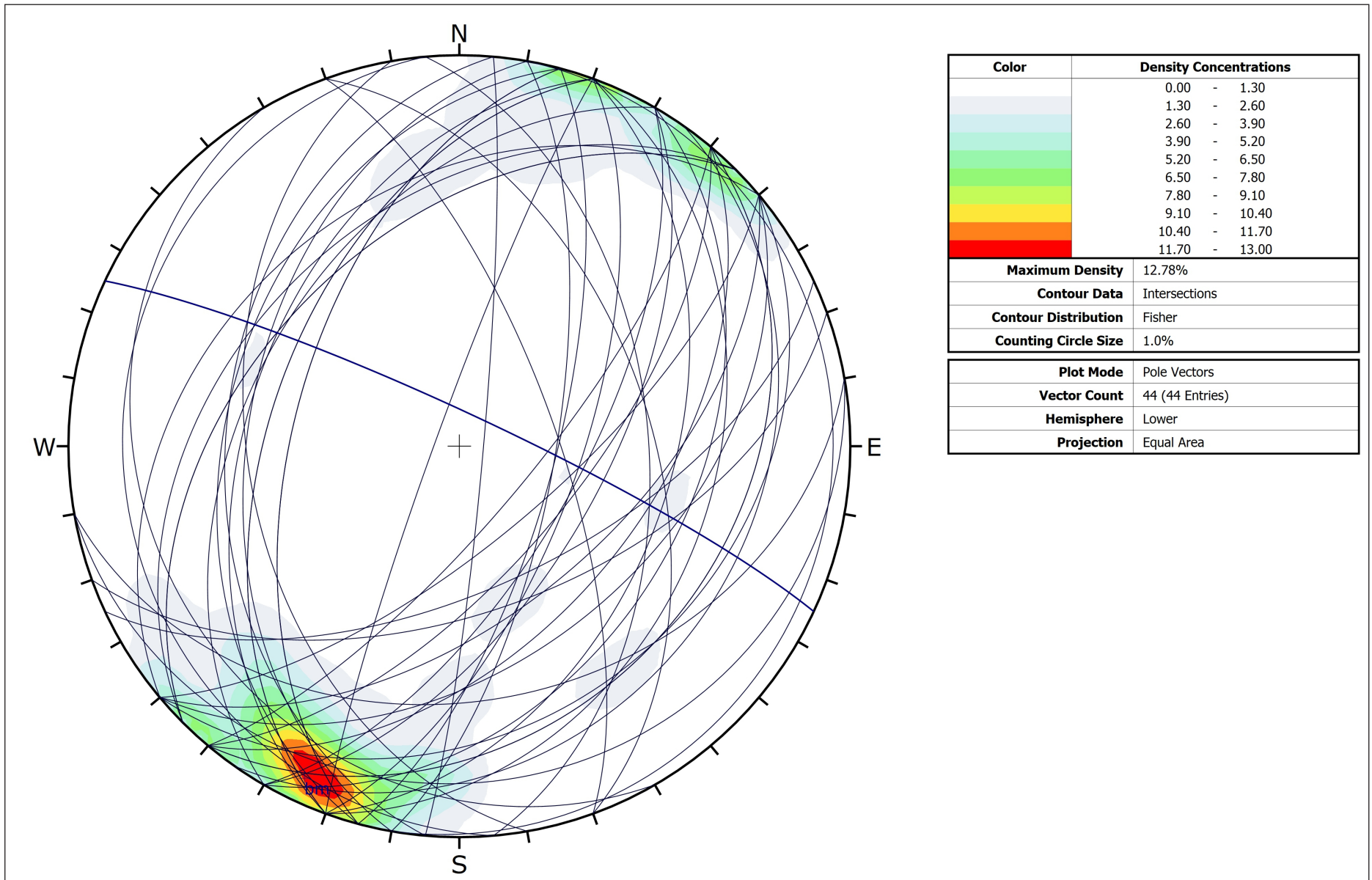


Figure 49: Intersection of bedding planes within Area 1 SE. Data indicate presence of shallow SSW plunging open folds

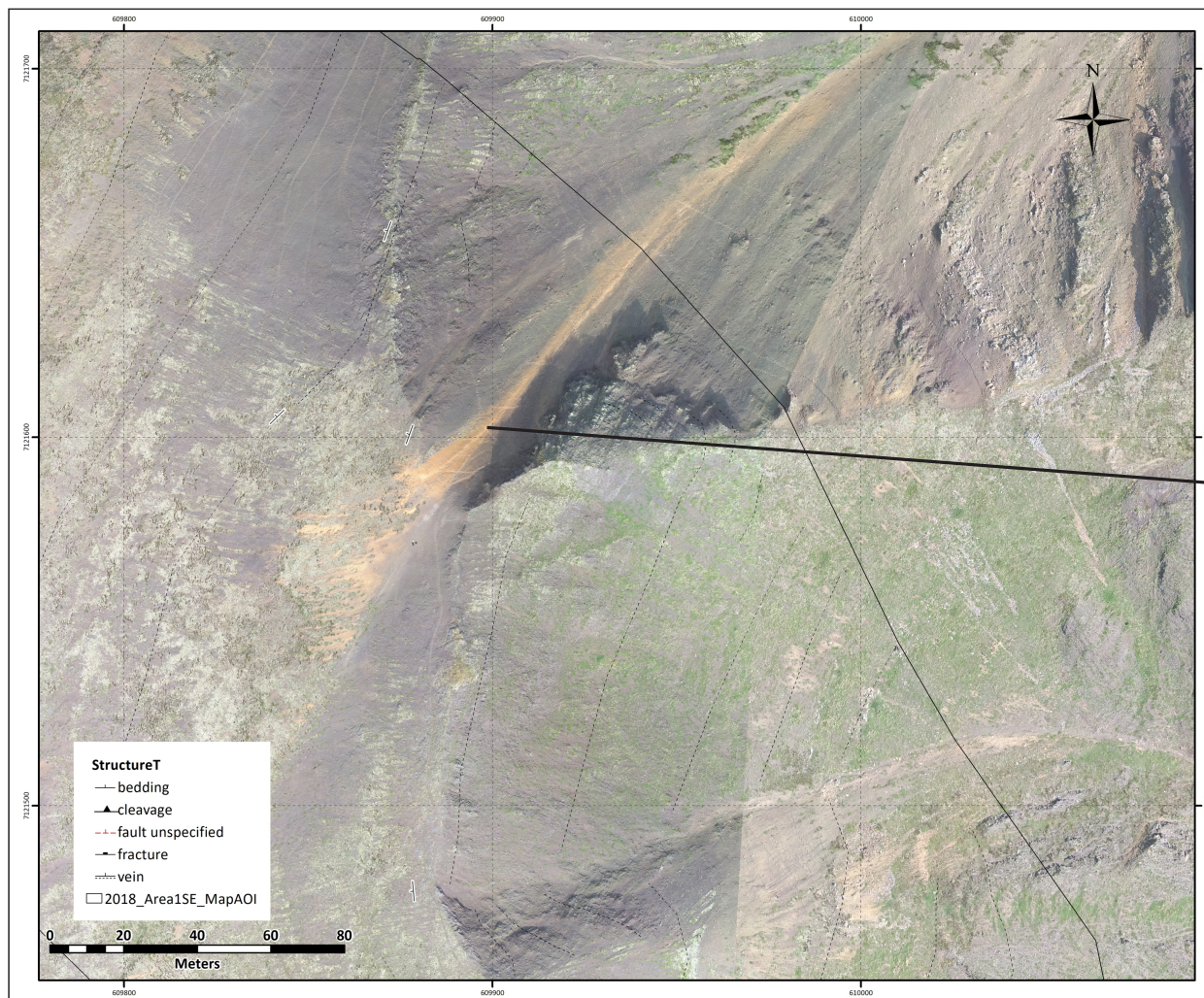


Figure 50: NE late brittle fault zone with barren limonite - carbonate breccia

AREA 1SE: 1 3000 Scale Structural/Stratigraphic Map

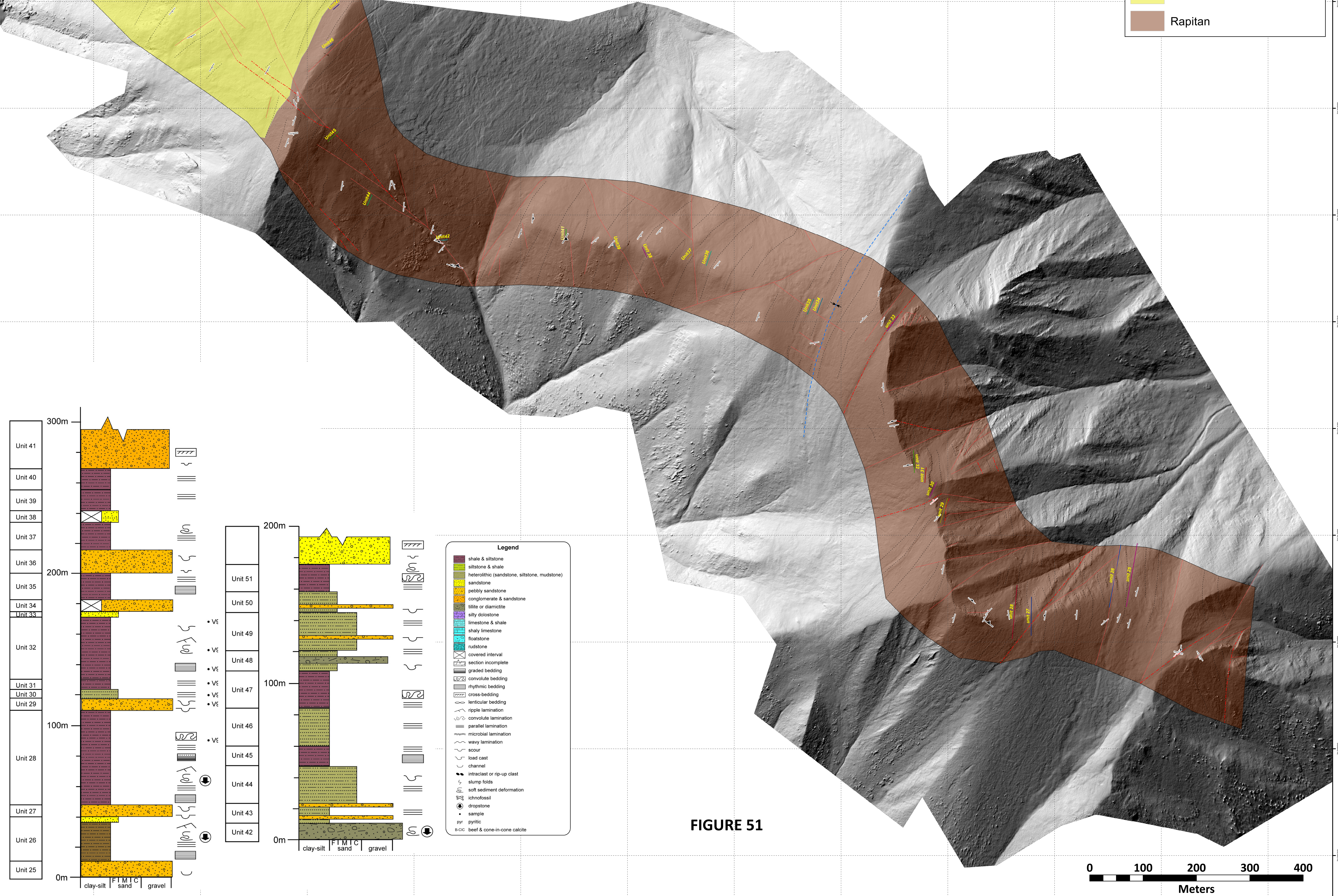
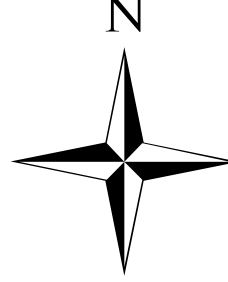
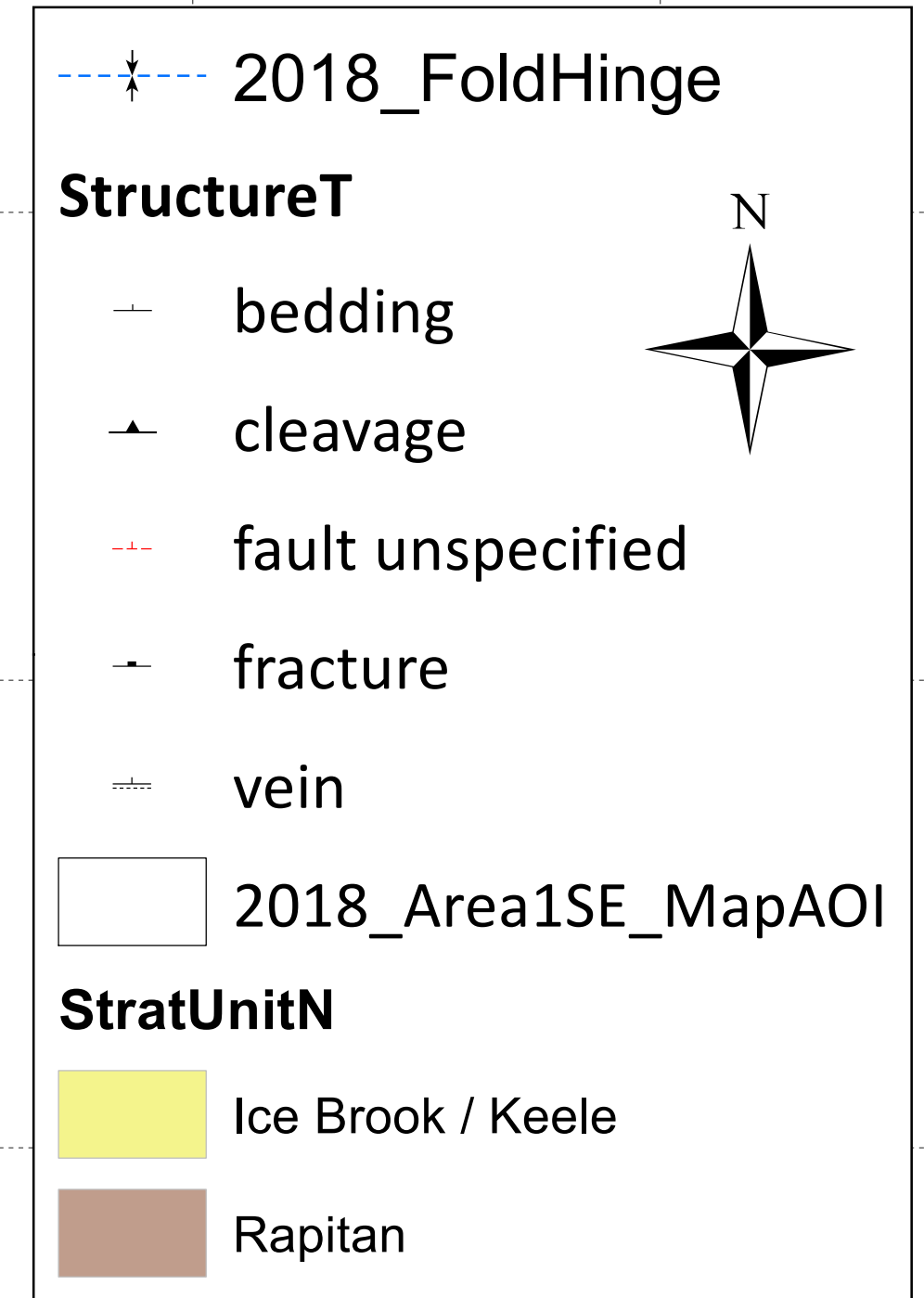


FIGURE 51

0 100 200 300 400
Meters

AREA 1 NW Transect

Figure 52 illustrates the location of the NW-SE mapping transect completed within the NW portion of Area 1. Note only reconnaissance work was carried out within the eastern third of the mapping transect. Drone imagery was not acquired over the reconnaissance area, however high resolution satellite data is publicly available for that portion of the mapping transect.

The area was not subdivided into structural domains like the previous two areas. The dominant structural grain is NNE trending and west dipping. The transect represents a reasonably structurally intact stratigraphic sequence (younging to the west). No thrust faults were observed.

Bedding reversals occur in association with a series of N, NE-ENE and NW brittle faults. A major NNW trending structure occurs approximately midway through the transect (**Fig. 53**). The NW and NE-ENE faults are not observed to offset the NNW faults and are interpreted as either coeval with the NNW faults (potential Riedel shear geometry?) or they predate them. No mineralization was observed on any of these late brittle structures.

The late brittle NE faults are associated with localized open ENE trending folding similar to areas 2 and 1SE, suggesting the presence of a regional deformation event (**Fig. 54**). No mineralization was observed associated with this generation of folding.

A 1:5000 scale structural/stratigraphic map interpretation is presented in **Fig. 55**. The stratigraphy represents six groups/formations of the Windermere Supergroup (Rapitan Group, Ice Brook/Keele Formation, Ravensthorpe Formation, Sheepbed Formation, Gametrail Formation and Blueflower Formation). A large format map is provided with stratigraphic logs and base of unit locations marked.

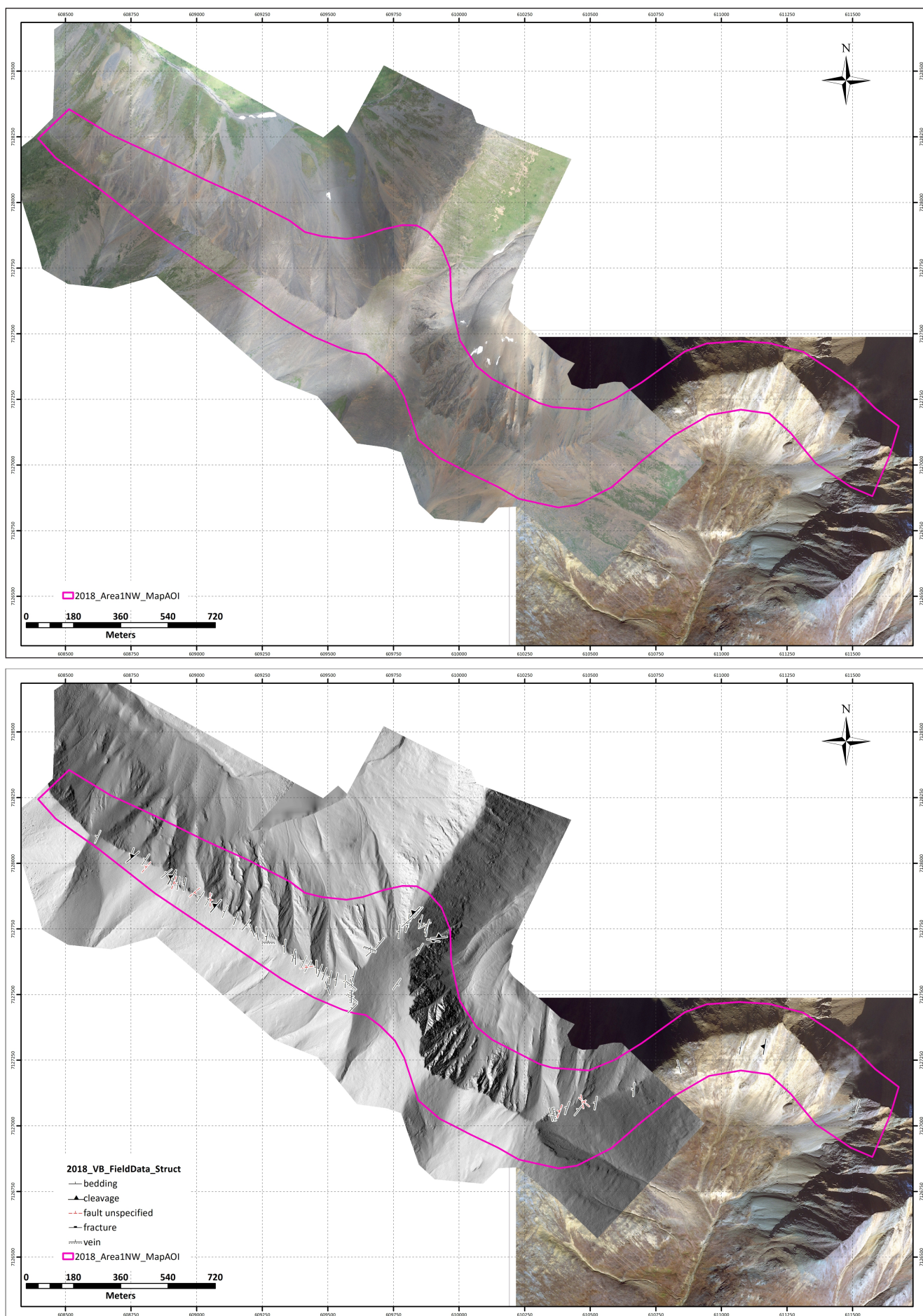


Figure 52: Orthophoto and hillshade model (illuminated from 270o azimuth) for Area 1NW transect.

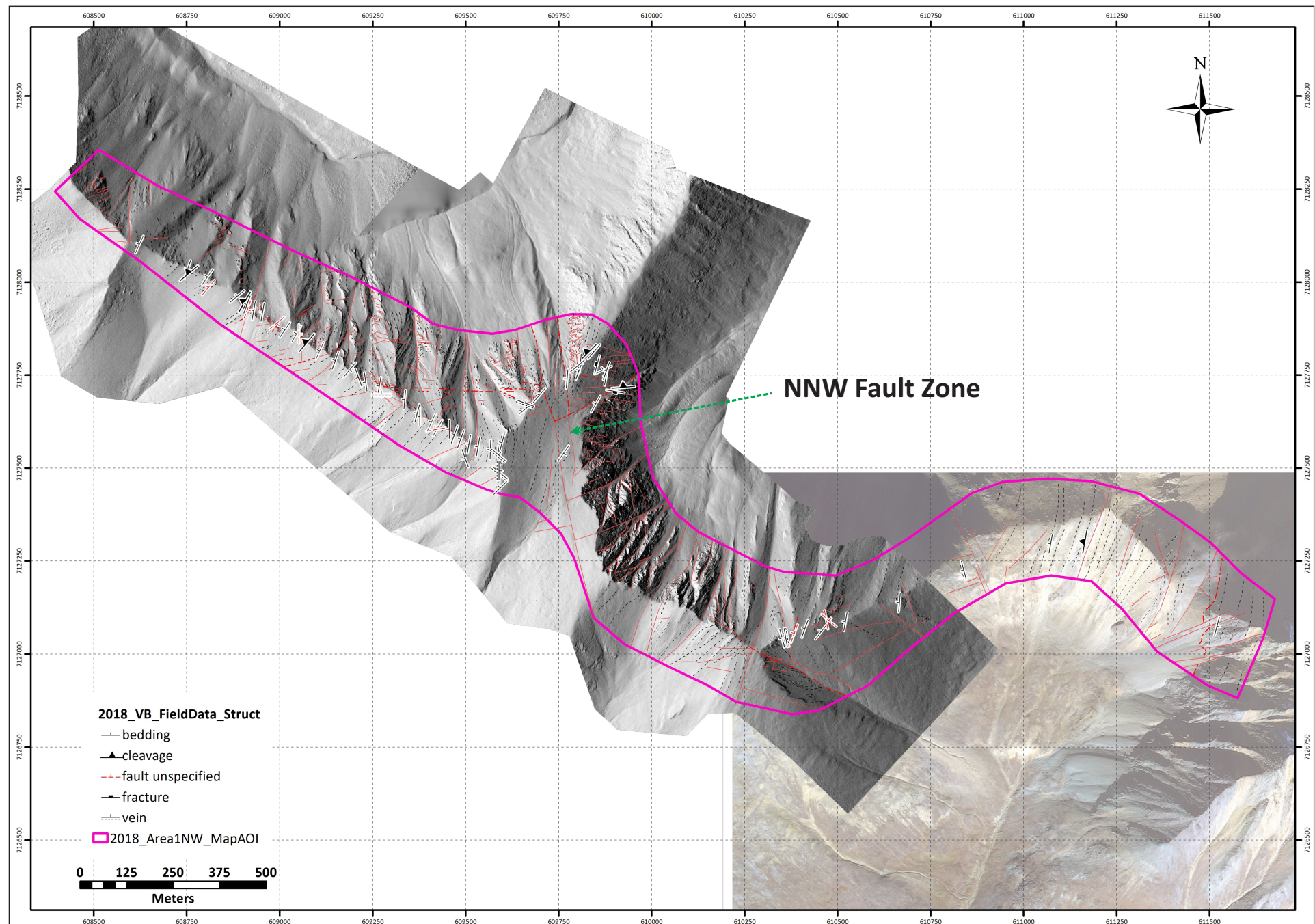


Figure 53: NNW trending late brittle fault zone occurring within the mapping transect

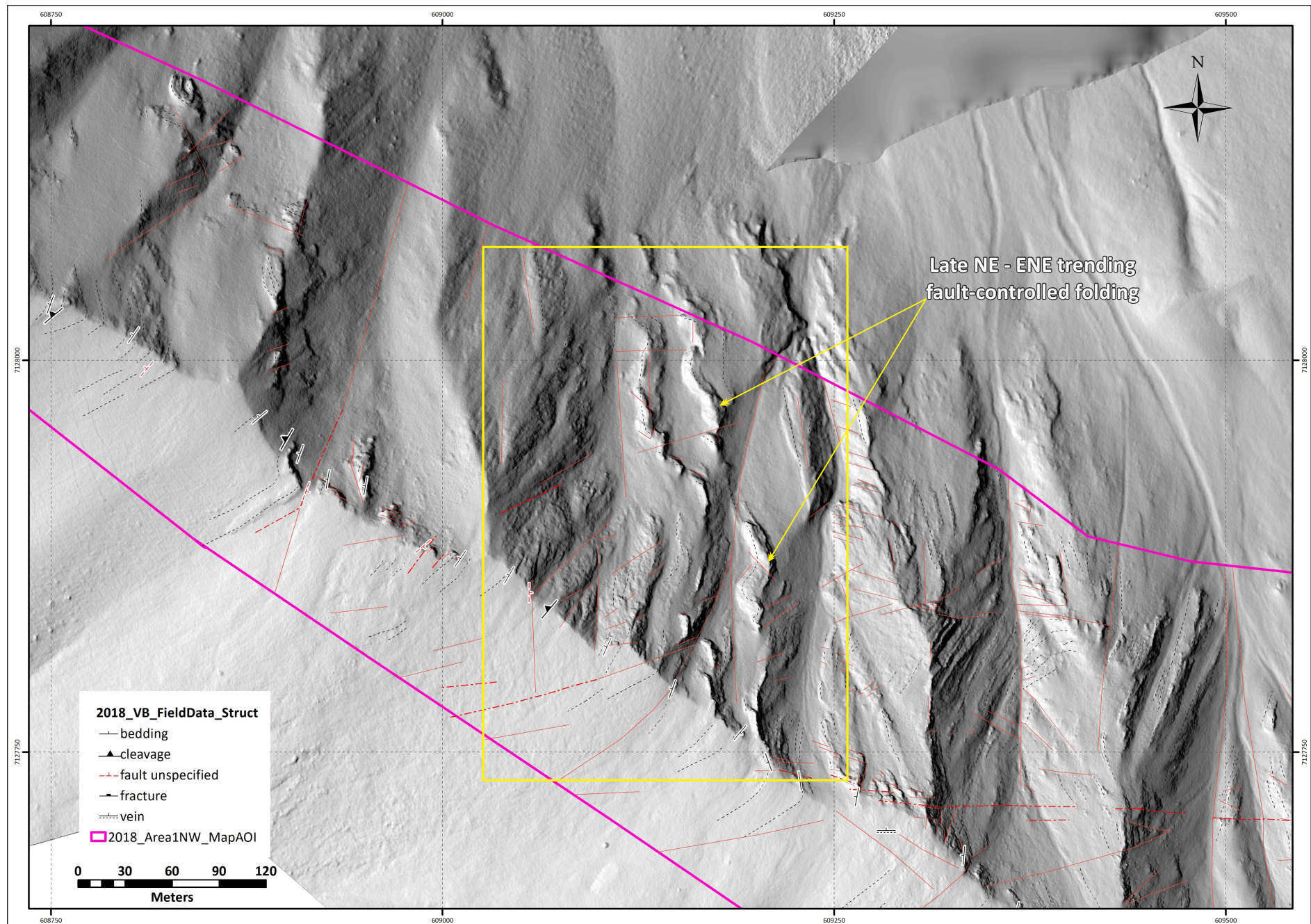
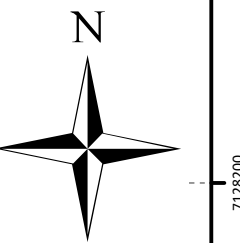


Figure 54: Late ENE-NE trending open fault-related folding, Area 1NW.

AREA 1NW: 1 5000 Scale Structural/ Stratigraphic Map



StratUnitN

- Blueflower
- Gametrail
- Sheepbed
- Raventhroat
- Ice Brook / Keele
- Rapitan

StructureT

- bedding
- cleavage
- fault unspecified
- fracture
- vein

2018_Area1NW_MapAOI

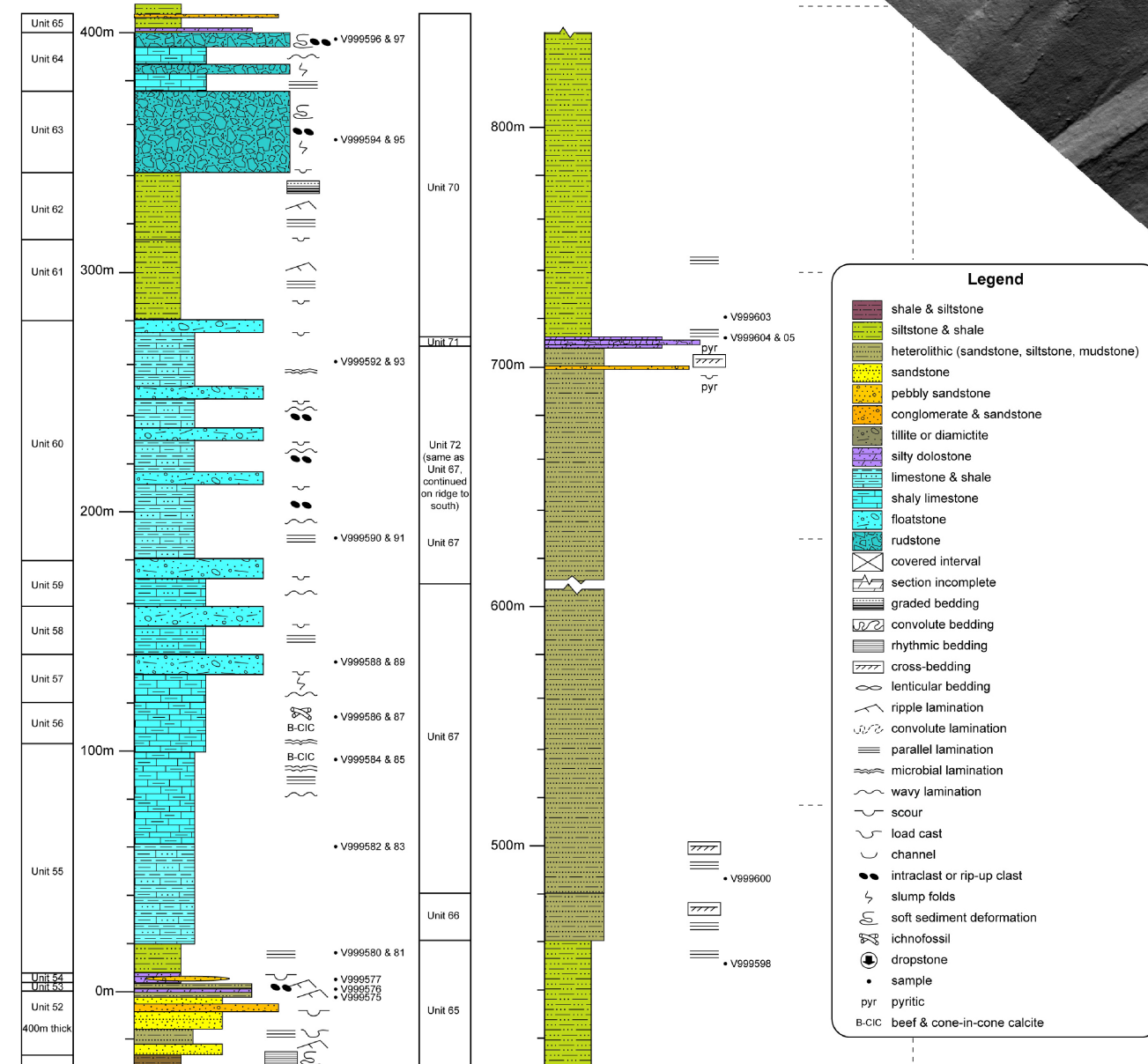


FIGURE 55

0 125 250 375 500
Meters

3.0 SUMMARY

Three detailed transects were completed in two areas of the CL and HJ claims of Carlincore Resources Ltd. The main objective was to place the rocks in a regional stratigraphic and structural context to better assess the potential for sediment hosted gold mineralization.

The stratigraphy in Area 2 remains unconstrained in a regional context, however, the predominance of siliciclastics over carbonate lithologies make this a less prospective target area for sediment-hosted gold. No major thrust faults or shears zones occur in the area (both of which are an important part of the mineralizing system at the Osiris cluster). The area is characterized by late brittle NE-ENE faults with only minor amounts of displacement. An important component of sediment hosted gold deposits is the presence of well-established, long-lived fault systems. Reactivated basement structures are excellent candidates to facilitate fluid flow. No such structures were observed within Area 2.

The south eastern portion of Area 1 consists of two stratigraphic units, the Rapitan Group and Ice Brook / Keele Formation. While these stratigraphic units are present within the Osiris cluster (NONAD), they are not mineralized hosts. Structures are dominantly late brittle NE and NW faults, although some early (F1) stage folding is present. No major shear zones or thrust faults were observed in this transect area.

The northwestern portion of Area 1 preserves the most intact section of stratigraphy through more prospective carbonate host rocks. The eastern half of the area is underlain by the Rapitan Group and Ice Brook / Keele Formation. The lack of carbonates within the succession make this section of the Windermere Supergroup unprospective for sediment hosted gold. Structures are very similar to those within the Area 1SE and are dominated by late brittle faults with only minor displacement.

The carbonate stratigraphy above the Ice Brook / Keele Formation represents the widest section of carbonate stratigraphy within the three transects mapped. Carbonate rocks include dolostone within the Ravenstthroat Formation, limestones within the Sheepbed Formation, Gametrail Formation, Blueflower Formation, and ?Risky Formation. No mineralization was observed in these units in the traverse areas, however, mineralization within the Osiris cluster occurs within the Nadaleen and Gametrail formations which are the stratigraphic equivalents to the Sheepbed and Gametrail formations.

REFERENCES

Aitken, J.D., 1991. The Ice Brook Formation and post-Rapitan, late Proterozoic glaciation, Mackenzie Mountains, Northwest Territories, Geological Survey of Canada. Bulletin 404, 43 p.

Colpron, M., Moynihan, D., Israel, S. and Abbott, G., 2013. Geological map of the Rackla belt, east-central Yukon (NTS 106C/1-4, 106D/1). Yukon Geological Survey, Open File 2013-13, 1:50 000 scale, 5 maps and legend.

Coulter, A.B., Lane, J. and Steiner, A., 2018. Osiris cluster Carlin-type gold, east-central Yukon. In: Yukon Exploration and Geology Overview 2017, K.E. MacFarlane (ed.), Yukon Geological Survey, p. 65-74.

Eisbacher, G.H., 1978. Re-definition and subdivision of the Rapitan Group, Mackenzie Mountains. Geological Survey of Canada, Paper 77-35, 21 p.

Hoffman, P.F., and Halverson, G.P., 2011. Neoproterozoic glacial record in the Mackenzie Mountains, northern Canadian Cordillera. In: Arnaud, E., Halverson, G.P., Shields- Zhou, G. (Eds.), The Geological Record of Neoproterozoic Glaciations. The Geological Society, London, pp. 397–412.

James, N.P., Narbonne, G.M., Kyser, T.K., 2001. Late Neoproterozoic cap carbonates: Mackenzie Mountains, northwestern Canada: precipitation and global glacial meltdown. Canadian Journal of Earth Sciences, v. 38, p. 1229–1262.

Macdonald, F.A., Strauss, J.V., Sperling, E.A., Halverson, G.P., Narbonne, G.M., Johnston, D.T., Kunzmann, M., Schrag, D.P., and Higgins, J.A., 2013. The stratigraphic relationship between the Shuram carbon isotope excursion, the oxygenation of Neoproterozoic oceans, and the first appearance of the Ediacara biota and bilaterian trace fossils in northwestern Canada; Chemical Geology, v. 362, p. 250-272.

Moynihan, D.P., 2016. Bedrock geology compilation of the eastern Rackla belt, NTS 105N/15, 105N/16, 105O/13, 106B/4, 106C/1, 106C/2, east-central Yukon. Yukon Geological Survey, Open File 2016-2, scale 1:75000, 2 sheets.

Narbonne, G.M. and Aitken, J.D., 1995. Neoproterozoic of the Mackenzie Mountains, northwestern Canada. Precambrian Research, v. 73, p. 101-121.

Ristorcelli, S., Ronning, P., Martin, C., and Christensen, O., 2018. Technical report and estimate of mineral resources for the Osiris Project, Yukon, Canada. Mining Development Associates, Mine Engineering Services, 118 p.

APPENDIX 1

2018 Stratigraphic Observations

XLS SHEET ATTACHED

APPENDIX 2

Drone Survey Method and Data Products

High resolution PPK (post processing kinematic) drone surveys were completed across the three main transect areas. The technique method involves the use of a custom modified DJI Phantom 4 Pro camera drone and a GNSS base station. The PPK P4P drone system has an additional L1 GNSS received mounted at a fixed height about the camera center.



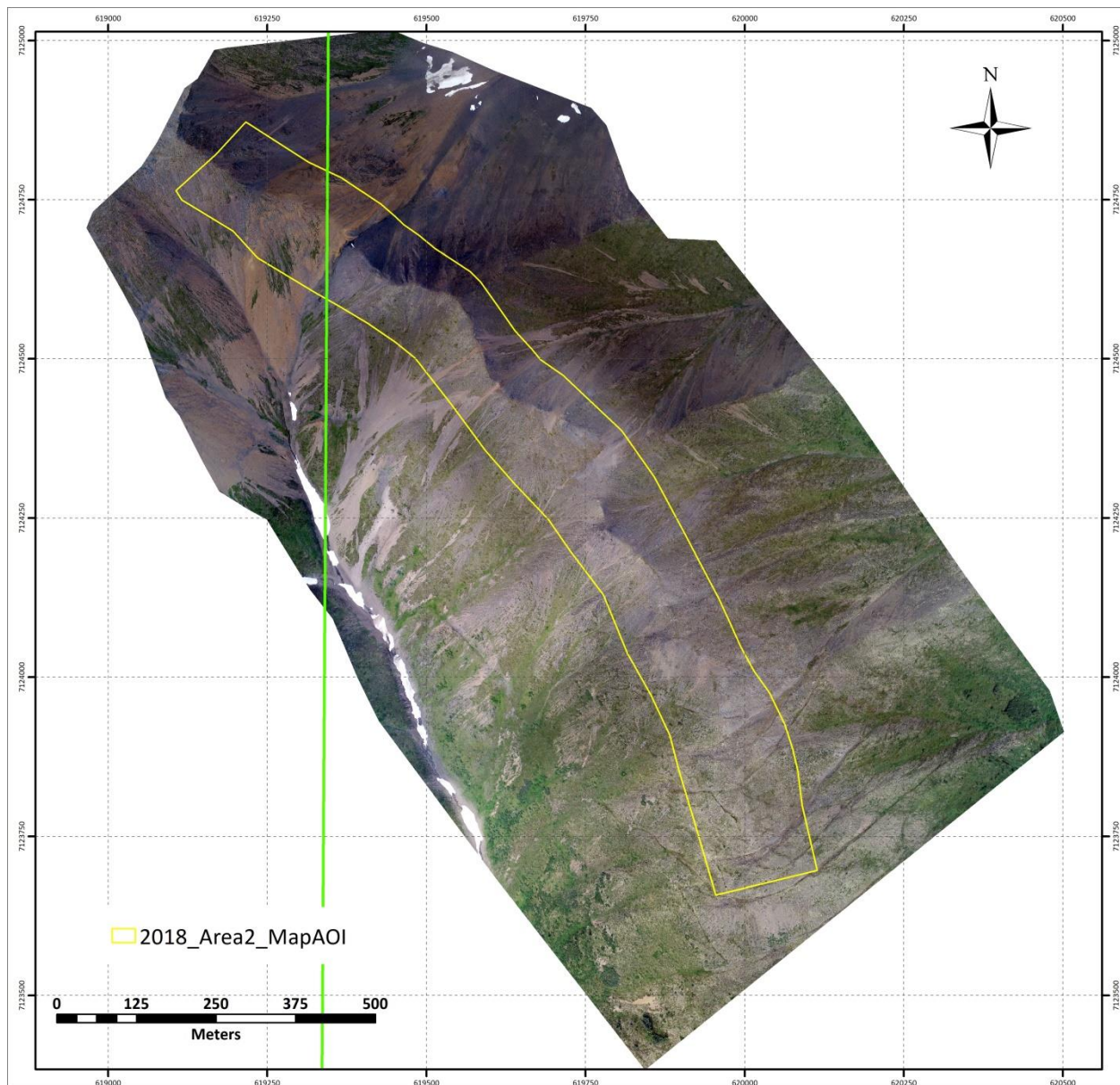
During drone missions, base and rover simultaneously collect positional information which are subsequently downloaded and used for post-processing. During post-processing, the original DJI gps positions are replaced with cm-accuracy coordinates in the photo EXIF data. The photos are then used to build orthophotos and digital elevation models. Spatial accuracy for orthophoto data ranges from 5-11 cm dependent on flight height and ground sampling distance. Resolution of digital elevation models ranges from 10-20 cm. Postional accuracy of final spatial data products ranges from 10 – 50cm. No ground control points were layed out during survey due to time constraints. The position of the base station was used to estimate final spatial variance.

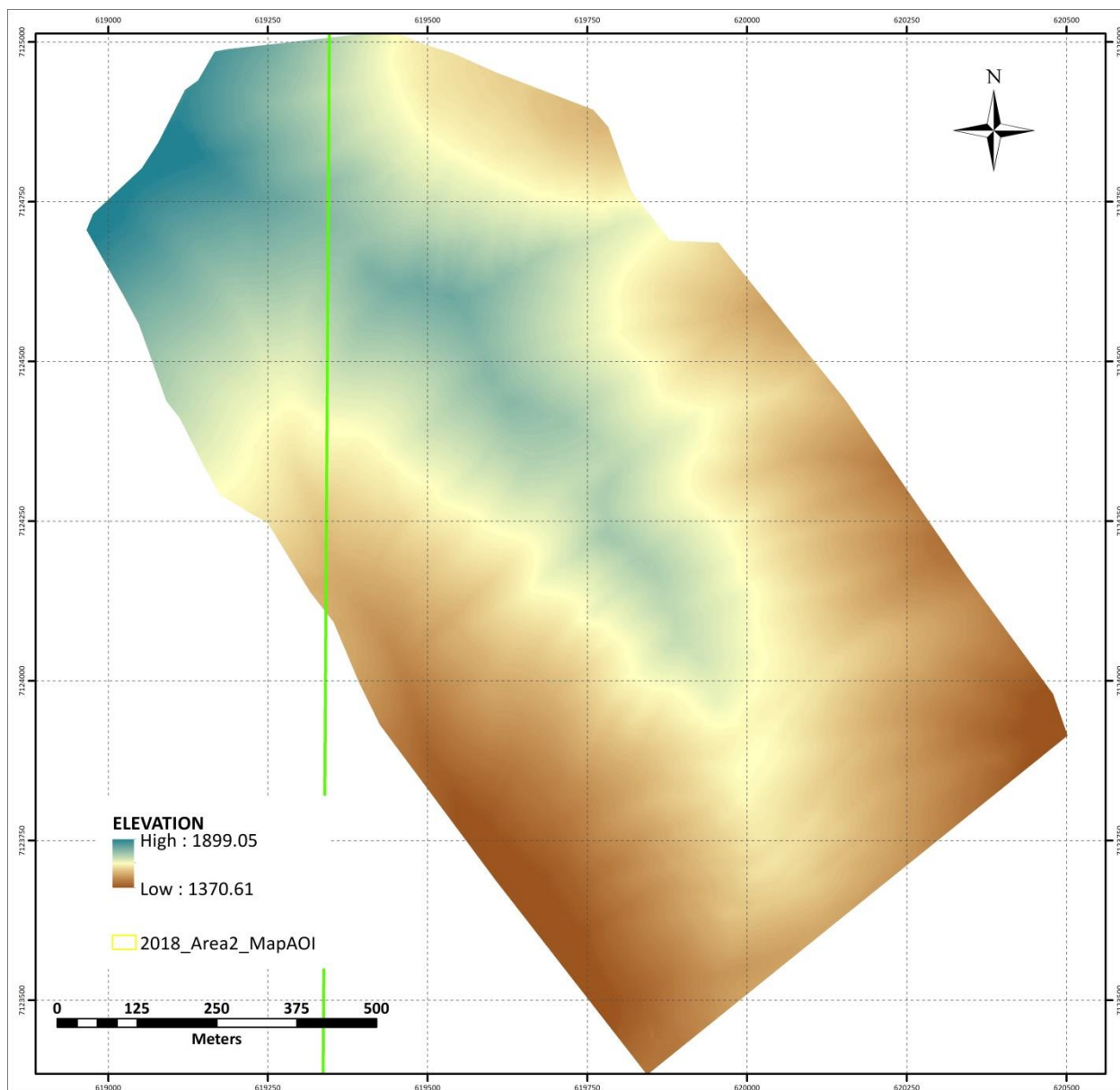
Three main sets of data products are provided including:

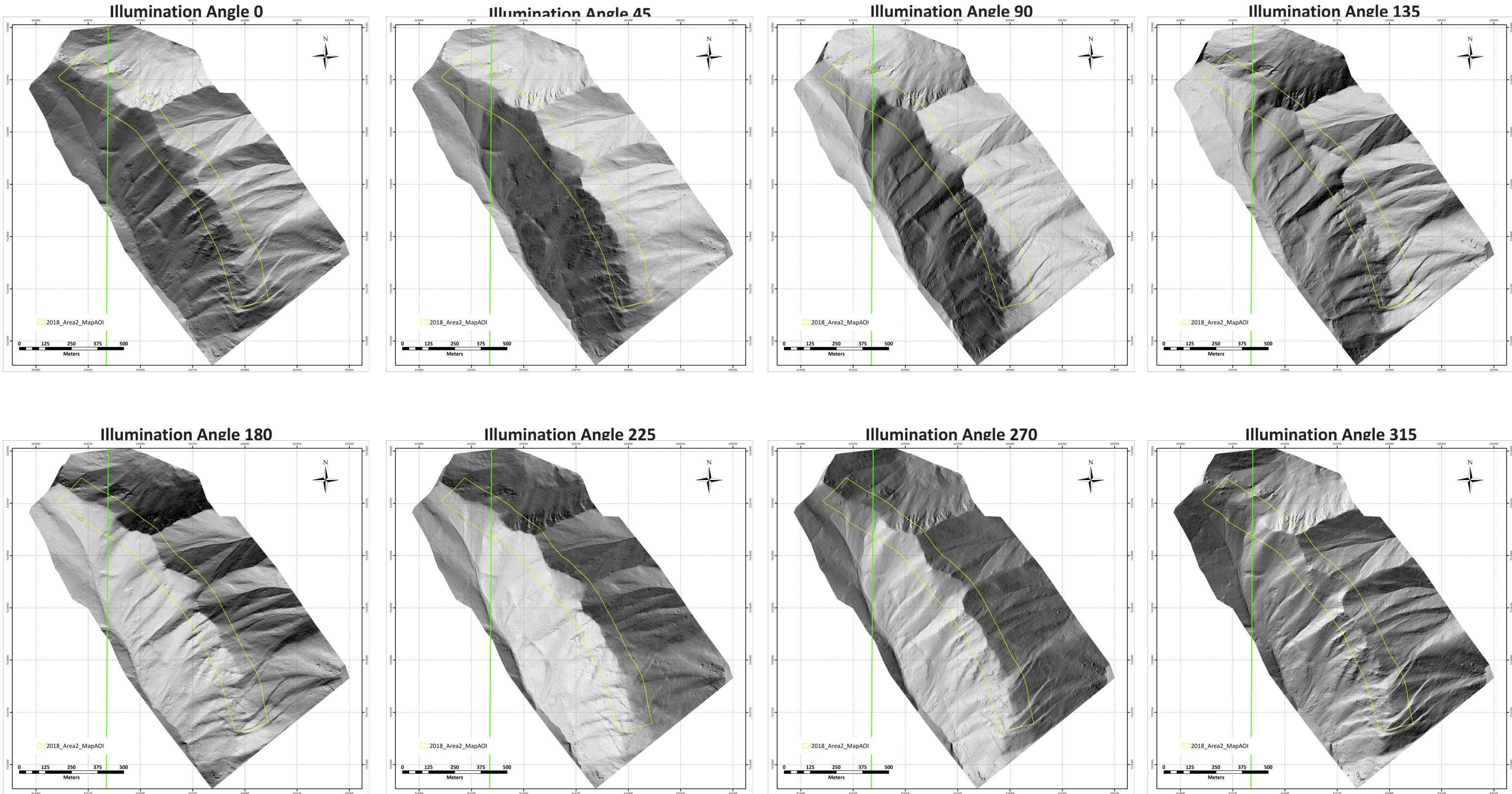
1. Orthophoto
2. Digital Elevation model
3. Eight derived hillshade models

<input type="checkbox"/>	<input checked="" type="checkbox"/> 2018_DRONE_IMAGERY
<input type="checkbox"/>	<input checked="" type="checkbox"/> AREA_1NW
<input type="checkbox"/>	<input type="checkbox"/> AREA_1SE
<input type="checkbox"/>	<input checked="" type="checkbox"/> AREA_2
<input type="checkbox"/>	<input checked="" type="checkbox"/> CC_A2_ORTHO_NAD83z8.img
<input type="checkbox"/>	<input type="checkbox"/> CC_A2_DEM_NAD83z8.img
<input type="checkbox"/>	<input checked="" type="checkbox"/> HILLSHADE
<input type="checkbox"/>	<input checked="" type="checkbox"/> A2_315_05.img
<input type="checkbox"/>	<input type="checkbox"/> A2_270_05.img
<input type="checkbox"/>	<input type="checkbox"/> A2_225_05.img
<input type="checkbox"/>	<input type="checkbox"/> A2_180_05.img
<input type="checkbox"/>	<input type="checkbox"/> A2_135_05.img
<input type="checkbox"/>	<input type="checkbox"/> A2_90_05.img
<input type="checkbox"/>	<input type="checkbox"/> A2_45_05.img
<input type="checkbox"/>	<input type="checkbox"/> A2_0_05.img

EXAMPLE OF ORTHOPHOTO (5cm spatial resolution)



EXAMPLE OF DEM (11cm resolution)

**Hillshade Model Data Products**

APPENDIX 3

Geochemical Sampling Results

In addition to C/O isotope analysis, assay geochemical sampling was completed for the 42 samples of clastic and carbonate rocks in both Areas 1 and 2. The objective was to use the geochemical data to better define geochemical trends within basin environments and in so doing identify basins with distinct different (or similar) geochemical settings.

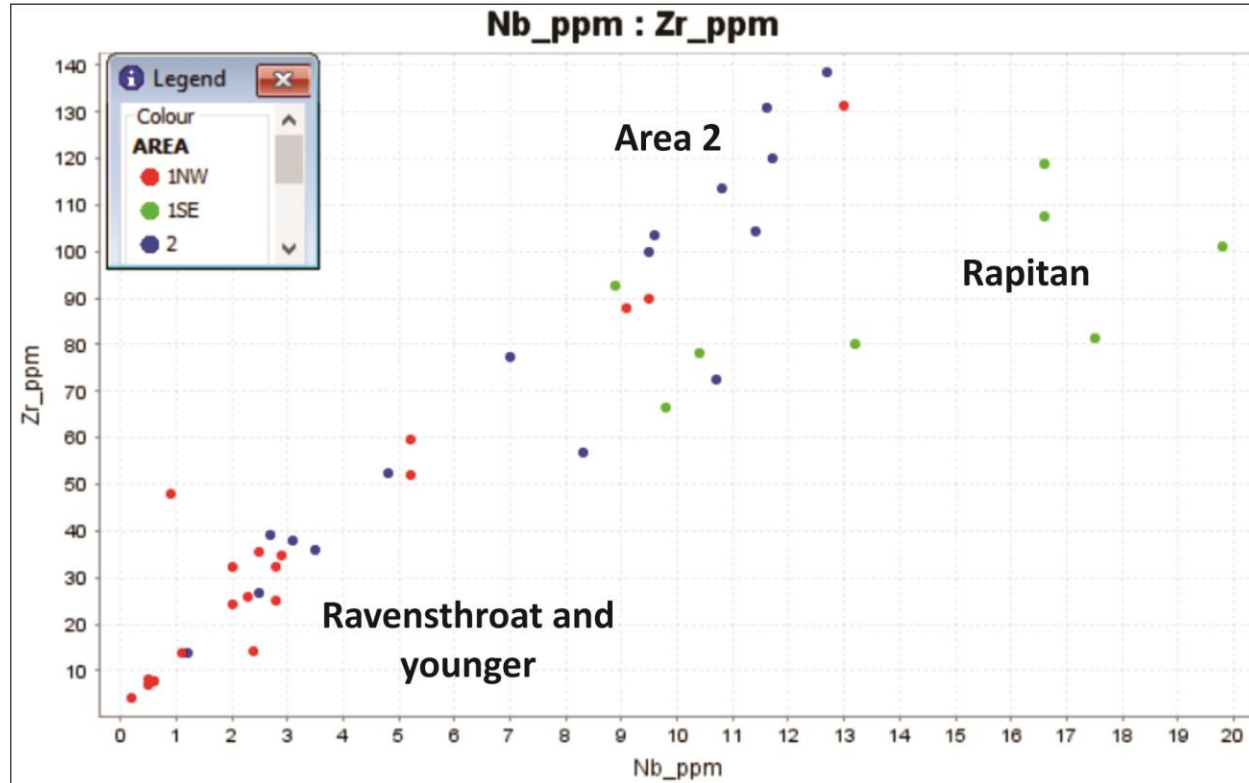
The samples were sent to ALS Geochemical Labs and analysed using the geochemical package MEMS 61. An excel spreadsheet of the compiled data is provided with this report (Appendix 3.xls).

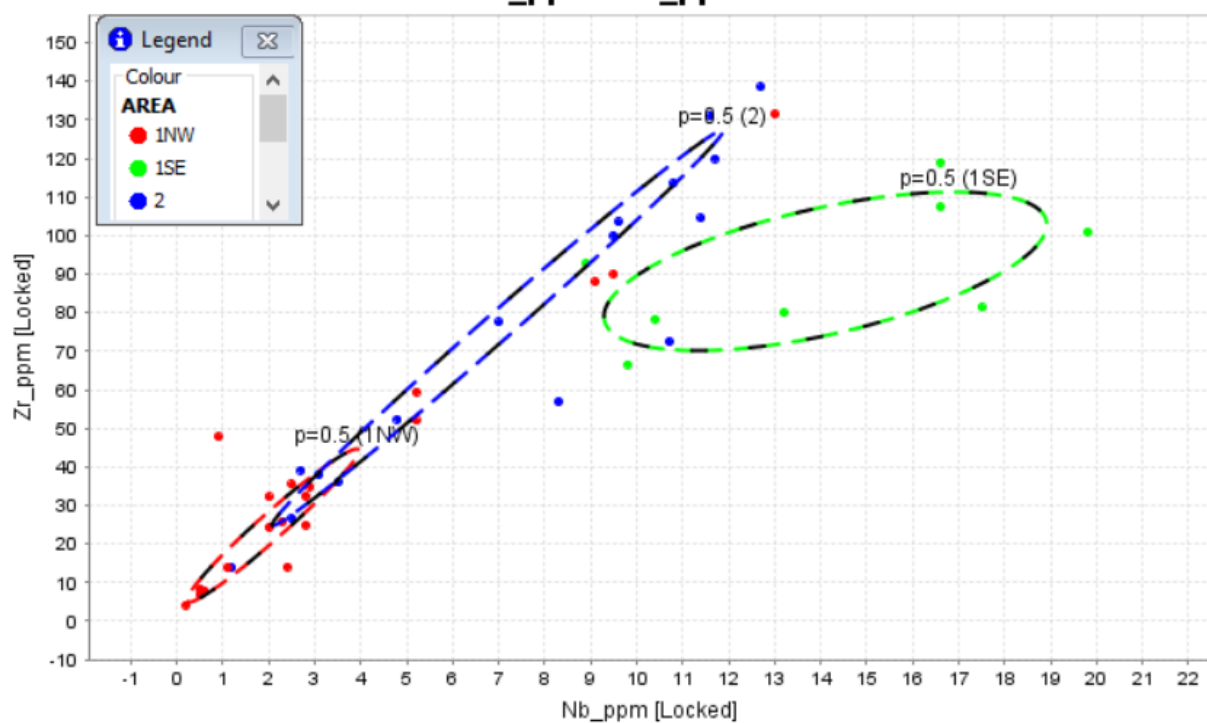
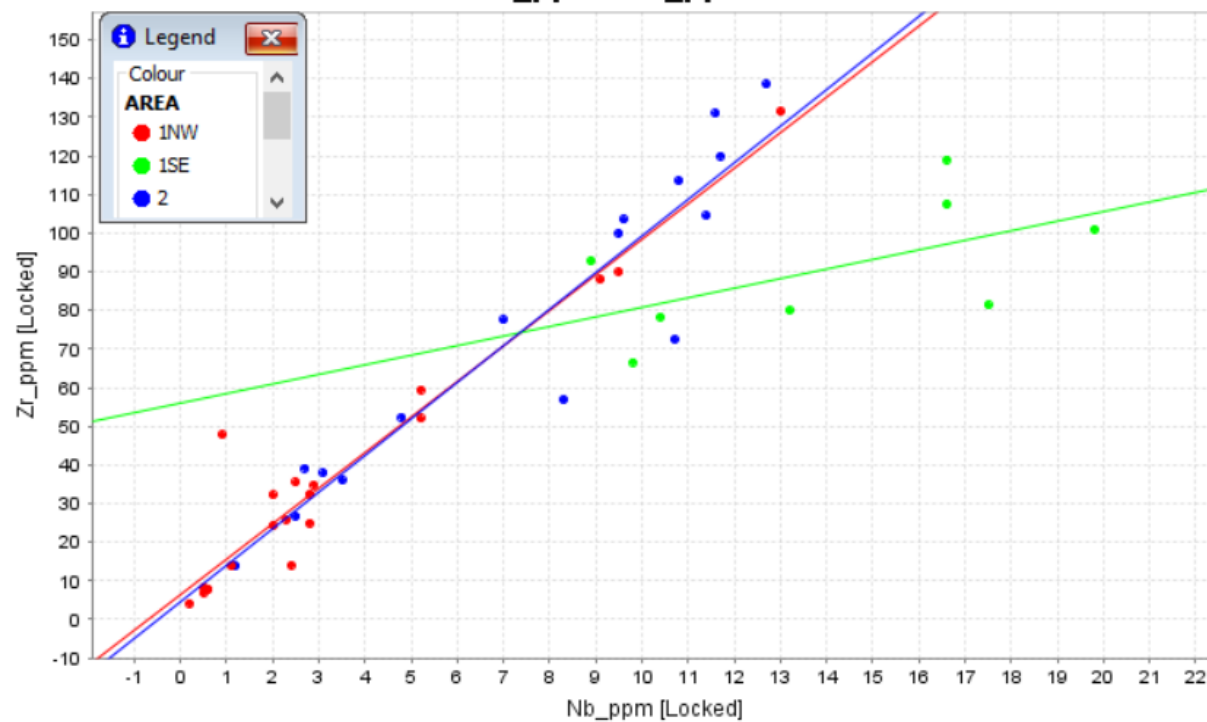
Two important observations come from X-Y scatterplots using element ratios that profile resistive mineral phases (e.g. zircon, ilmenite, rutile) that better represent source material, including:

1. Sedimentary material forming in the Rapitan basinal environment is distinctly different from younger overlying stratigraphy and the unknown stratigraphy of Area 2. Samples from the Rapitan formation area elevated in Fe, Ti, Zr Sc and Nb concentrations
2. The poorly constrained stratigraphy of Area 2 has a geochemical affinity more akin to Stratigraphy within and younger than the Ravensthorpe Formation.

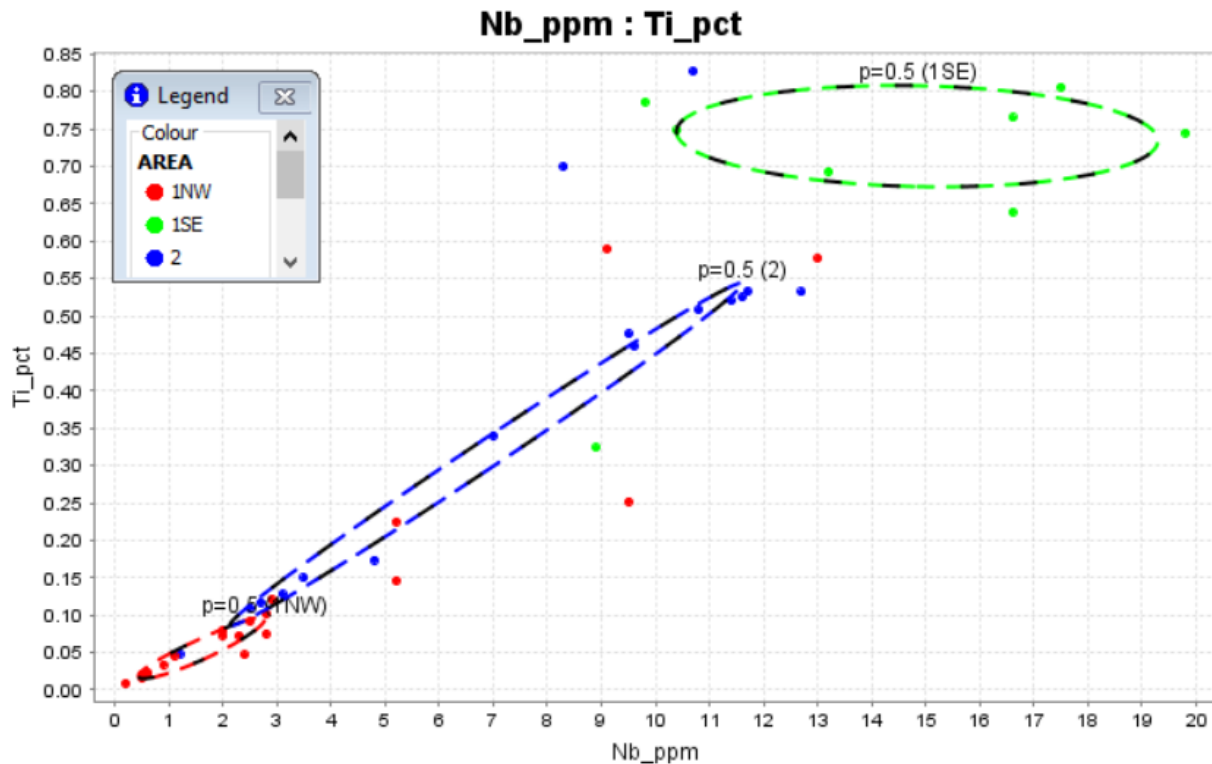
Useful element ratios that highlight these observations include:

- **Nb vs Zr**

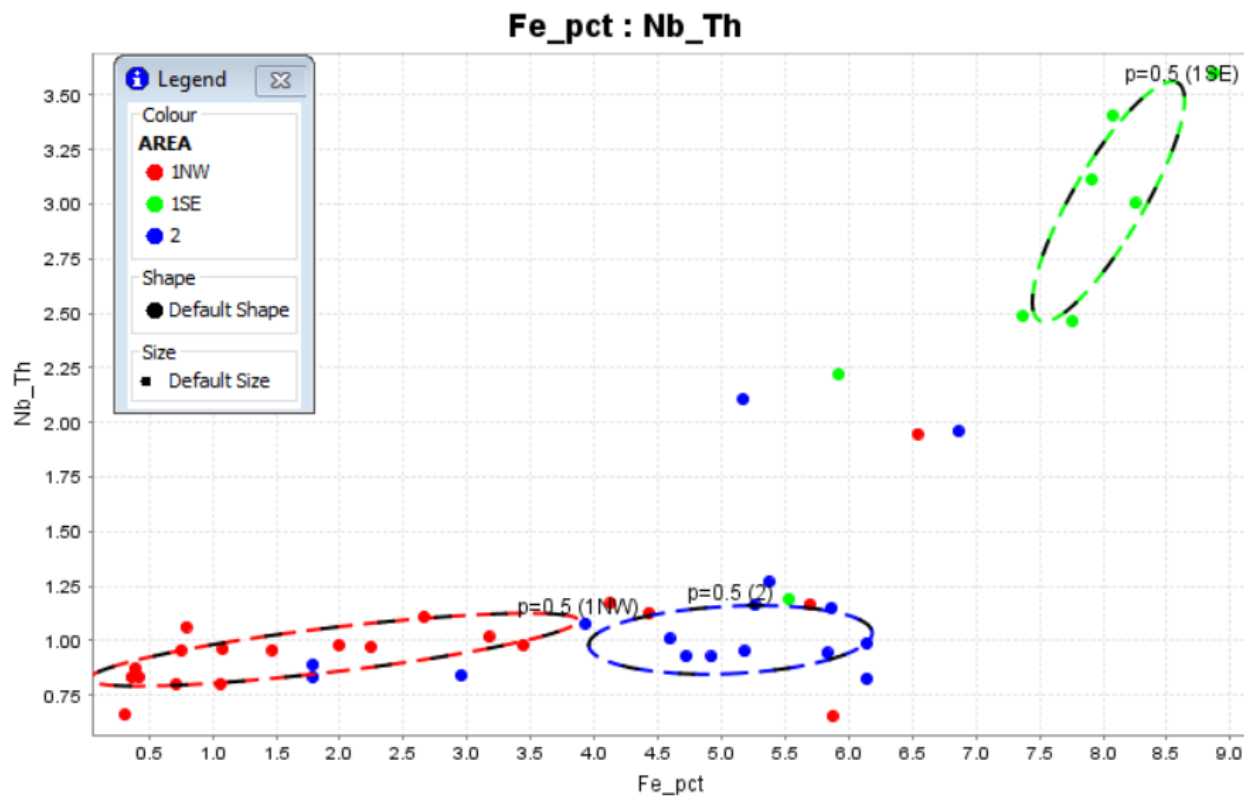


Nb_ppm : Zr_ppm**Nb_ppm : Zr_ppm**

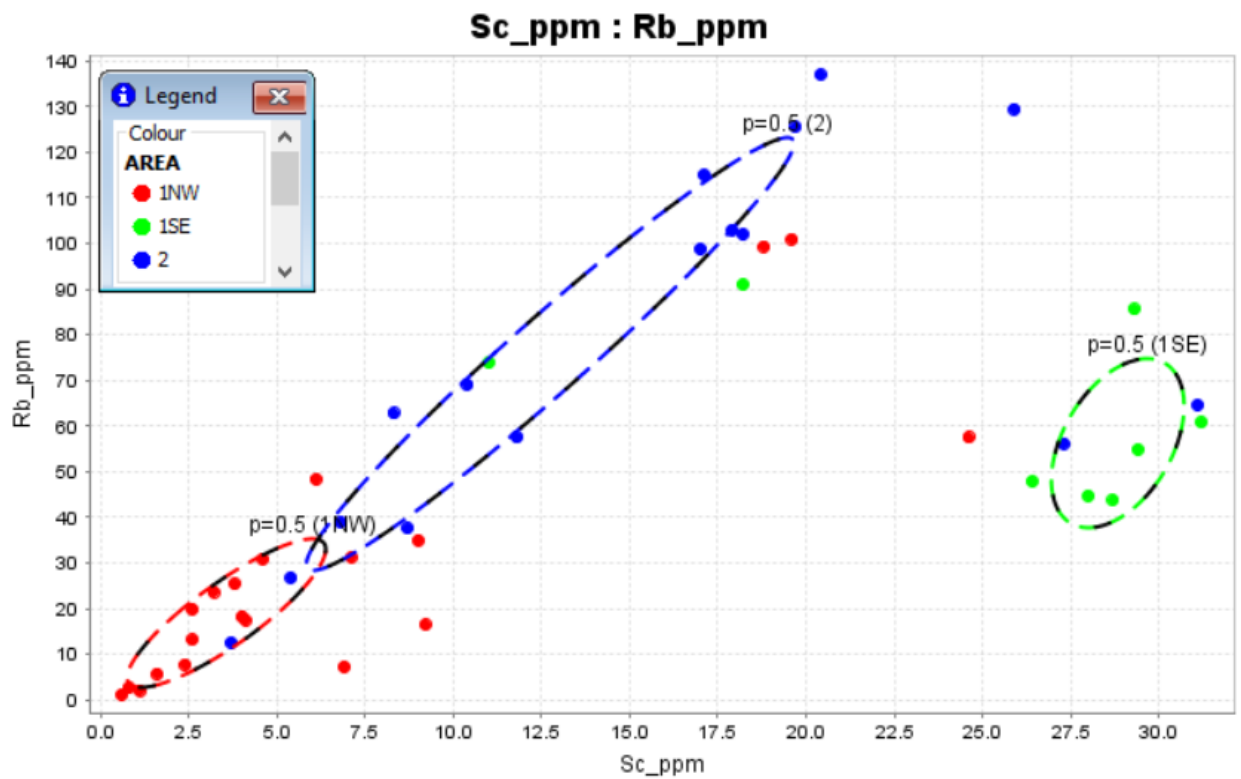
- ## • Nb vs Ti



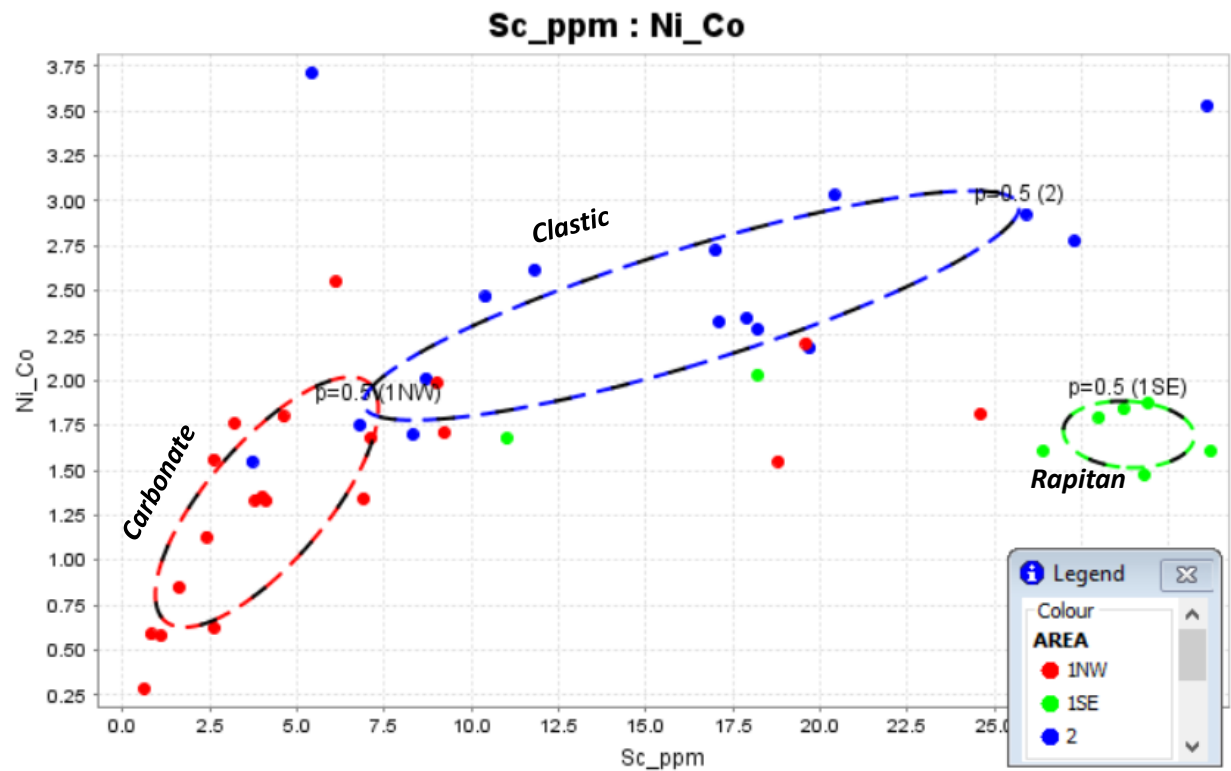
- Fe vs Nb/Th



- Sc vs Rb



- Sc vs Ni/Co



APPENDIX 4

Mappt™ Mobile GIS and Data Capture Software - Overview

- Mappt is a versatile, user-friendly mobile GIS application available for android devices:

<https://www.mappt.com.au/>

- Product and software developers from the Takor Group who designed and maintain Mappt have been working with Geomantia Consulting during 2018 to customize the application for mineral exploration needs. This is an ongoing process.
- Projects are setup in the app, much like desktop GIS software. The app actively taps into onboard GPS units (or external GPS units through Bluetooth connection). Raster and vector data can be loaded into the project. Any custom raster imagery can be easily uploaded to the app.
- Data collection templates can be built to suite any existing database structure.
- The app also also for real time capture and display of structural data either through manual entry of measurement or by using the onboard digital compass.
- An extended zoom view feature allows the user to tap into high resolution drone imagery.
- Point, polyline and polygon data can be capture in the field.

MAPPT MAIN INTERFACE

The screenshot displays the MAPPT software interface, specifically version 3.11.2 Professional, titled "carlincore 2018.mp". The interface includes a top navigation bar with icons for file operations, zoom, orientation, and settings. On the left, a "View Layers" panel lists several data sources, with "2014_SOIL_LOC" highlighted in blue. The main area shows a geological map with a dark background and a textured surface. Several white callout bubbles contain labels such as "2014_CCvb116", "2018CCvb118", "2018CCvb119", and "2018CCvb120". Red X marks are placed on the rock surface near these labels. A legend icon in the bottom right corner indicates the presence of a legend or information panel.

carlincore 2018.mp

Mappt 3.11.2 Professional

View Layers

Search...

CC POINT DATA

CC PHOTOS

DETrital ZIRCON SAMPLES

Linework

2014_SOIL_LOC

2015_SOIL_LOC

2014_Rock

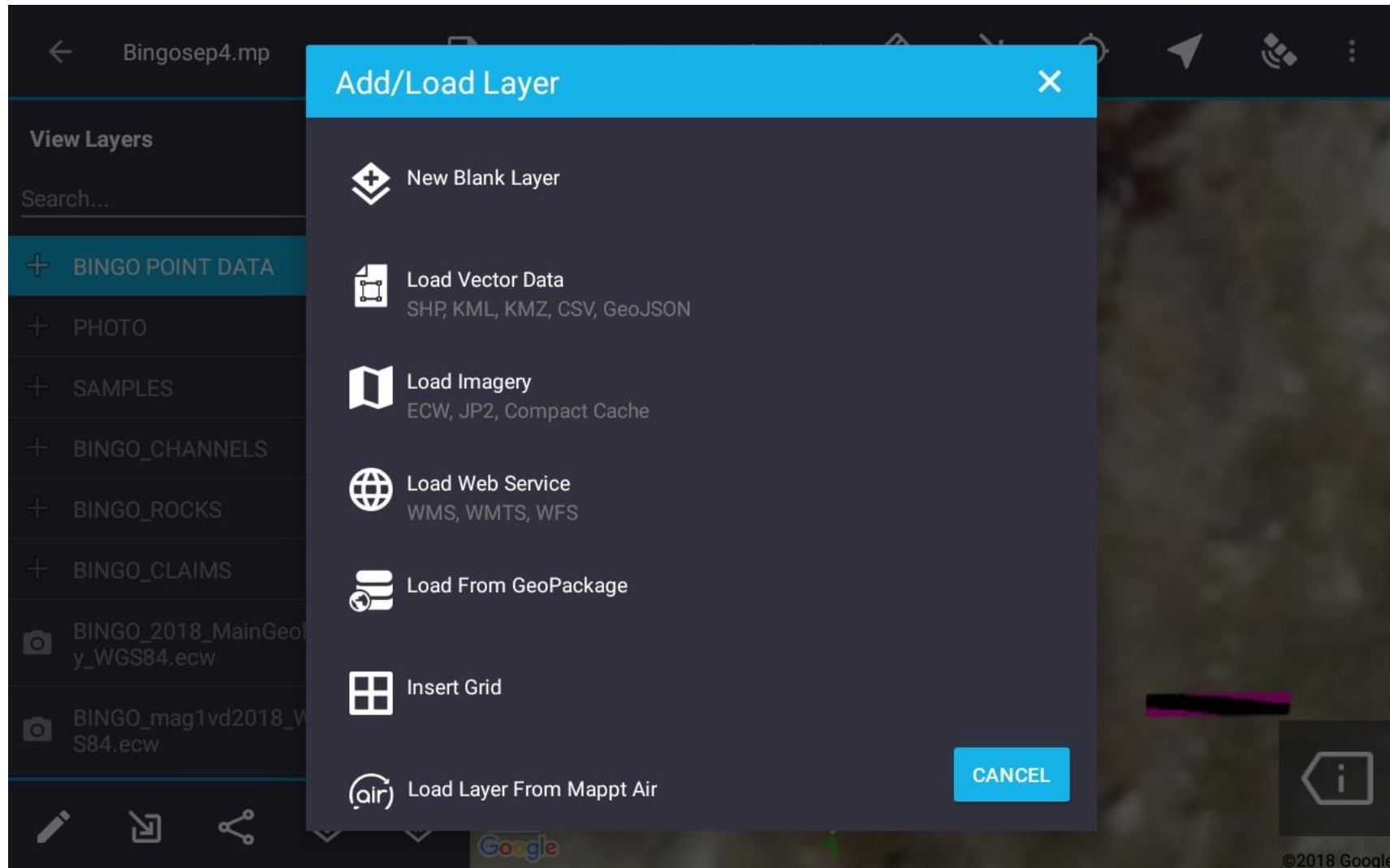
2015_Rock

2016_Rock

Google

©2018 Google

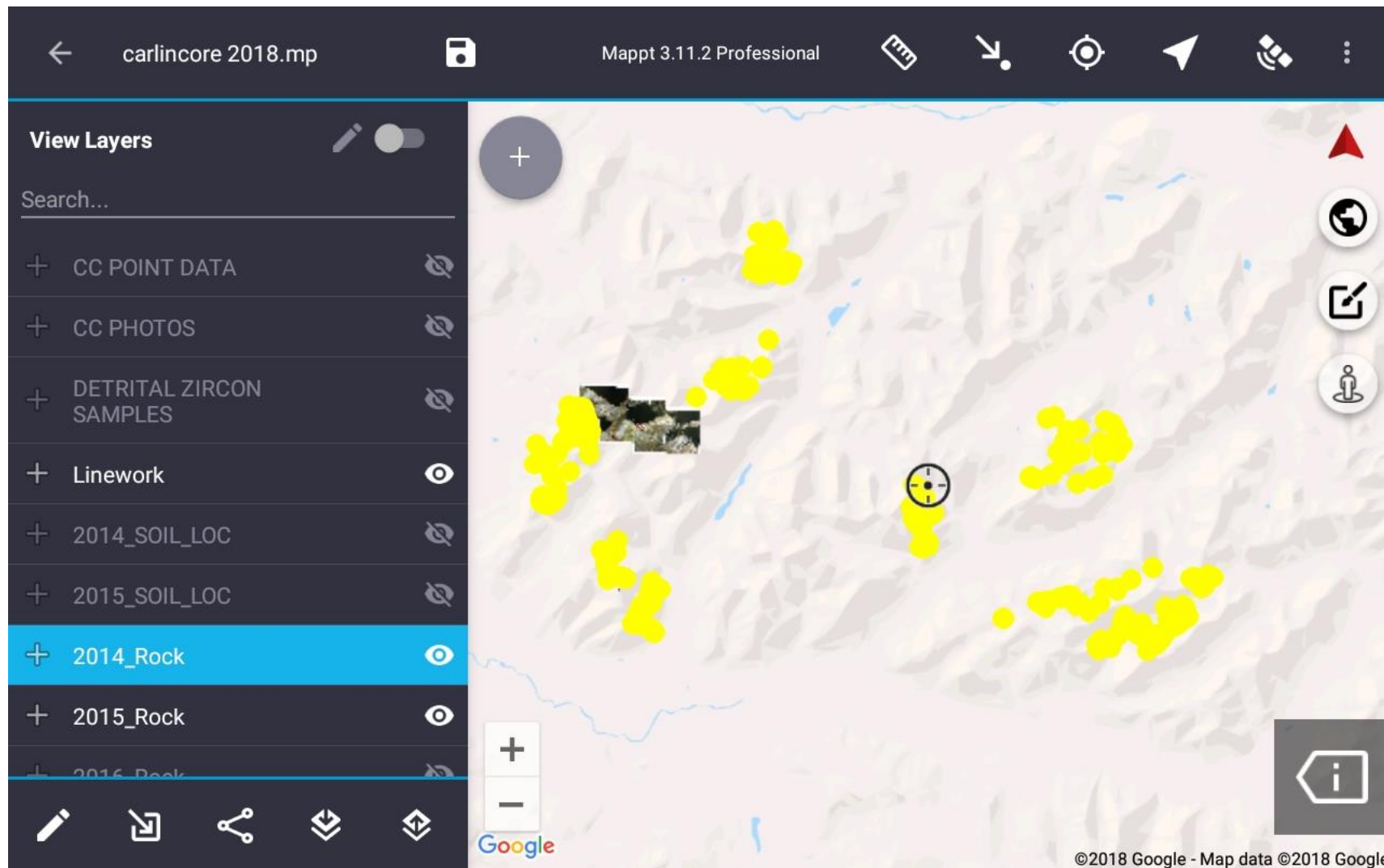
UPLOAD VECTOR and RASTER IMAGERY



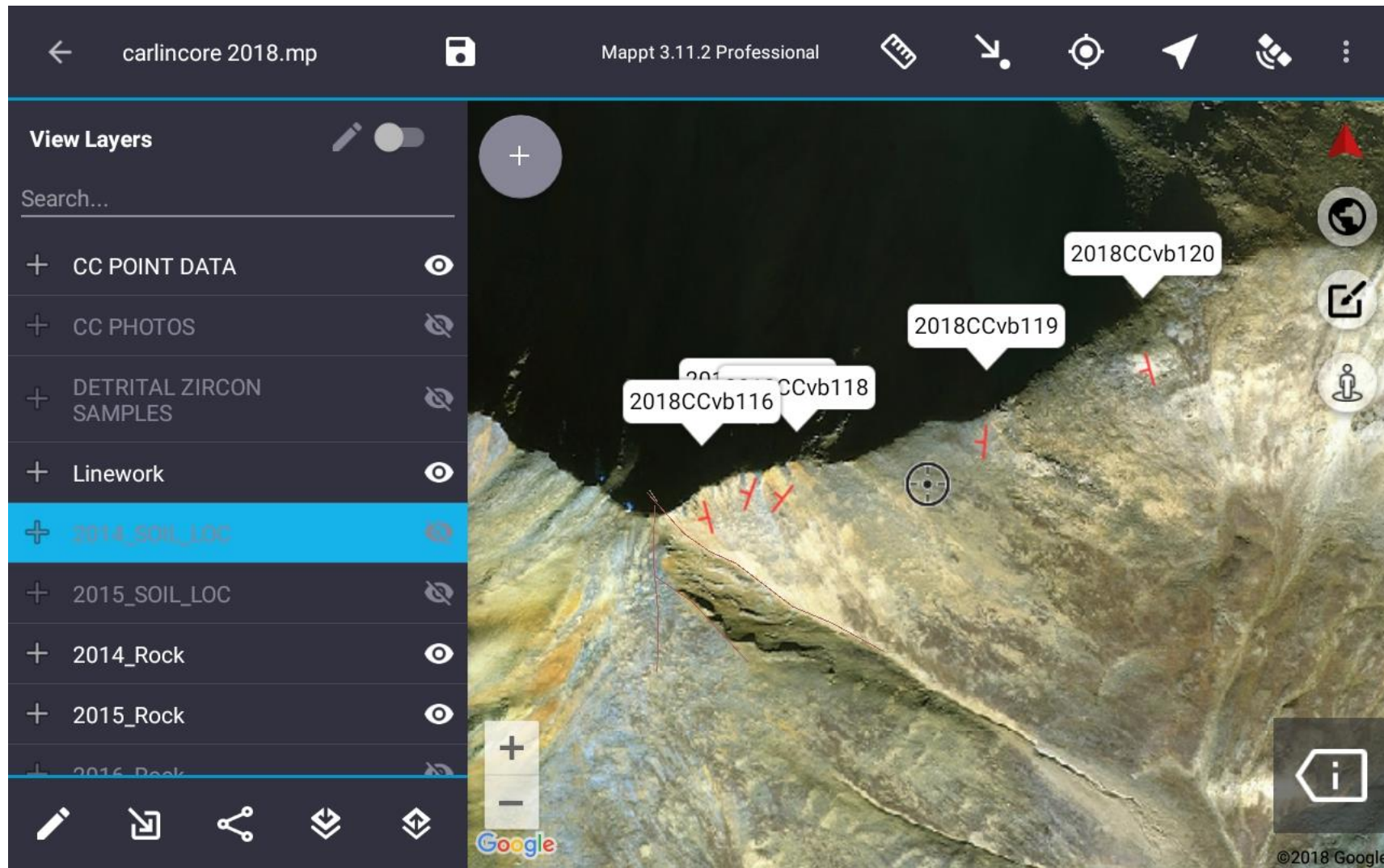
CUSTOM RASTER DATA (High Resolution Free Satellite Data)

The screenshot shows the Mappt 3.11.2 Professional application interface. The top bar includes a back arrow, the file name "carlincore 2018.mp", a save icon, the version "Mappt 3.11.2 Professional", and several tool icons. On the left, a "View Layers" panel lists geological data layers: "Linework", "2014_SOIL_LOC", "2015_SOIL_LOC", "2014_Rock" (selected and highlighted in blue), "2015_Rock", "2016_Rock", "Area1NW3_5k.ecw", "Area1_NW_PtB_1.ecw", and "Area1_NW_PtB_2.ecw". Each layer has an eye icon to toggle visibility. The main workspace displays a geological map with various rock units and soil locations. A central inset provides a detailed view of a specific rock outcrop with a circular measurement tool overlaid. To the right, there are three smaller image thumbnails showing different geological features. The bottom of the screen features a toolbar with icons for edit, search, share, and download, along with a "Google" button.

Vector data (Carlincore 2014/2015 Rocks)



Collect Point data(2018 vb field data with custom structural symbols)



Digital Compass

Device Orientation

Pitch	-38.04°
Roll	-9.16°
Yaw	318.03°

(Positive C/W from North)

Strike&Dip

Strike	48.03°
Dip	38.04°
Dip Direction	138.03°

Use True North

CANCEL RECAPTURE READINGS OK

DESIGN DATA COLLECTION FORMS

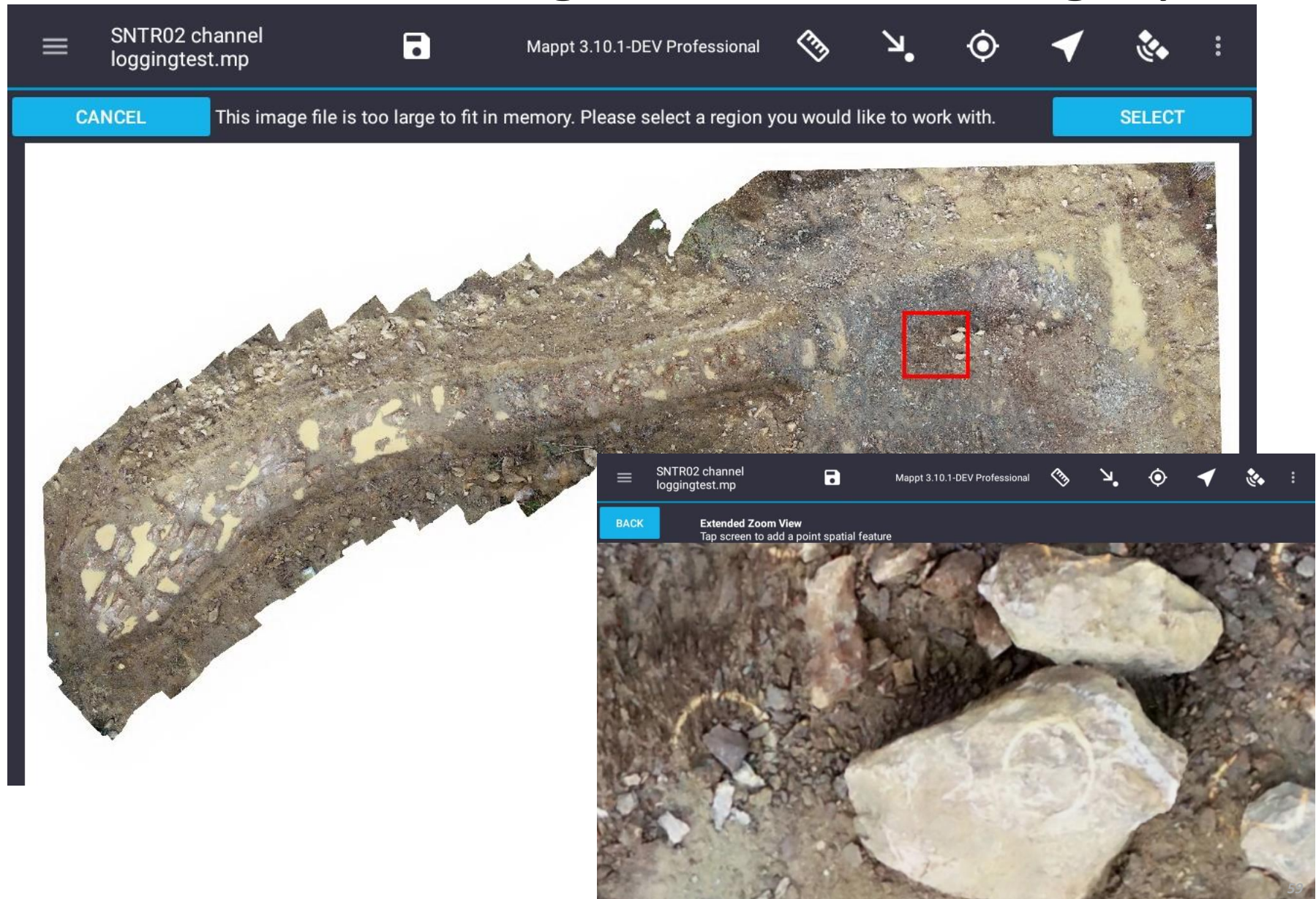
Edit Layer

DESCRIPTION		ATTRIBUTES		STYLE	CLASSIFICATION	CLASS STYLES
Name	Type	Required	Include in Wizard?	Constraints		
StationID	Text	<input checked="" type="checkbox"/>	<input checked="" type="checkbox"/>	-		
ObservationID	Number	<input type="checkbox"/>	<input checked="" type="checkbox"/>	Min: 1, Max: -		
Area	Dropdown	<input type="checkbox"/>	<input checked="" type="checkbox"/>	area1 SE, area1 NW, area2		
ELEVATION	Decimal	<input type="checkbox"/>	<input type="checkbox"/>	Min: -, Max: -		
Lithology	Dropdown	<input type="checkbox"/>	<input checked="" type="checkbox"/>	siltstone, mudstone, carbonate, dolostone, sandstone		
CommentLithology	Text	<input type="checkbox"/>	<input checked="" type="checkbox"/>	-		
StructureType	Dropdown	<input type="checkbox"/>	<input checked="" type="checkbox"/>	bedding, cleavage, foliation, joint, fracture, fault unspec		
CommentStructure	Text	<input type="checkbox"/>	<input checked="" type="checkbox"/>	-		

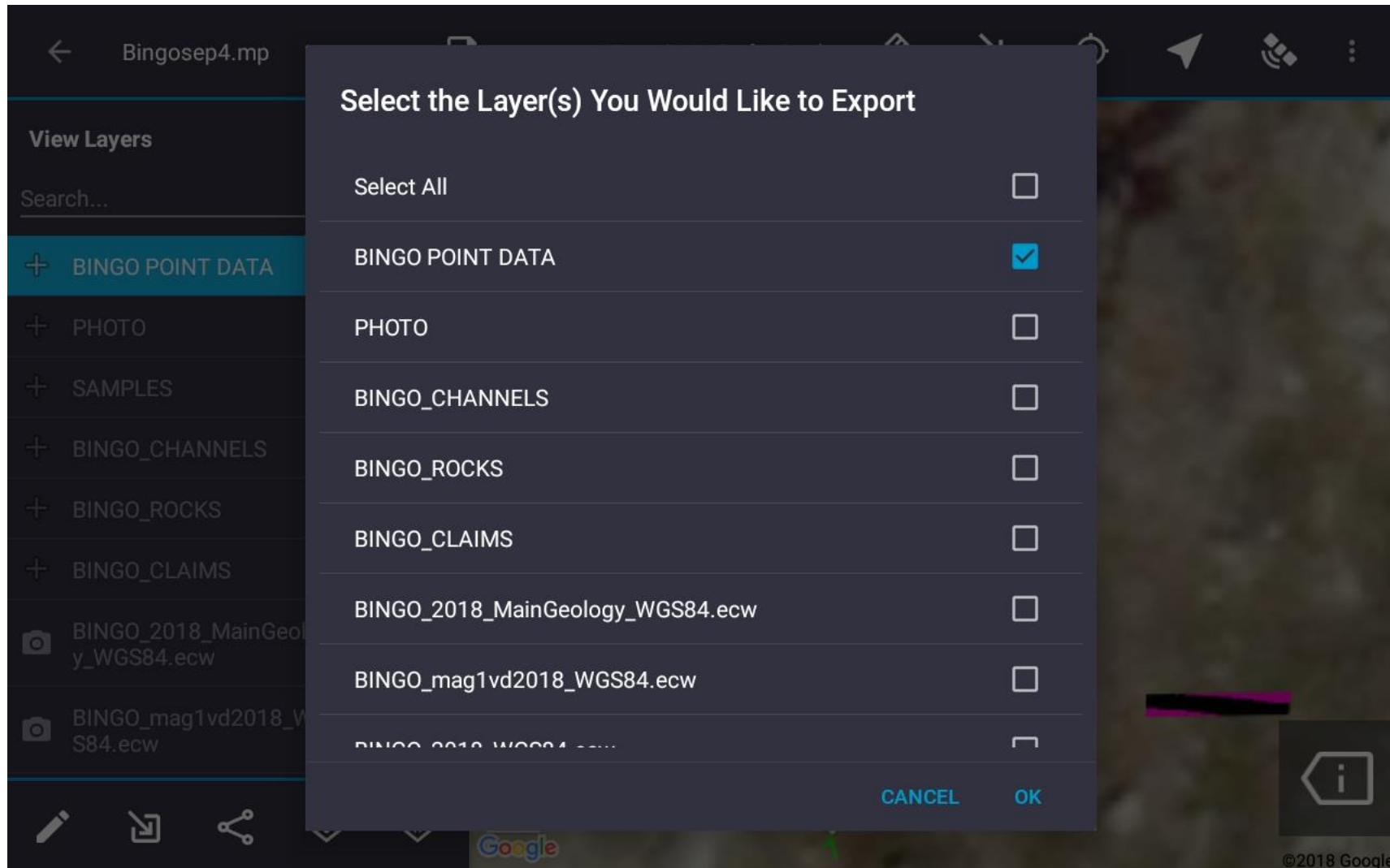
LOAD **EXPORT** **ADD** **EDIT** **DELETE** **OK**

Google ©2018 Google - Map data ©2018 Google

Access Drone High Resolution Imagery



EXPORT TO MULTIPLE FORMATS



EXPORT TO MULTIPLE FORMATS

